

Supporting information for:

Diruthenium(II) Capped Oligothiénylethynyl Bridged Highly Soluble Organometallic Wires for Long-Range Electronic Coupling

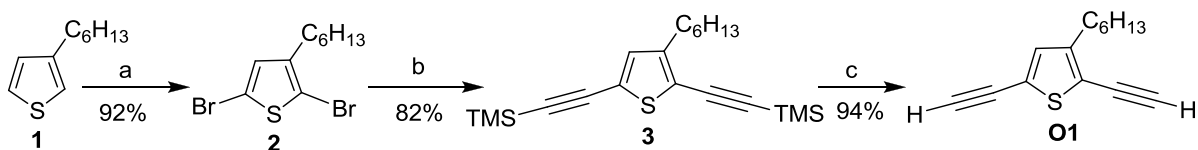
Sourav Saha Roy,^a Amit Sil,^a Dipanjan Giri^a Sabyasachi Roy Chowdhury,^a Sabyashachi Mishra^{*a} and Sanjib K. Patra^{*a}

^a*Department of Chemistry, Indian Institute of Technology Kharagpur, Kharagpur-721302, WB, INDIA, E-mail: skpatra@chem.iitkgp.ac.in; Tel: +913222283338*

1. Synthesis and Characterization.....	S2-S50
1a. Synthesis.....	S2-S6
1b. NMR spectra.....	S7-S39
1c. Mass spectrometry.....	S40-S43
1d. FTIR spectra.....	S44-S48
1e. CHN analysis.....	S48-S50
2. Photophysical studies.....	S50-S51
3. Thermal analysis.....	S51-S52
3a. TGA.....	S51-S51
3b. DSC.....	S52
4. Electrochemical Characterization.....	S53
5. Crystallographic data.....	S54-S55
6. Estimation of intermetallic distances in the synthesized diruthenium(II) complexes.....	S56-S57
7. UV-vis-NIR measurements.....	S57-S58
8. Selected Frontier molecular orbitals obtained from DFT calculations.....	S59
9. References.....	S60

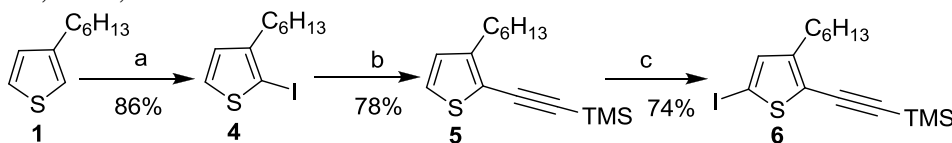
1. Synthesis and Characterization

1a. Synthesis and Characterization



Scheme S1: Synthesis of 2,5-bis(ethynyl)-3-hexylthiophene (**O1**)

Reagents and conditions: a) 2.5 eqv. NBS, THF, 25 °C, 12h; b) 3.6 eqv. Ethynyltrimethylsilane, 3 mol% Pd(PPh₃)₂Cl₂, 3 mol% CuI, Et₃N, DCM, 25 °C, 12h; c) K₂CO₃, MeOH/DCM, 25 °C, 2h.



Scheme S2. Synthesis of 5-iodo-2-ethynyl(trimethylsilyl)-3-hexylthiophene (**6**)

Reagents and conditions: a) 1.2 eqv. NIS, DCM/AcOH, 0 °C, 12h; b) 1.3 eqv. Ethynyltrimethylsilane, 3 mol% Pd(PPh₃)₂Cl₂, 3 mol% CuI, Et₃N, DCM, 25 °C, 12h; c) LDA, -78 °C, I₂, THF, 12h.

2,5-bis[ethynyl(trimethylsilyl)]-3-hexylthiophene (3). To a solution of 3-hexyl-2,5-dibromothiophene (0.5 g, 1.53 mmol), bis(triphenylphosphine) palladium(II) chloride (0.03 g, 0.05 mmol, 3 mol%), copper(I) iodide (0.01 g, 0.05 mmol, 3 mol%), and DCM (15 mL) were added. Then triethylamine (5 mL, 34 mmol) was added to it at room temperature while stirring. The resulting clear orange solution was stirred for 5 min before (trimethylsilyl)-acetylene (0.8 mL, 5.5 mmol) was added. The whole reaction mixture was stirred for 12h at room temperature and poured into water, and the aqueous layer was extracted with DCM. The organic layer was dried over anhydrous MgSO₄, and the crude product was concentrated *in vacuo*. The product was purified using silica gel column chromatography (hexane as eluent) to get dark yellow oily product with 0.45 g, (82% yield). ¹H NMR (400MHz, CDCl₃) δ(ppm): 6.98 (s, 1H, CH thienyl), 2.61 (t, J=6Hz, 2H, CH₂-C₅H₁₁), 1.57 (m, 2H, Th-CH₂-CH₂-C₄H₉), 1.31(m, 6H), 0.93(m, 3H), 0.24(s, 18H, SiMe₃). ¹³C {¹H} NMR (100MHz, CDCl₃) δ (ppm): 148.5, 133.6 (CH thienyl), 123.0, 120.1, 101.9, 99.6, 97.6, 97.1, 31.8, 30.1, 29.5, 28.9, 22.8, 14.3, 0.03 (SiMe₃).

2-[ethynyl(trimethylsilyl)]-3-hexylthiophene (5). To a solution of 3-hexyl-2-iodothiophene (0.5 g, 1.69 mmol), bis(triphenylphosphine) palladium(II) chloride (0.04 g, 0.05 mmol, 3 mol%), copper(I) iodide (0.01 g, 0.05 mmol, 3 mol%), and DCM (10 mL) were added. Then triethylamine(5 mL, 34 mmol) was added to it at room temperature while stirring. The

resulting clear orange solution was stirred for 5 min before (trimethylsilyl)-acetylene (0.3 mL, 2.02 mmol) was added. The reaction mixture was stirred for 12h at room temperature and poured into water, and the aqueous layer was extracted with DCM. The organic layer was dried over anhydrous MgSO_4 , and the crude product was concentrated *in vacuo*. It was chromatographed on silica gel using hexane as eluent to get dark yellow oily product with 0.25 g (78% yield). ^1H NMR (400MHz, CDCl_3) δ (ppm): 7.12 (d, $J=4$ Hz, 1H, 5 position CH thienyl), 6.83 (d, $J=4$ Hz, 1H, 4 position CH thienyl), 2.69 (t, $J=8$ Hz, 2H, $\text{Th-CH}_2\text{-C}_5\text{H}_{11}$), 1.61 (m, 2H, $\text{Th-CH}_2\text{-CH}_2\text{-C}_4\text{H}_9$), 1.31(m, 6H), 0.88 (m, 3H), 0.24(s, 9H, SiMe_3). ^{13}C $\{^1\text{H}\}$ NMR (100MHz, CDCl_3) δ (ppm): 148.5, 133.6 (CH thienyl), 123.0, 120.1, 101.9, 99.6, 97.6, 97.1, 31.8, 30.1, 29.5, 28.9, 22.8, 14.3, 0.03 (SiMe_3).

3-hexyl-5-iodo-2-((trimethylsilyl)ethynyl)thiophene (6). To a solution of diisopropylamine (1.6 mL, 11.7 mmol) in THF (8 mL) at -78°C was added dropwise *n*-butyllithium (14.68 mL, 23.5mmol, 1.6 M in hexanes). The mixture was warmed to 0°C for 30 min and then recooled to -78°C . 2-[ethynyl(trimethylsilyl)]-3-hexylthiophene(1.50 g, 5.34 mmol) in THF (10 mL) at room temperature was then added dropwise, and the solution was warmed from -78°C to 0°C for next 10 min. Next, the solution was recooled to -78°C . While at -78°C , iodine (3.26 g, 12.8 mmol) in THF (10 mL) was added via cannula, and the solution was allowed to warm up to room temperature overnight. The mixture was quenched with water, and the aqueous layer was extracted with diethyl-ether. The organic extracts were washed with brine and aqueous sodium thiosulfate. The ether layers were dried over anhydrous MgSO_4 . The solvent was removed by rotary evaporation, and the residue was purified by flash chromatography (silica gel, hexane) to provide 2.10 g (74% yield) of the title product as a yellow liquid. ^1H NMR (400 MHz, CDCl_3), δ (ppm): 6.99 (s, 1H, CH thienyl), 2.63 (t, $J =4$ Hz, 2H, $\text{Th-CH}_2\text{-C}_5\text{H}_{11}$), 1.57 (m, 2H, $\text{Th-CH}_2\text{-CH}_2\text{-C}_4\text{H}_9$), 1.31 (m, 6H), 0.87 (m, 3H), 0.24 (s, 9H, SiMe_3). ^{13}C $\{^1\text{H}\}$ NMR (100 MHz, CDCl_3) δ (ppm): 150.5, 138.1 (CH thienyl), 124.7, 102.8, 96.3, 74.1 (C-I thienyl), 31.7, 30.1, 29.3, 29.0, 22.8, 14.3, 0.1 (SiMe_3).

2,5-bis(ethynyl)-3-hexylthiophene (O1). 2,5-Bis[ethynyl(trimethylsilyl)]-3-hexylthiophene(1 g, 2.97 mmol) and potassium carbonate (0.82 g, 5.94 mmol) were dissolved in a solution of DCM (15 mL) and methanol (10 mL). The solution was allowed to stir at room temperature for 2h. The reaction mixture was poured into water and extracted with DCM. The organic extract was washed with brine. The combined organic layers were dried over anhydrous MgSO_4 . The solvent was removed by rotary evaporation. It was purified using silica gel column chromatography (hexane as eluent) to afford 2,5-bis(ethynyl)-3-hexylthiophene as yellowish oil with 0.6 g (94% yield). ^1H NMR (400 MHz, CDCl_3) δ (ppm): 7.01 (s, 1H, CH thienyl),

3.44 (s, 1H, -C≡CH), 3.32 (s, 1H, -C≡CH), 2.64 (t, J=6 Hz, 2H, Th-CH₂-C₅H₁₁), 1.58 (m, 2H, Th-CH₂-CH₂-C₄H₉), 1.31 (m, 6H), 0.89 (m, 3H). ¹³C{¹H} NMR (100 MHz, CDCl₃) δ (ppm): 148.9, 133.9 (CH thienyl), 122.2, 119.0, 84.1 (-C≡CH), 81.8 (-C≡CH), 76.8 (-C≡CH), 76.2 (-C≡CH), 31.8, 30.1, 29.5, 28.9, 22.8, 14.3. UV-Vis (1, 2 DCE) λ_{max}: 298 nm, (ε = 4.5×10⁴ M⁻¹ cm⁻¹).

Synthesis of Bis(trimethylsilylethynyl) thienylethynyl Derivatives (7-9)

Compound 7: An oven dried Schlenk flask were charged with dialkynyl derivative **O1** (0.31 g, 1.43 mmol), 5-iodo-2-ethynyl(trimethylsilyl)-3-hexylthiophene **6** (1.17 g, 3.00 mmol, 2.1 eq.), tetrakis(triphenylphosphine) palladium(0) (0.12 g, 0.1 mmol, 3.5 mol%), copper(I) iodide (0.01 g, 0.04 mmol, 3 mol%) and dry DCM/Et₃N (v/v, 2/1). The mixture was stirred at room temperature under argon atmosphere for 12h. After completion of reaction, the reaction mixture was extracted with DCM. The combined organic extracts were washed with water and brine, and then dried over anhydrous MgSO₄. After removal of solvents under reduced pressure, the residue product was purified through column chromatography eluting with 3% ethyl acetate-hexane mixture to afford **7** as yellow oil (0.72 g, 68%). ¹H NMR (600 MHz, CDCl₃) δ (ppm): 7.03 (s, 1H, CH thienyl), 7.00 (s, 2H, CH thienyl), 2.68-2.62 (m, 6H, Th-CH₂-C₅H₁₁), 1.65-1.58 (m, 6H, Th-CH₂-CH₂-C₄H₉), 1.32-1.31 (m, 20H), 0.90-0.84 (m, 12H), 0.26 (s, 18H, SiMe₃). ¹³C {¹H} NMR (150 MHz, CDCl₃) δ (ppm): 148.9, 148.6, 133.4 (CH thienyl), 133.3 (CH thienyl), 133.0 (CH thienyl), 123.2, 122.6, 122.3, 120.8, 120.6, 120.1, 102.8, 102.6, 96.9, 89.8, 87.6, 86.9, 86.2, 31.8, 31.7, 30.2, 30.1, 29.7, 29.6, 29.1, 29.0, 22.8, 14.3, 0.1 (SiMe₃). MALDI-TOF (m/z): C₄₄H₆₀S₃Si₂, calculated value 740.339 (M⁺), found 740.749 (M⁺).

Compound 8: Compound **8** was prepared by similar procedure to that for **7**. From **O3** (0.4 g, 0.67 mmol), 5-iodo-2-ethynyl(trimethylsilyl)-3-hexylthiophene **6** (0.55 g, 1.41 mmol, 2.1 eq.), tetrakis(triphenylphosphine) palladium(0) (0.06 g, 0.05 mmol, 3.5 mol%), copper(I) iodide (0.004 g, 0.02 mmol, 3 mol%), **8** was obtained as orange oil (0.53 g, 71%). ¹H NMR (600 MHz, CDCl₃) δ (ppm): 7.05-7.04 (m, 3H, thienyl), 6.99 (s, 2H, thienyl), 2.69-2.62 (m, 10H, Th-CH₂-C₅H₁₁), 1.65-1.60 (m, 10H, Th-CH₂-CH₂-C₄H₉), 1.31 (br, 35H), 0.90-0.87 (m, 18H), 0.26 (s, 18H, SiMe₃). ¹³C{¹H} NMR (150 MHz, CDCl₃) δ (ppm): 148.9, 148.6, 133.5, 133.3, 133.1, 133.0, 123.4, 123.2, 123.1, 122.6, 122.5, 120.6, 120.2, 120.1, 120.0, 102.7, 96.9, 89.9, 89.8, 87.6, 87.5, 86.9, 86.3, 86.2, 31.8, 31.7, 30.3, 30.2, 30.1, 29.8, 29.7, 29.6, 29.0, 22.8, 14.3, 0.1 (SiMe₃). MALDI-TOF (m/z): C₆₈H₈₈S₅Si₂, calculated value 1121.511 (M+H)⁺, found 1121.271 (M+H)⁺.

Compound 9: Compound **9** was prepared by similar procedure to that for **8**. From **O5** (0.2 g, 0.20 mmol), 5-iodo-2-ethynyl(trimethylsilyl)-3-hexylthiophene **6** (0.17 g, 0.42 mmol, 2.1 eq.), tetrakis(triphenylphosphine) palladium(0) (0.02 g, 0.01 mmol, 3.5 mol%), copper(I) iodide (0.001 g, 0.01 mmol, 3 mol%), **9** was obtained as orange red oil (0.2 g, 68%). ¹H NMR (600 MHz, CDCl₃) δ (ppm): 7.05-7.04 (m, 5H, CH thienyl), 6.99 (s, 2H, CH thienyl), 2.70-2.63 (m, 14H, Th-CH₂-C₅H₁₁), 1.66-1.61 (m, 14H, Th-CH₂-CH₂-C₄H₉), 1.33-1.32 (m, 51H), 0.91-0.88 (m, 25H), 0.26 (s, 18H, SiMe₃). ¹³C {¹H} NMR (150 MHz, CDCl₃) δ(ppm): 148.9, 148.7, 148.6, 133.5 (CH thienyl), 133.3 (CH thienyl), 133.2 (CH thienyl), 133.0 (CH thienyl), 123.5, 123.4, 123.3, 123.2, 122.6, 120.6, 120.1, 120.0, 119.9, 102.7, 96.9, 89.9, 87.6, 86.9, 86.3, 31.8, 31.8, 31.7, 30.3, 30.2, 30.1, 29.8, 29.7, 29.6, 29.1, 22.8, 14.3, 0.1 (SiMe₃). MALDI-TOF (m/z): C₉₂H₁₁₆S₇Si₂, calculated value 1501.674 (M+H)⁺, found 1501.431 (M+H)⁺.

Synthesis of the thienylethynyl derivatives O3, O5, O7: To a solution of **7** (0.5 g, 0.67 mmol) in DCM (10 mL) and methanol (10 mL) was added potassium carbonate (0.23 g, 1.68 mmol). The reaction mixture was allowed to stir at room temperature for 2h before being poured into water. The aqueous layer was extracted with DCM and the organic extracts were washed with brine. The combined organic layers were dried over anhydrous MgSO₄. The final product was purified by column chromatography using 5% ethyl acetate-hexane mixture to afford **O3** (0.36 g, 91%) as orange-yellow oil. ¹H NMR (600 MHz, CDCl₃) δ (ppm): 7.04 (s, 1H, CH thienyl), 7.02 (s, 1H, CH thienyl), 7.01 (s, 1H, CH thienyl), 3.49 (s, 2H, -C≡CH) 2.68-2.64 (m, 6H, CH₂-C₅H₁₁), 1.63-1.60 (m, 6H, CH₂-CH₂-C₄H₉), 1.32-1.30 (m, 25H), 0.90-0.88 (m, 12H). ¹³C {¹H} NMR (150 MHz, CDCl₃) δ (ppm): 149.3, 148.7, 133.5 (CH thienyl), 133.2 (CH thienyl), 133.0 (CH thienyl), 123.8, 122.1, 120.1, 119.4, 119.2, 119.1, 89.6, 87.4, 86.9, 86.3, 84.7, 84.6, 84.0 (-C≡CH), 76.4 (-C≡CH), 76.1, 31.8, 30.2, 29.7, 29.6, 29.5, 29.1, 29.0, 22.6, 14.3. MALDI-TOF (m/z): C₃₈H₄₄S₃, calculated value 596.260 (M⁺), found 596.642 (M⁺). UV-Vis (1,2-DCE) λ_{max}: 393 nm, (ε = 5.03 × 10⁴ M⁻¹ cm⁻¹).

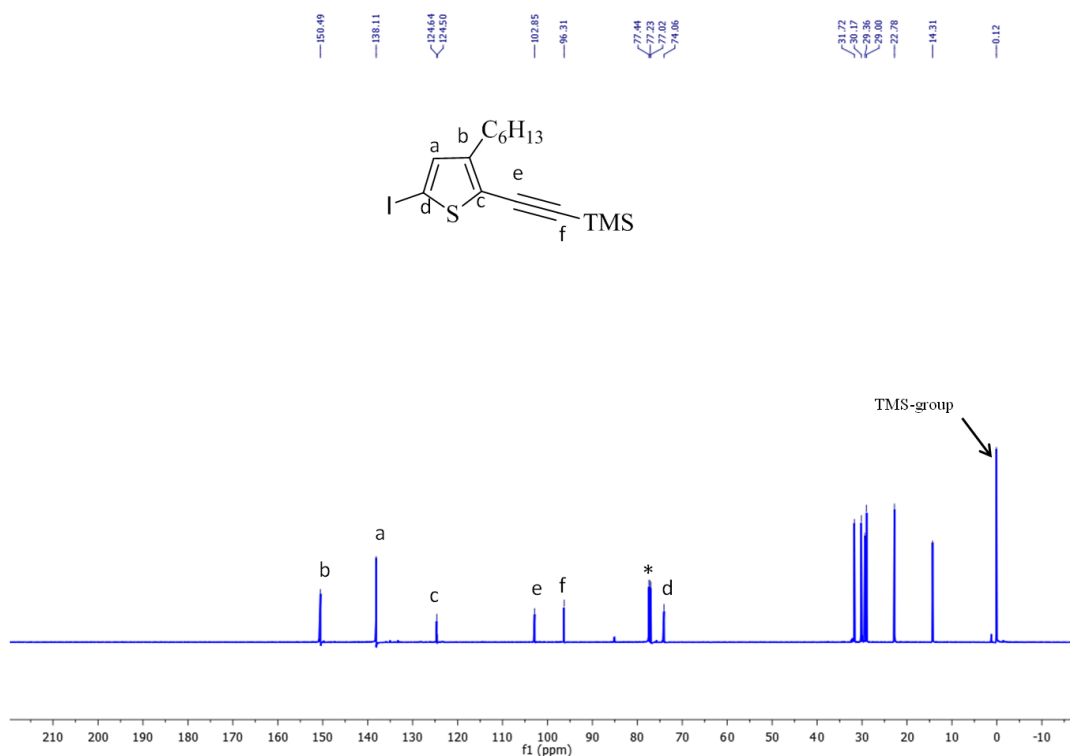
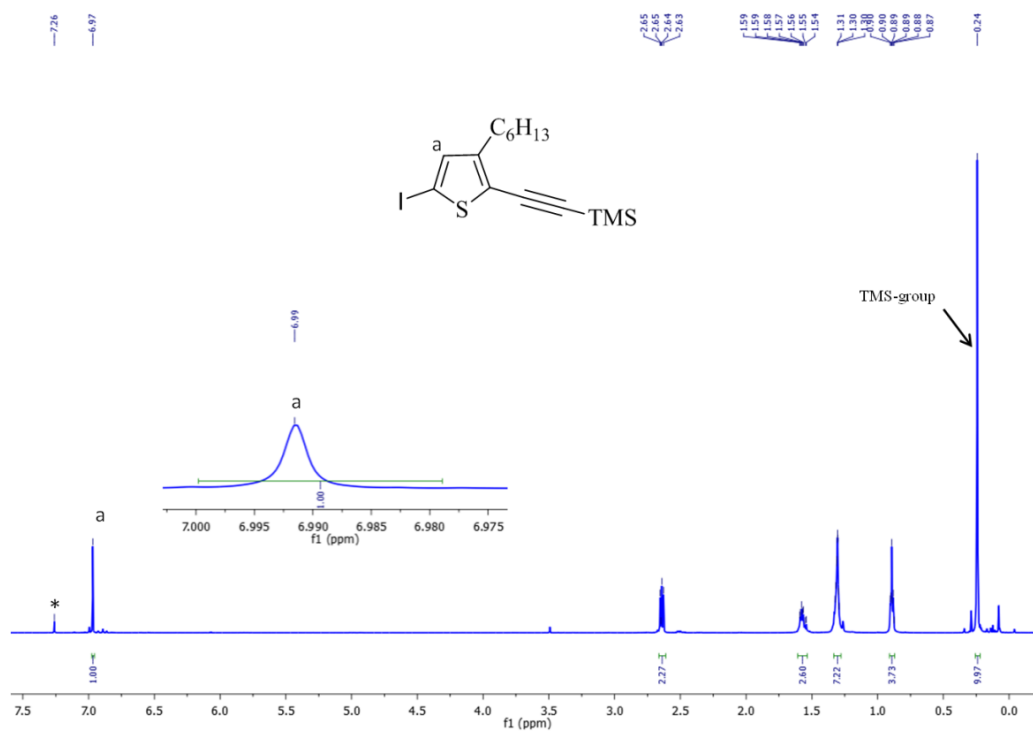
Compound O5: Compound **O5** was prepared by an analogues method to that for **O3**. From **8** (0.18 g 0.16 mmol) and potassium carbonate (0.06 g, 0.4 mmol), **O5** was obtained as orange oil (0.15 g, 94%). ¹H NMR (600 MHz, CDCl₃) δ (ppm): 7.05-7.04 (m, 3H, CH thienyl), 7.01 (s, 2H, CH thienyl), 3.49 (s, 2H, -C≡CH), 2.70-2.64 (m, 10H, CH₂-C₅H₁₁), 1.66-1.60 (m, 10H, CH₂-CH₂-C₄H₉), 1.32-1.31 (m, 42H), 0.90-0.86 (m, 20H). ¹³C {¹H} NMR (150 MHz, CDCl₃) δ (ppm): 149.3, 148.7, 133.6 (CH thienyl), 133.5 (CH thienyl), 133.3 (CH thienyl), 133.0 (CH thienyl), 132.9 (CH thienyl), 123.4, 123.2, 123.1, 122.9, 122.8, 120.1, 120.0, 119.9, 119.3, 119.2, 89.8, 89.6, 89.5, 87.6,

87.5, 86.9, 86.4, 86.3, 84.6 (-C≡CH), 76.4 (-C≡CH), 31.8, 30.3, 30.2, 29.8, 29.7, 29.6, 29.5, 29.1, 29.0, 22.8, 14.3. MALDI-TOF (m/z): C₆₂H₇₂S₅, calculated value 976.423 (M⁺), found 976.449 (M⁺). UV-Vis (1,2-DCE) λ_{max}: 412 nm, (ε = 5.72×10⁴ M⁻¹ cm⁻¹).

Compound O7: Compound **O7** was prepared by an analogues method to that for **O3**. From **9** (0.2 g 0.13 mmol) and potassium carbonate (0.05 g, 0.36 mmol), **O7** was obtained as dark red oil (0.16, 92%). ¹H NMR (600 MHz, CDCl₃) δ (ppm): 7.05-7.04 (m, 5H, CH thienyl), 7.01 (s, 2H, CH thienyl), 3.49 (s, 2H, -C≡CH), 2.70-2.65 (m, 14H, CH₂-C₅H₁₁), 1.65-1.60 (m, 14H, CH₂-CH₂-C₄H₉), 1.32-1.30 (m, 75H), 0.90-0.87 (m, 29H). ¹³C {¹H} NMR (150 MHz, CDCl₃) δ (ppm): 149.3, 148.7, 133.6 (CH thienyl), 133.3 (CH thienyl), 133.2 (CH thienyl), 133.0 (CH thienyl), 132.9 (CH thienyl), 123.5, 123.4, 123.2, 122.9, 120.1, 120.0, 119.9, 119.8, 119.3, 89.8, 89.7, 89.6, 87.6, 87.0, 86.4, 84.6 (-C≡CH), 76.1 (-C≡CH), 32.1, 31.8, 30.3, 30.2, 29.8, 29.9, 29.7, 29.6, 29.5, 29.0, 22.9, 22.8, 14.3. MALDI-TOF (m/z): C₈₆H₁₀₀S₇, calculated value 1356.587 (M⁺), found 1356.629 (M⁺). UV-Vis (1,2-DCE) λ_{max}: 432 nm, (ε = 6.59×10⁴ M⁻¹ cm⁻¹).

Compound 13. A mixture of **12** (0.16 g, 0.14 mmol), phenylacetylene(0.02 g, 0.17 mmol), NaPF₆ (0.03 g, 0.17 mmol) and Et₃N (1 mL) in dry DCM (10 mL) were stirred at room temperature for 16h. The solution was filtered through Schlenk frit containing activated Celite 545 to remove NaCl by-product and unreacted NaPF₆, if any. The solvent was evaporated to dryness. First the residue was washed with diethyl-ether to remove the excess phenylacetylene. Finally it was purified by column chromatography (silica gel) using 30% ethyl acetate-hexane mixture eluent in inert atmosphere to afford **13** (0.13 g, 79%) as .yellow solid. ¹H NMR (600 MHz, CDCl₃) δ (ppm): 7.96-7.94 (m, 10H, Ph of dppe), 7.24-7.2 (m, 5H, Ph of dppe+Ph of phenylacetynyl), 7.14-7.08 (m, 14H, Ph of dppe+Ph of phenylacetynyl), 7.04-6.82 (m, 19H+H, Ph of dppe+Ph of phenylacetylene+CH of thienyl) 2.85-2.71 (m, 6H, CH₂ of dppe+Th-CH₂-C₅H₁₁), 2.60-2.52 (m, 4H, CH₂ of dppe) 1.96-1.93 (m, 2H), 1.26-1.15 (m, 5H) 0.83-0.80 (m, 3H). ¹³C {¹H} NMR (150 MHz, CDCl₃,) δ (ppm): 139.4, 135.2, 134.6, 134.1, 129.5, 129.0, 128.5, 127.7, 127.3, 127.2, 127.1, 126.9 (Ru-C≡C-), 32, 31.3 (quint. PCH₂PCH₂, ¹J_{P,C}+³J_{P,C}=24Hz), 30.3, 29.9, 29.6, 28.9, 22.9, 14.4.. ³¹P {¹H} NMR (162 MHz, CDCl₃,) δ (ppm): 54 .8 (s, dppe). FTIR (KBr, cm⁻¹): ν̄(Ru-C≡C)= 2025. HRMS-ESI (m/z): C₆₈H₆₆NP₄SRu, calculated value 1154.2910 (M-Ph+CH₃CN)⁺, found 1154.2993(M-Ph+CH₃CN)⁺.

1b. NMR Spectra



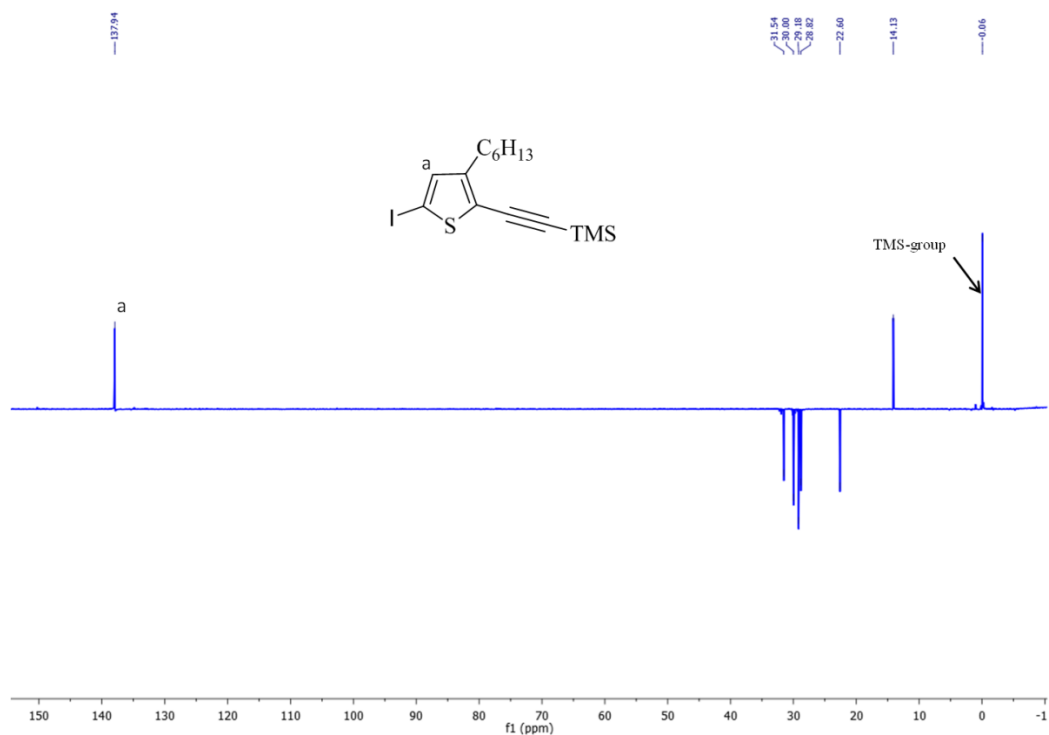


Fig. S1c: DEPT-135 (100MHz, CDCl₃) spectrum of **6**

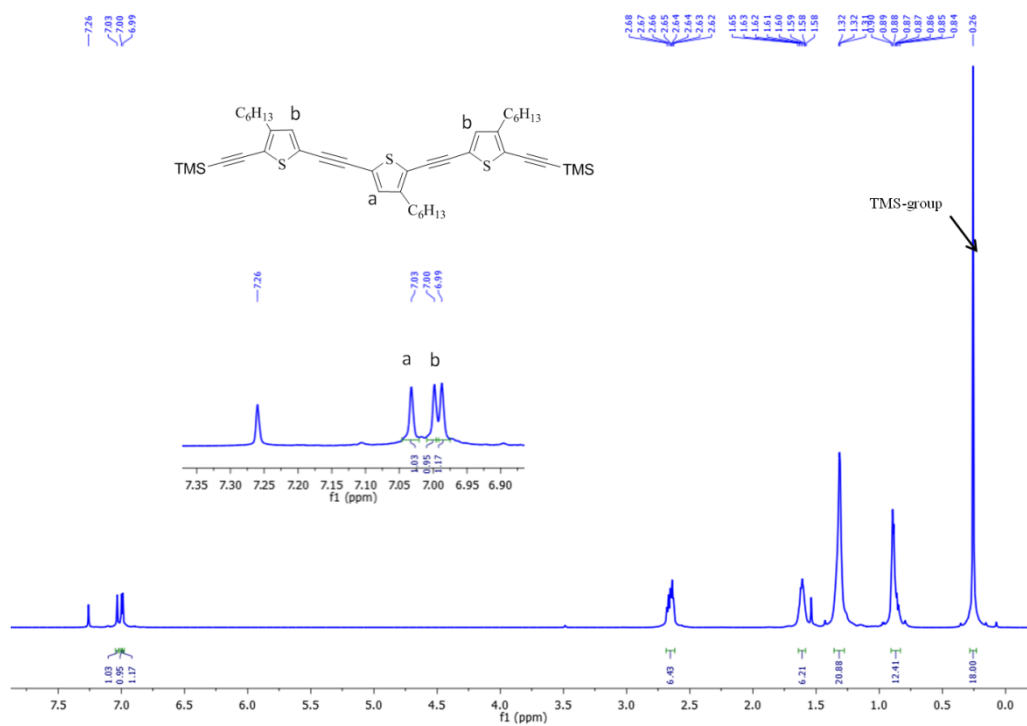


Fig. S2a: ¹H-NMR (600MHz, CDCl₃) spectrum of **7**

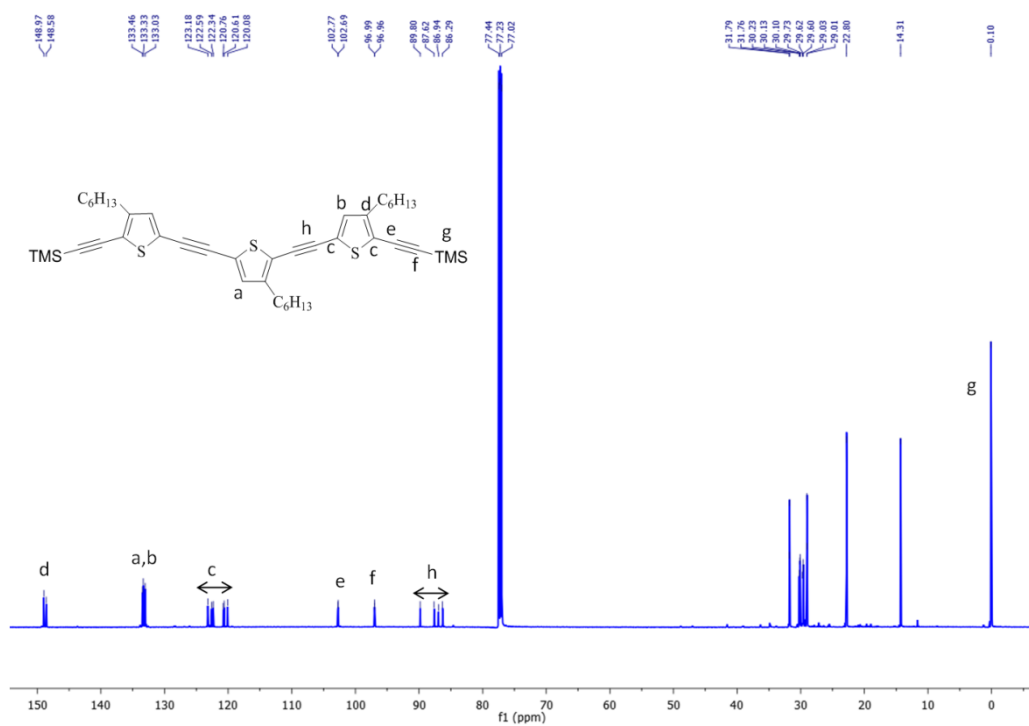


Fig. S2b: ¹³C{¹H}-NMR (150MHz, CDCl₃) spectrum of **7**

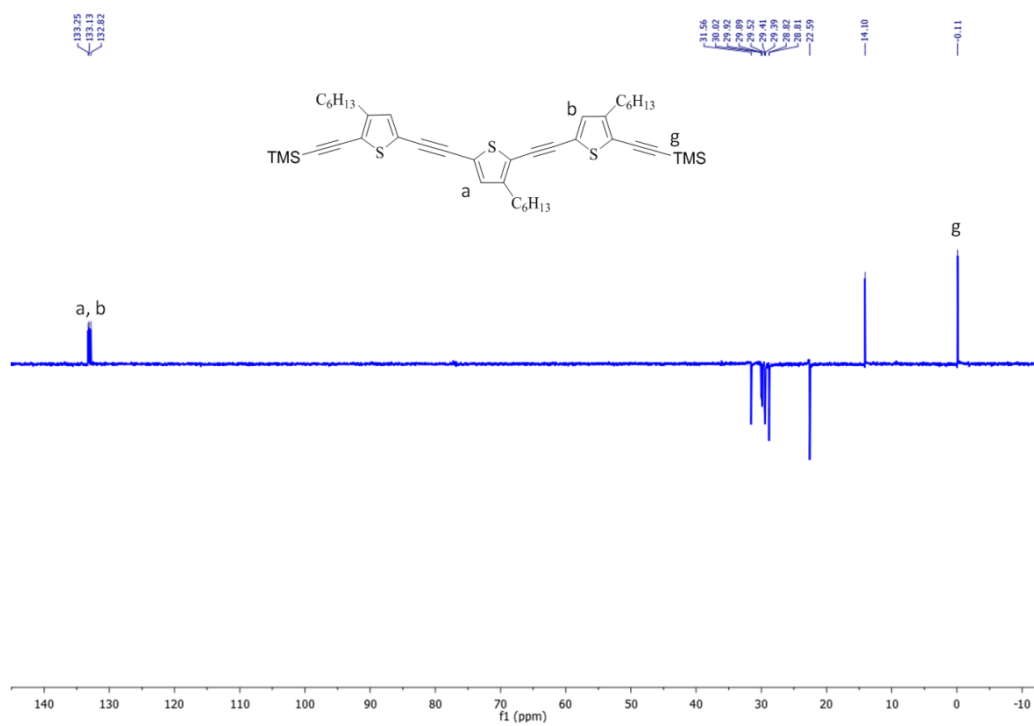


Fig. S2c: DEPT-135 (150MHz, CDCl₃) spectrum of **7**

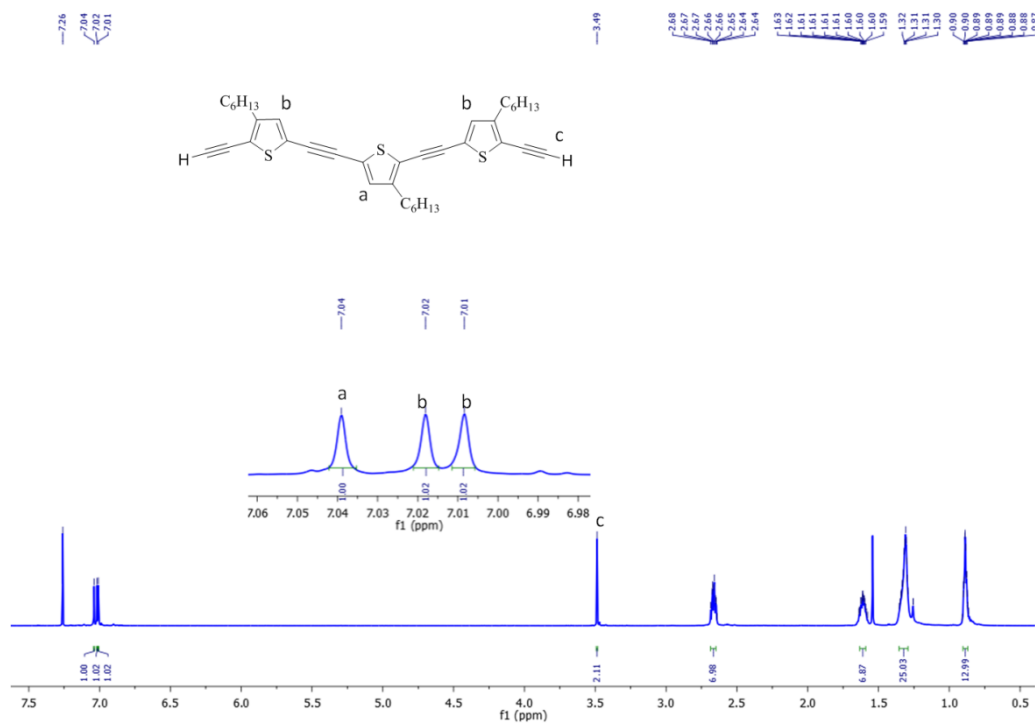


Fig. S3a: $^1\text{H-NMR}$ (600 MHz, CDCl_3) spectrum of **O3**

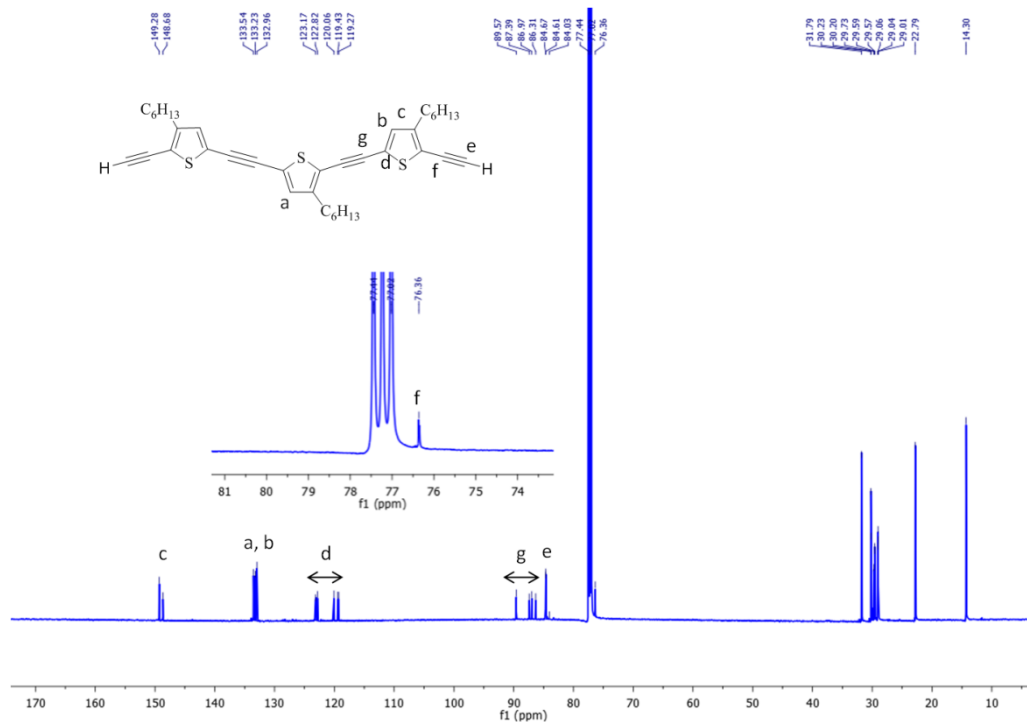


Fig. S3b: $^{13}\text{C}\{^1\text{H}\}\text{-NMR}$ (150 MHz, CDCl_3) spectrum of **O3**

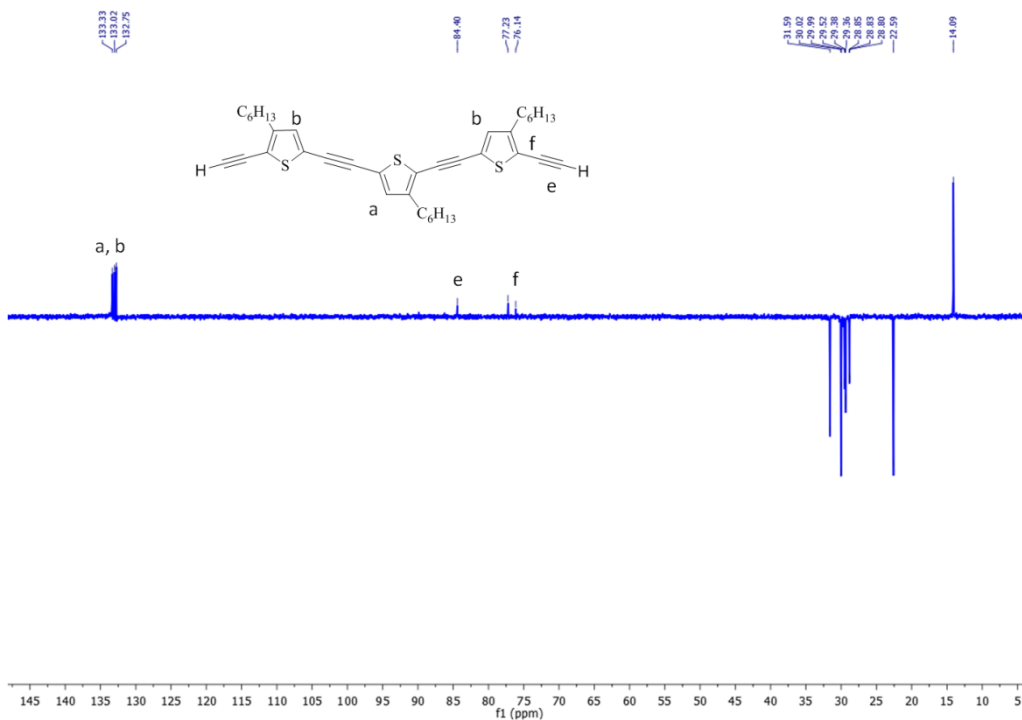


Fig. S3c: DEPT-135 (150MHz, $CDCl_3$) spectrum of **O3**

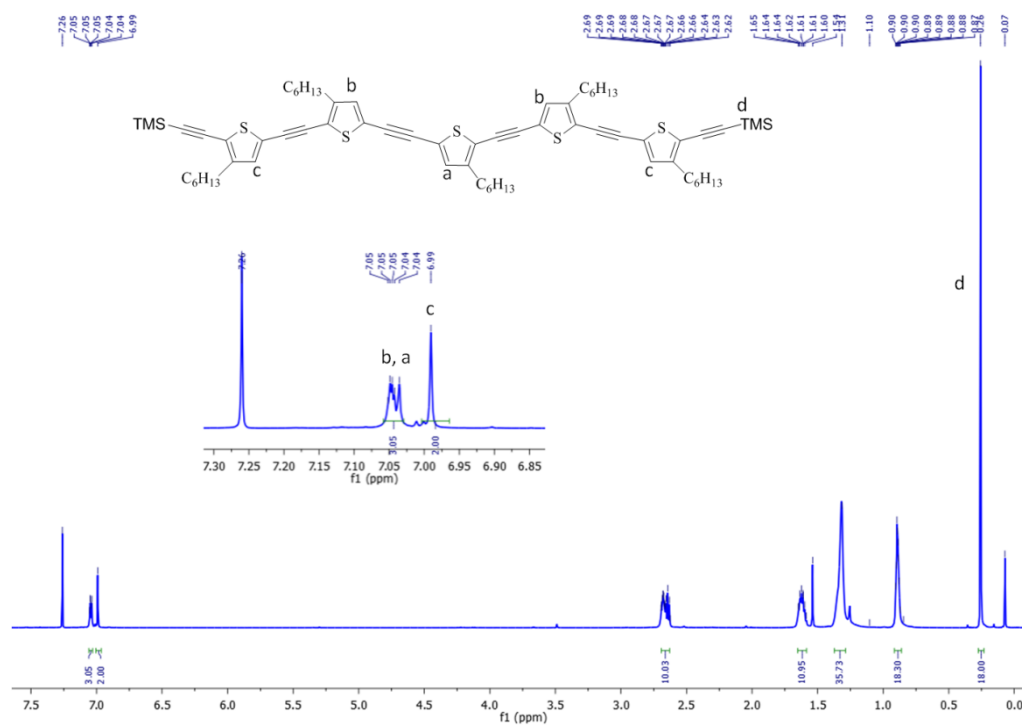


Fig. S4a: 1H -NMR (600MHz, $CDCl_3$) spectrum of **8**

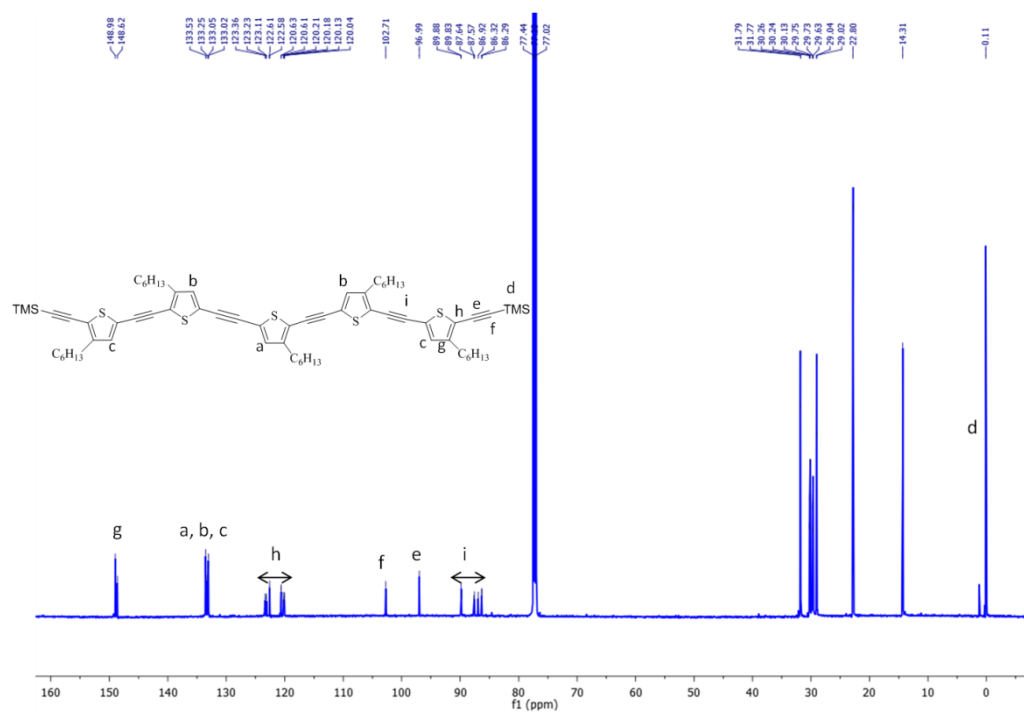


Fig. S4b: $^{13}\text{C}\{^1\text{H}\}$ -NMR (150MHz, CDCl_3) spectrum of **8**

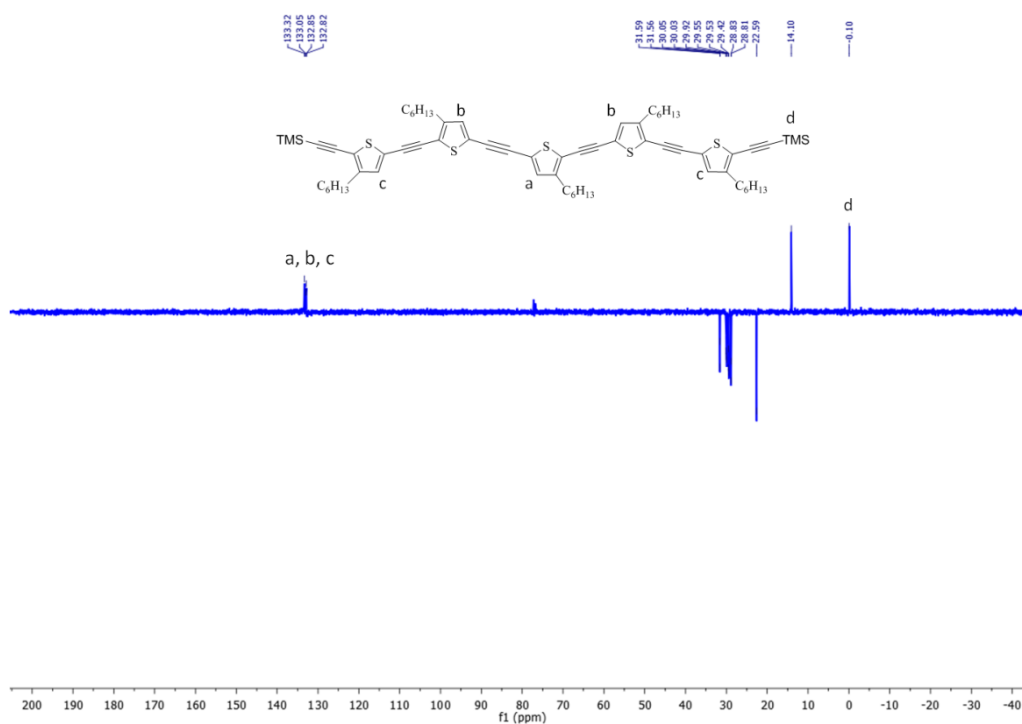


Fig. S4c: DEPT-135 (150MHz, CDCl_3) spectrum of **8**

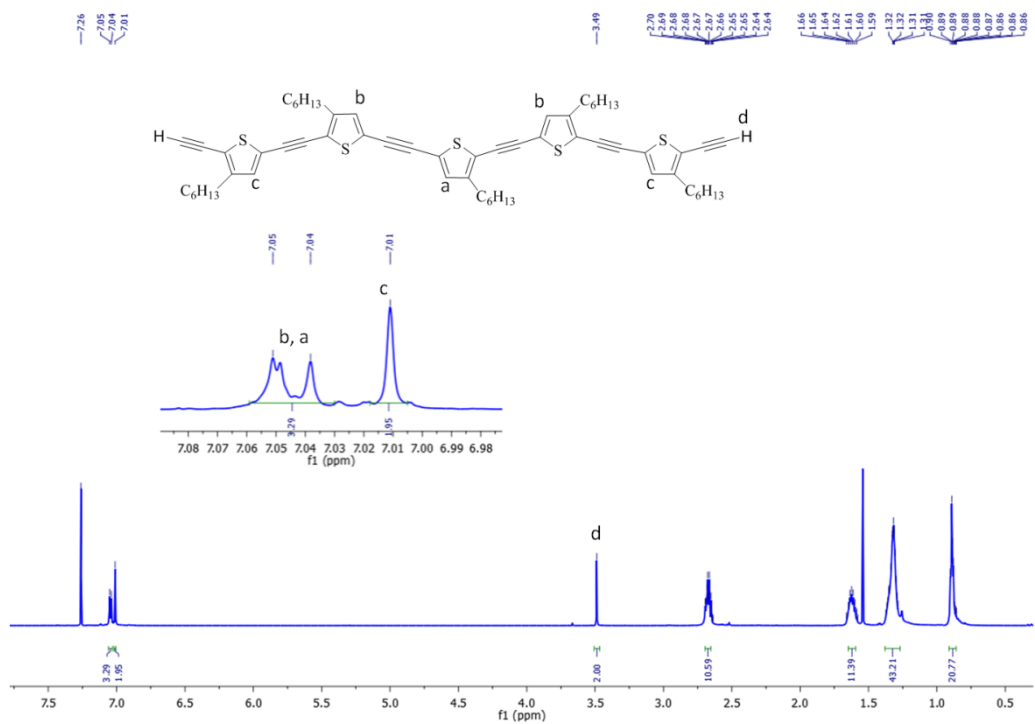


Fig. S5a: ¹H-NMR (600MHz, CDCl₃) spectrum of **O5**

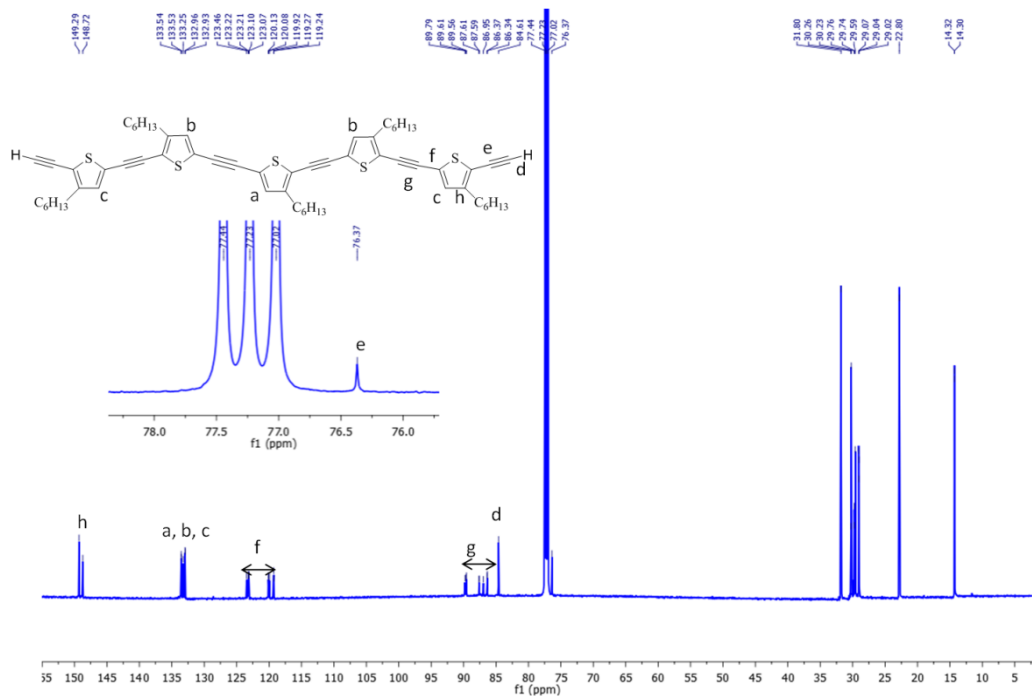


Fig. S5b: ¹³C{¹H}-NMR (150MHz, CDCl₃) spectrum of **O5**

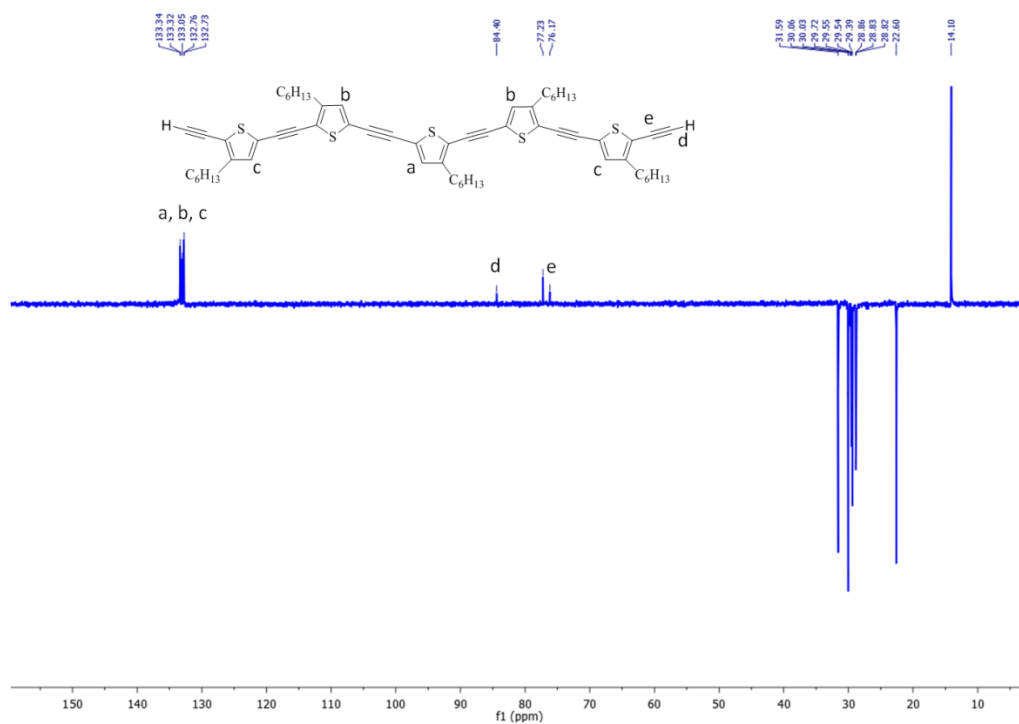


Fig. S5c: DEPT-135 (150MHz, CDCl₃) spectrum of **O5**

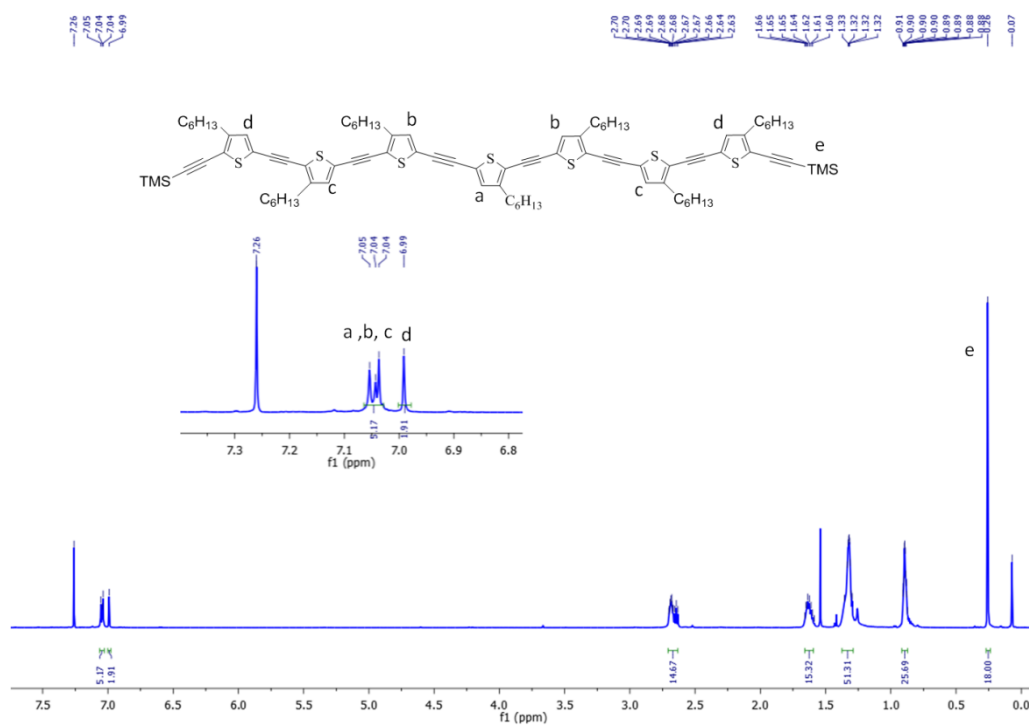


Fig. S6a: ¹H-NMR (600MHz, CDCl₃) of **9**

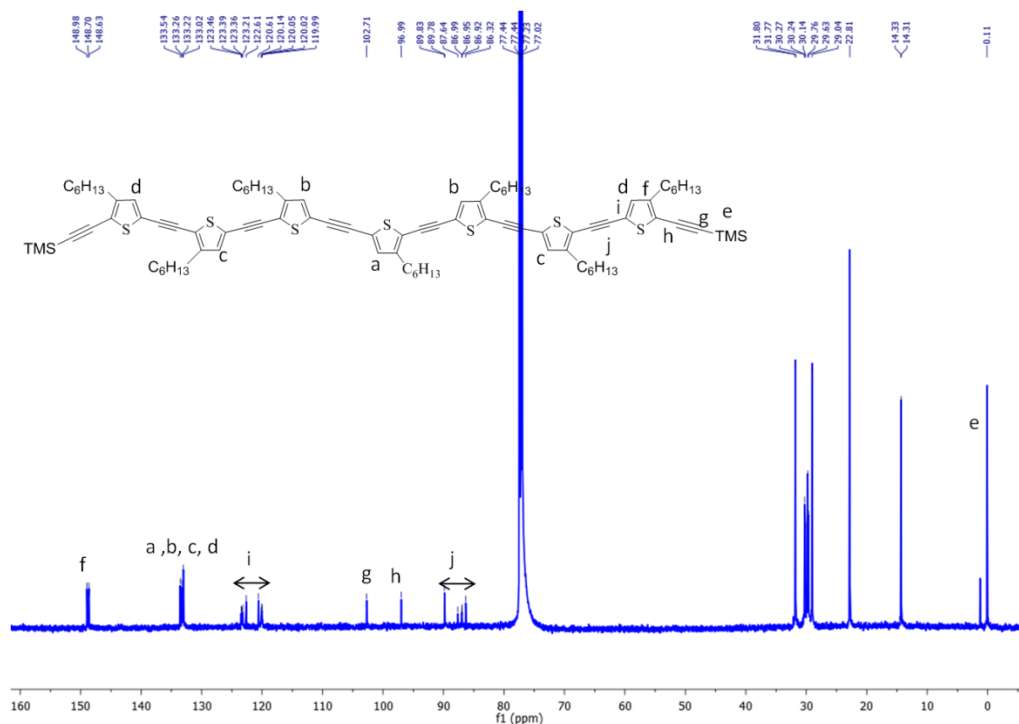


Fig. S6b: $^{13}\text{C}\{^1\text{H}\}$ -NMR (150MHz, CDCl_3) spectrum of **9**

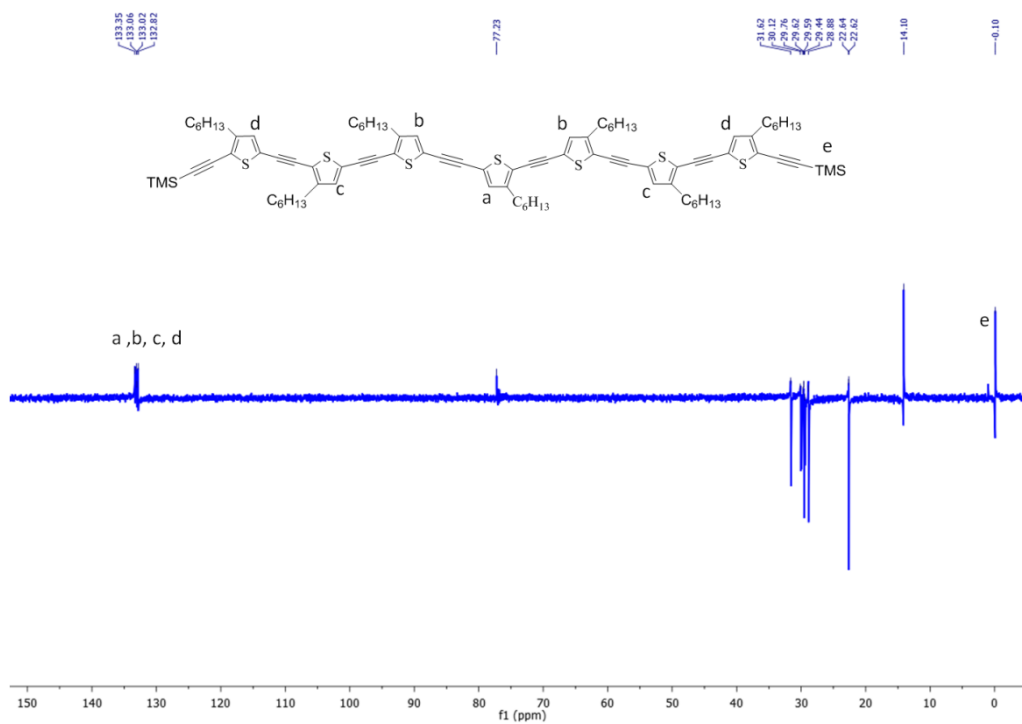


Fig. S6c: DEPT-135 (150MHz, CDCl_3) spectrum of **9**

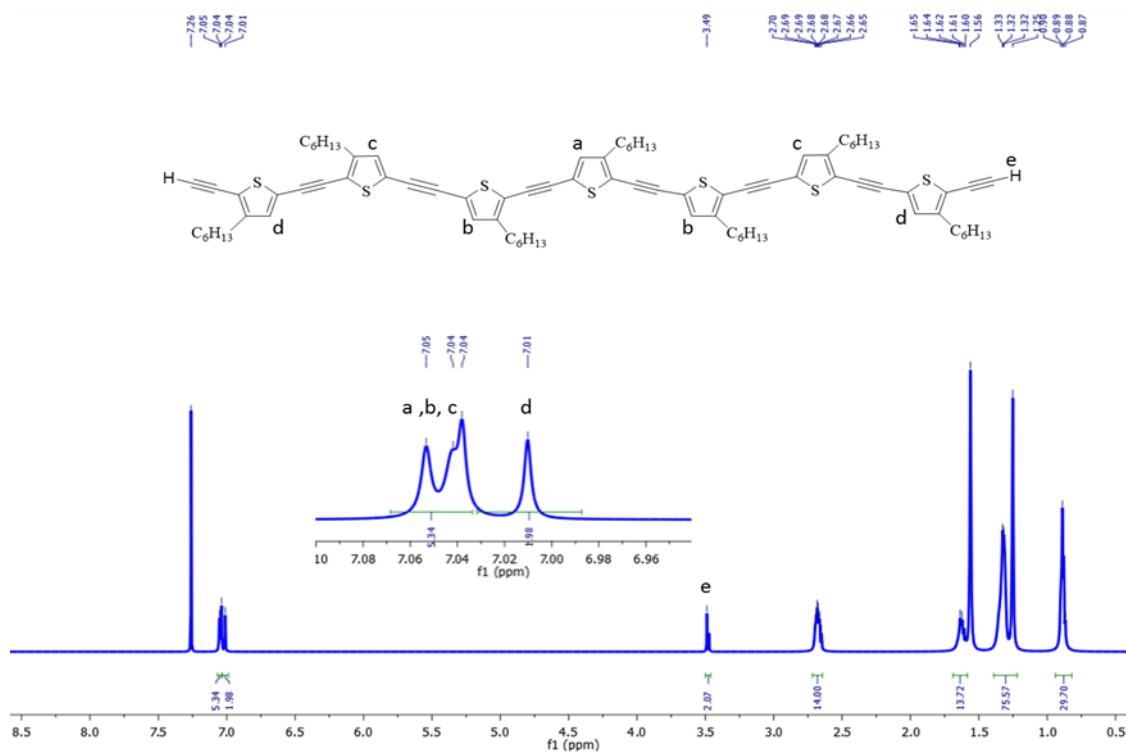


Fig. S7a: ¹H-NMR (600MHz, CDCl₃) spectrum of **O7**

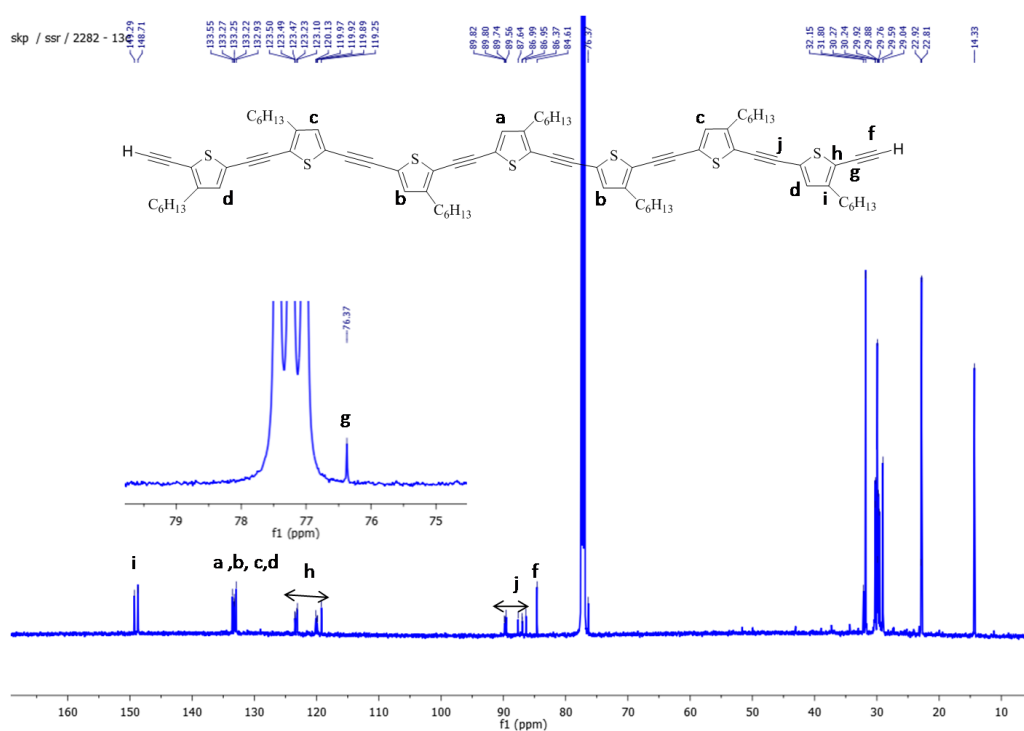


Fig. S7b: ¹³C{¹H}-NMR (150MHz, CDCl₃) spectrum of **O7**

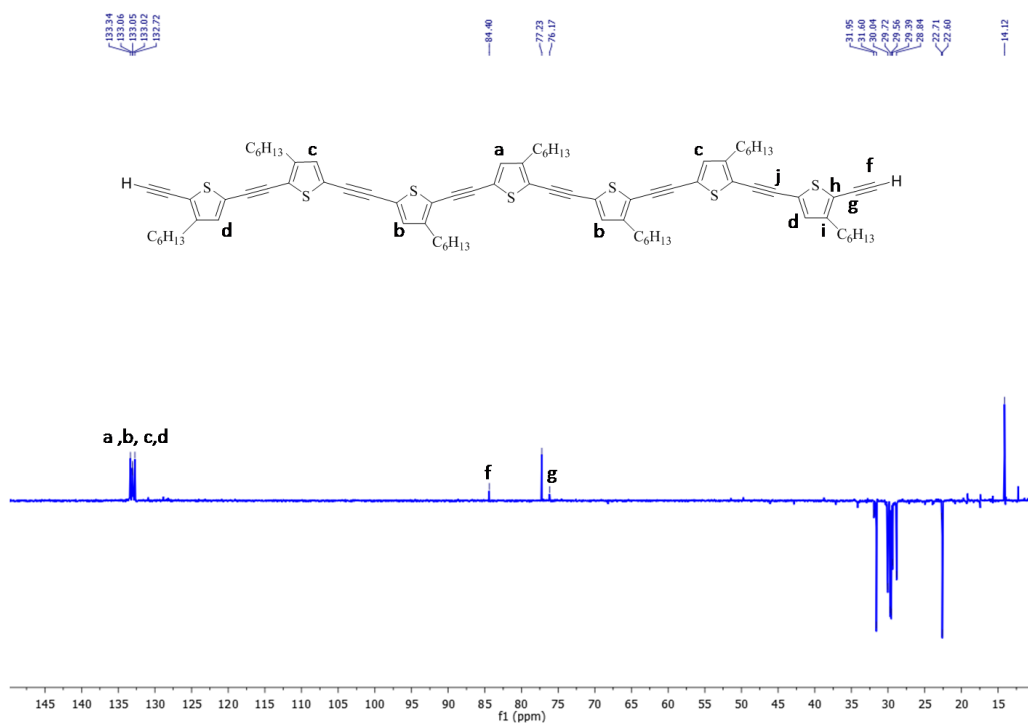


Fig. S7c: DEPT-135 (150MHz, CDCl_3) spectrum of **O7**

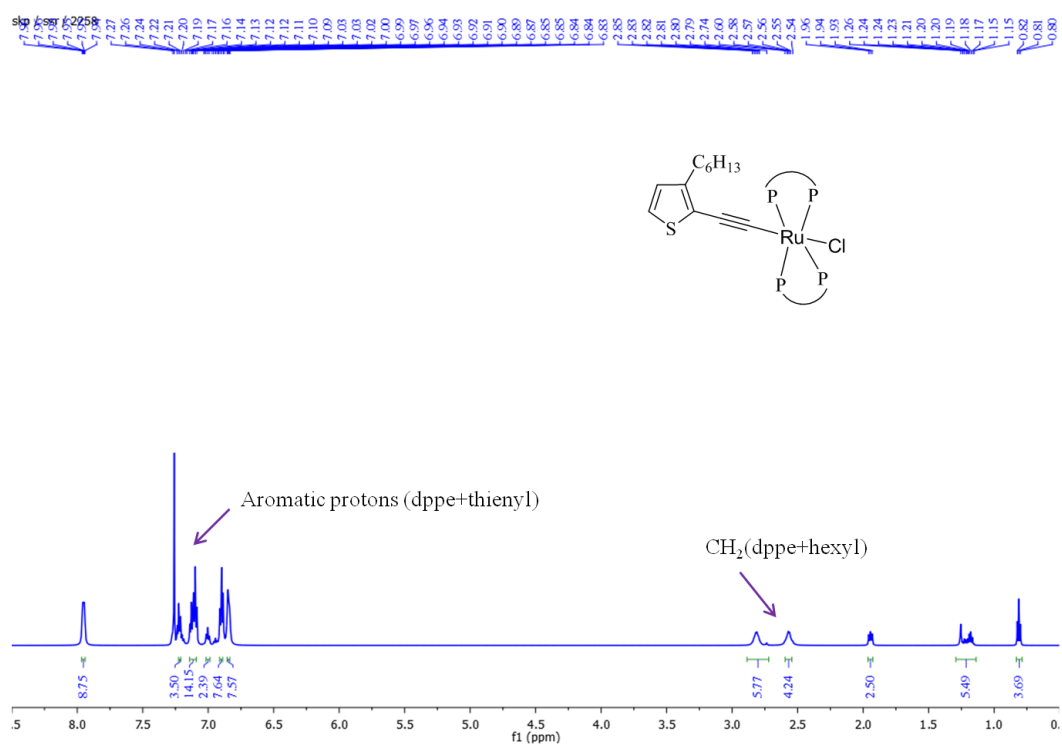


Fig. S8a: ^1H -NMR (600MHz, CDCl_3) spectrum of **12**

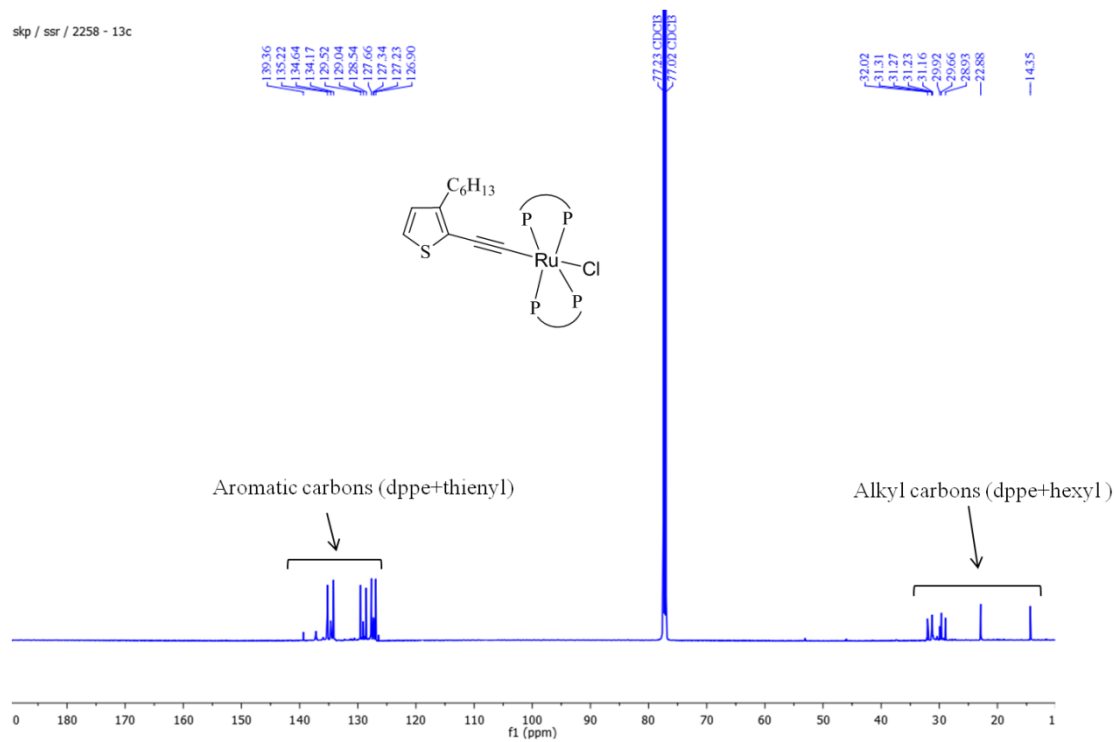


Fig. S8b: $^{13}\text{C}\{^1\text{H}\}$ -NMR (150MHz, CDCl_3) spectrum of **12**

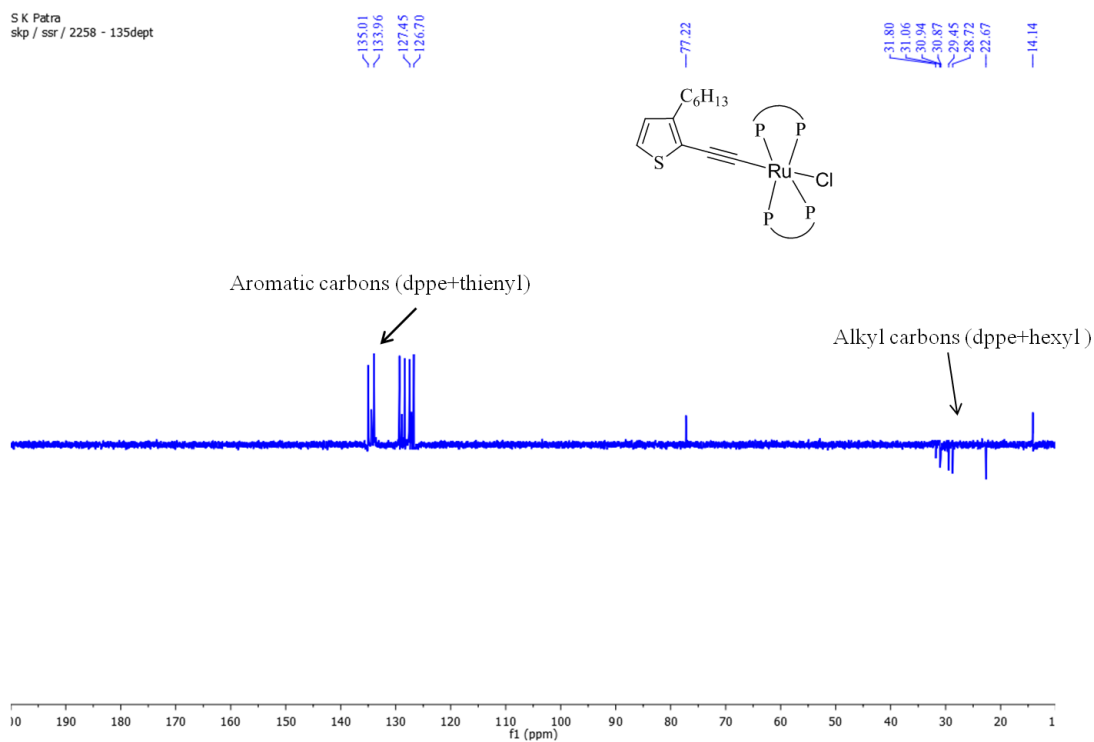


Fig. S8c: DEPT-135 (150MHz, CDCl_3) spectrum of **12**

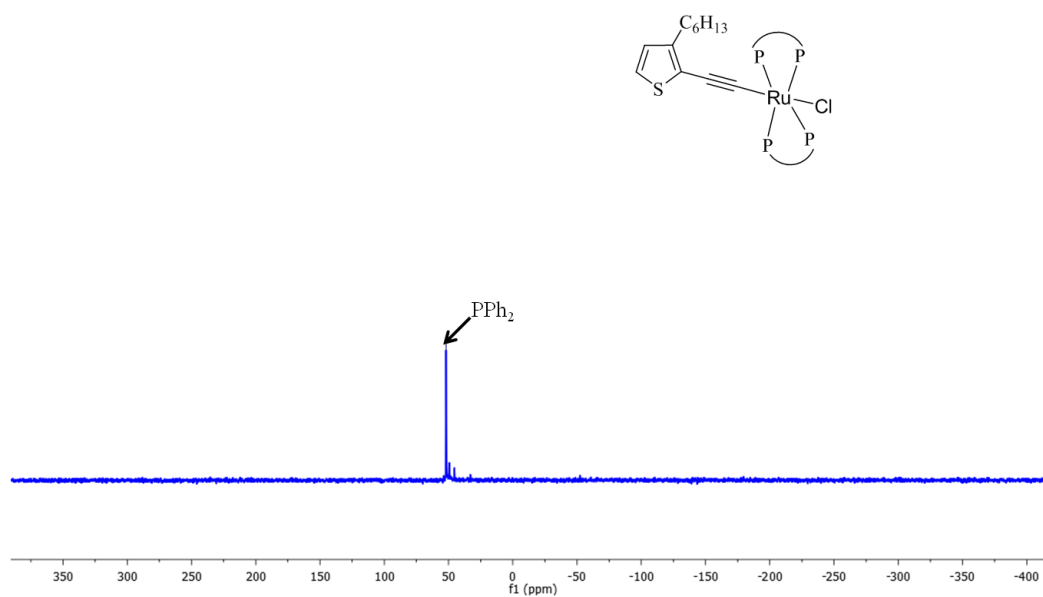


Fig. S8d: $^{31}\text{P}\{^1\text{H}\}$ -NMR (162MHz, CDCl_3) spectrum of **12**

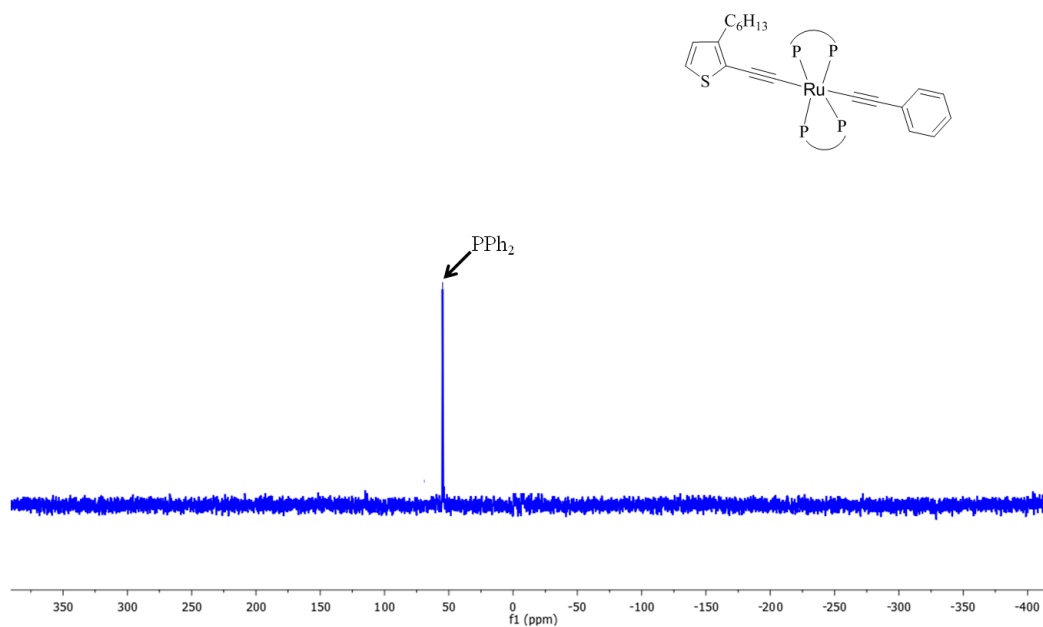


Fig. S9a: $^{31}\text{P}\{^1\text{H}\}$ -NMR (162MHz, CDCl_3) spectrum of **13**

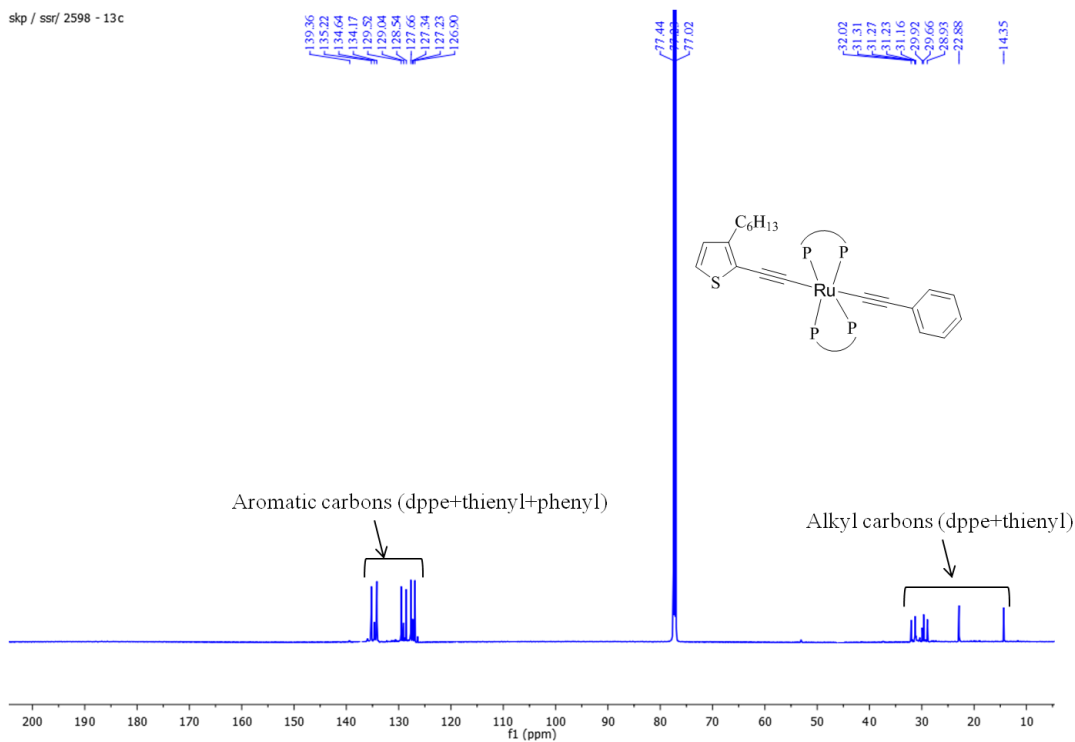


Fig. S9b: ¹³C{¹H}-NMR (150MHz, CDCl₃) spectrum of **13**

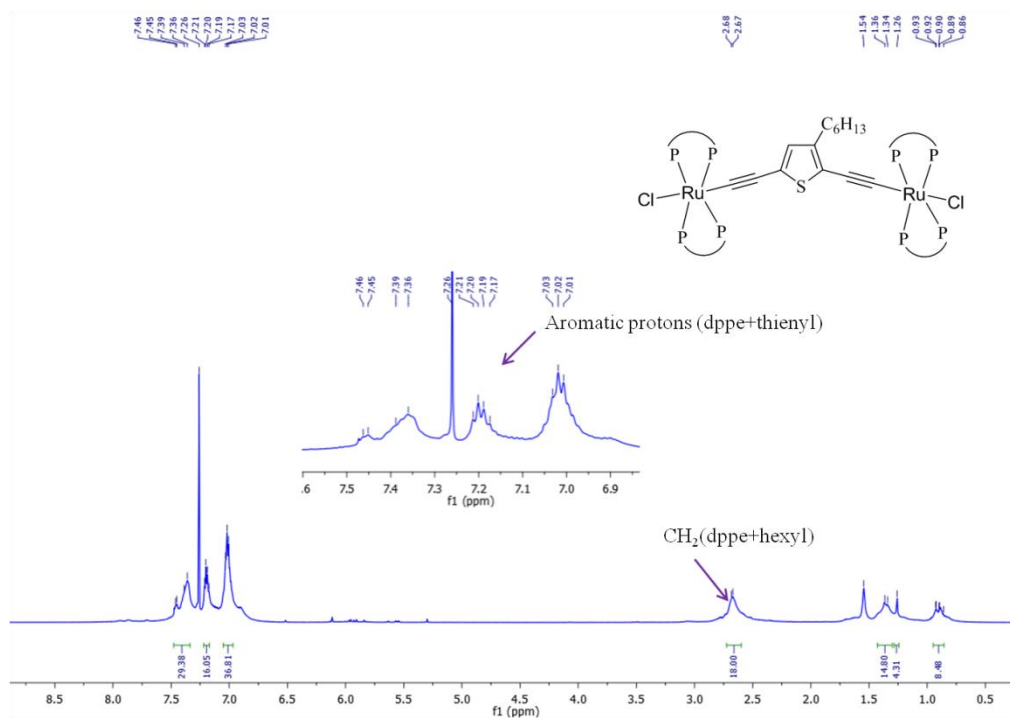


Fig. S10a: ¹H-NMR (600MHz, CDCl₃) spectrum of **O1-Ru₂**

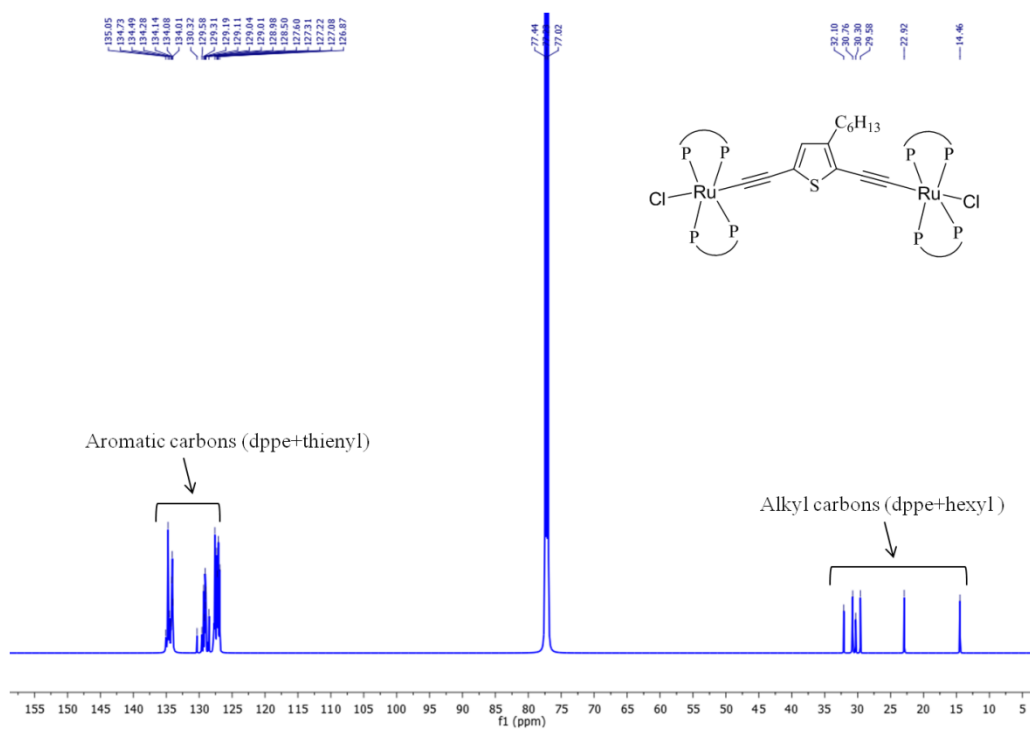


Fig. S10b: $^{13}\text{C}\{^1\text{H}\}$ -NMR (150MHz, CDCl_3) spectrum of **O1-Ru₂**

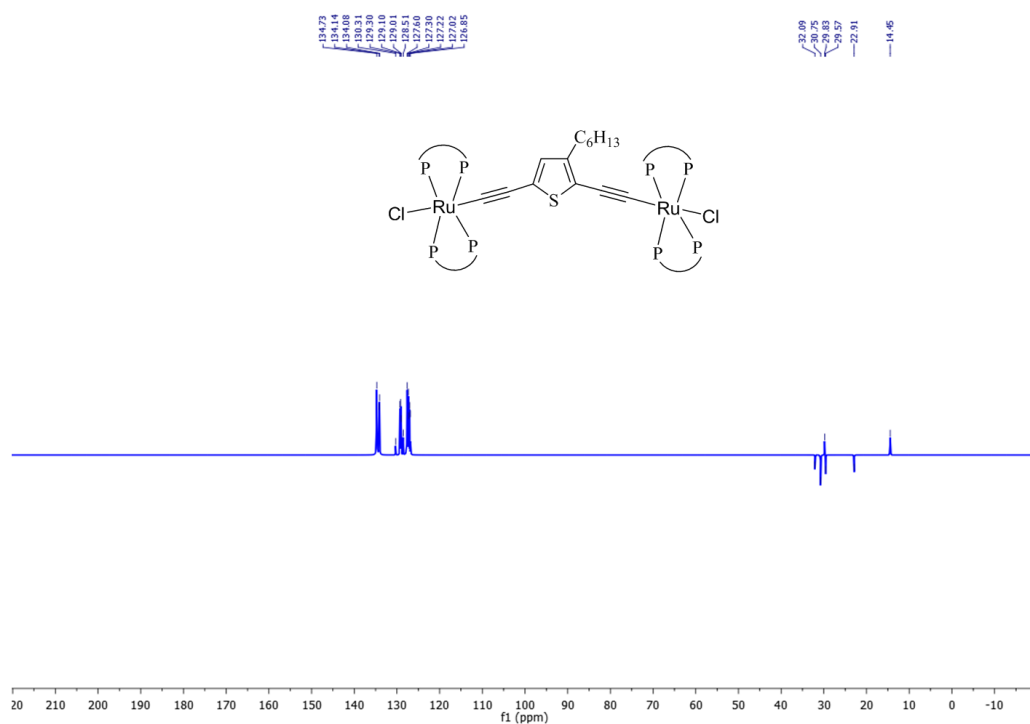


Fig. S10c: DEPT-135 (150MHz, CDCl_3) spectrum of **O1-Ru₂**

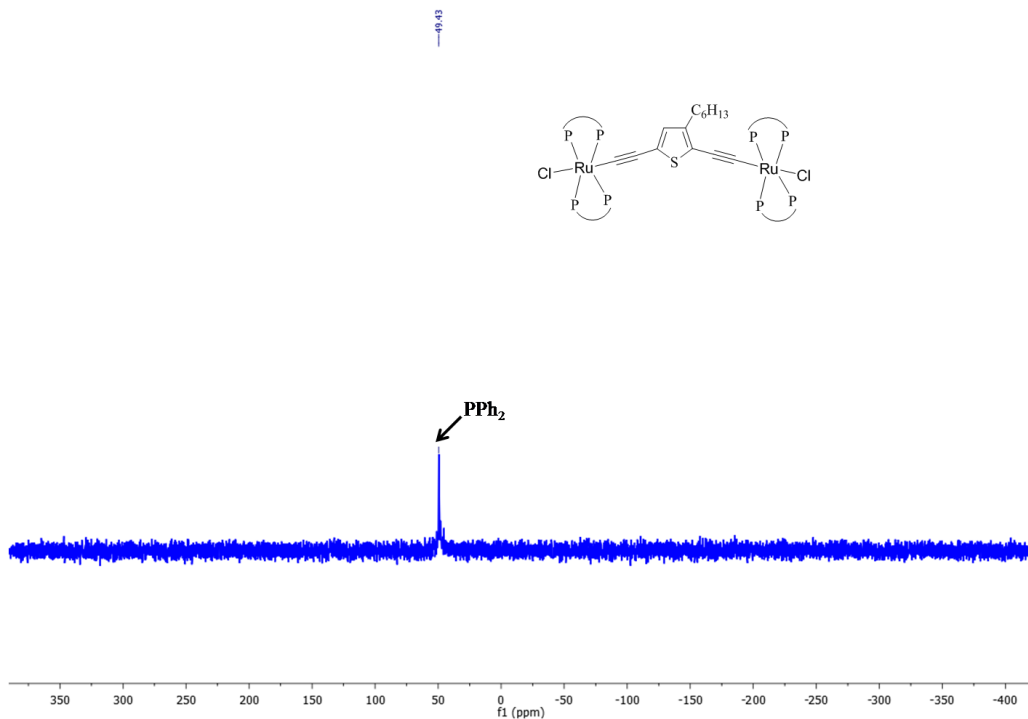


Fig. S10d: $^{31}\text{P}\{^1\text{H}\}$ -NMR (162MHz, CDCl_3) spectrum of **O1-Ru2**

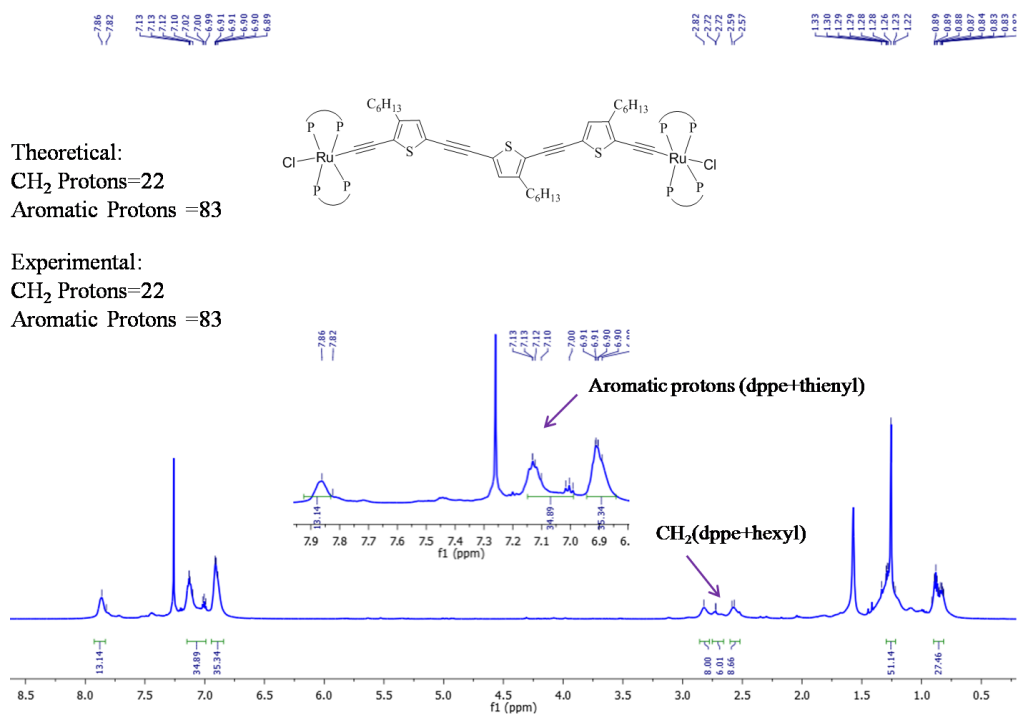


Fig. S11a: $^1\text{H-NMR}$ (600MHz, CDCl_3) spectrum of **O3-Ru₂**

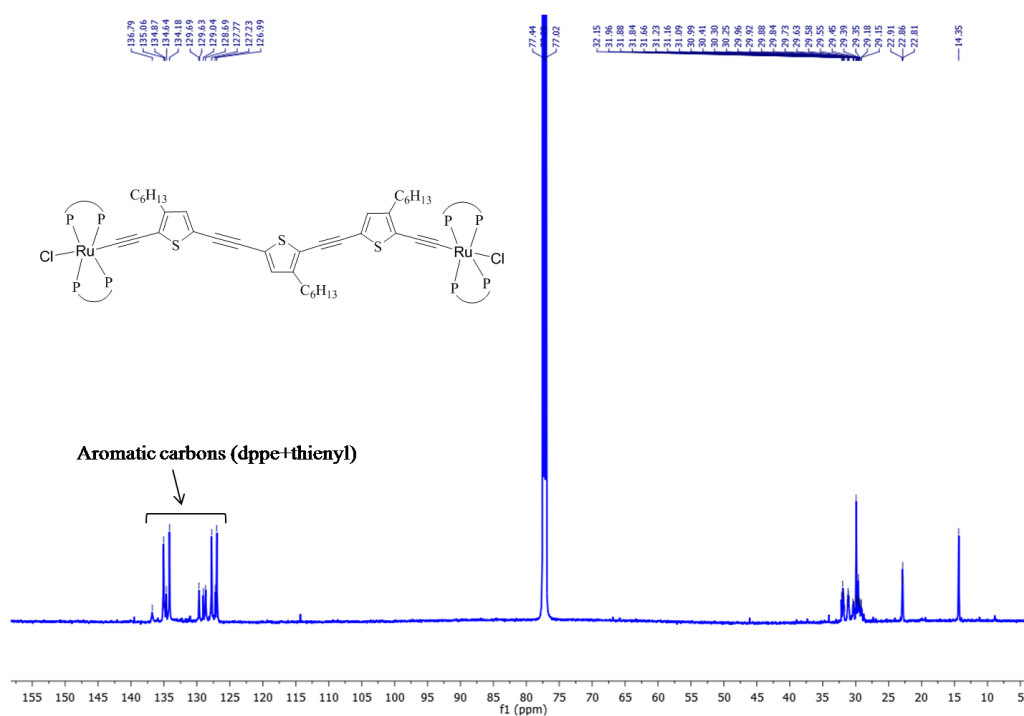


Fig. S11b: $^{13}\text{C}\{^1\text{H}\}$ -NMR (150MHz, CDCl_3) spectrum of **O3-Ru₂**

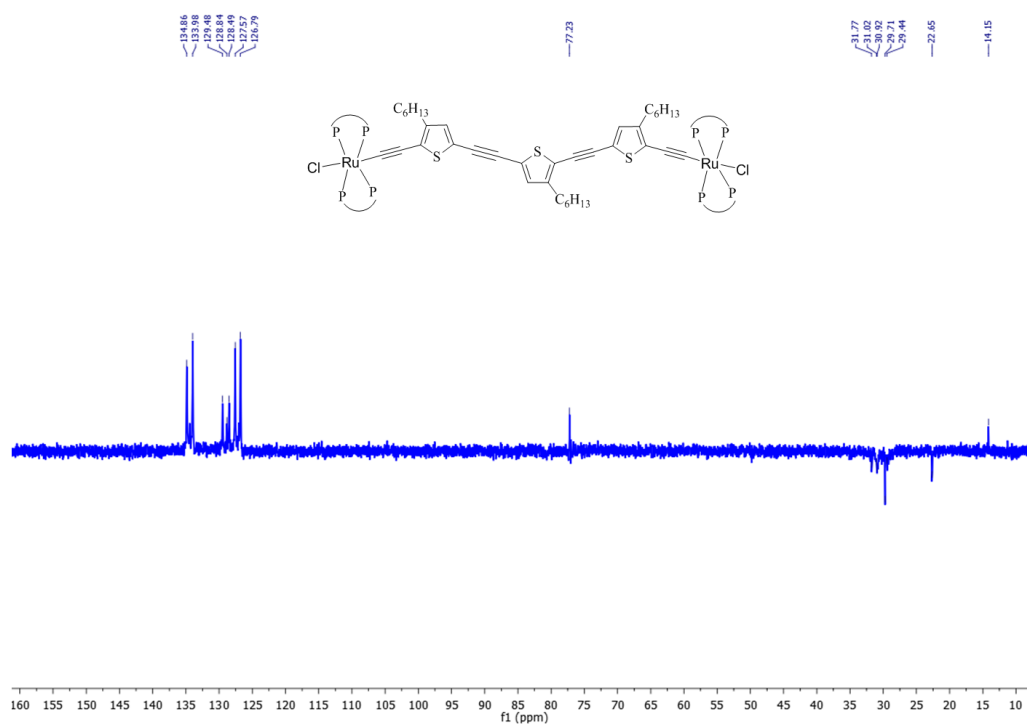


Fig. S11c: DEPT-135 (150MHz, CDCl_3) spectrum of **O3-Ru₂**

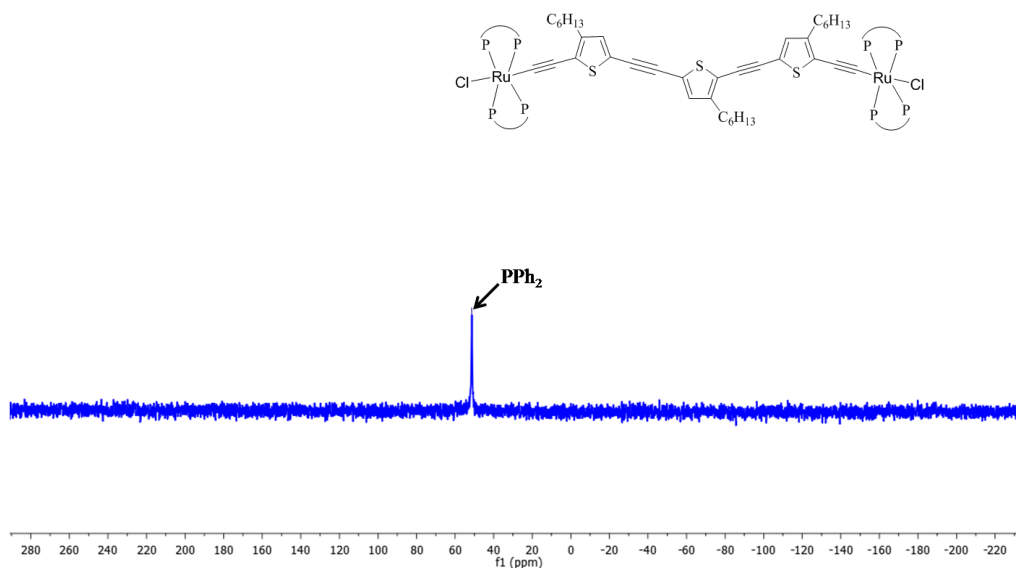


Fig. S11d: ³¹P{¹H}-NMR (162MHz, CDCl₃) spectrum of **O3-Ru₂**

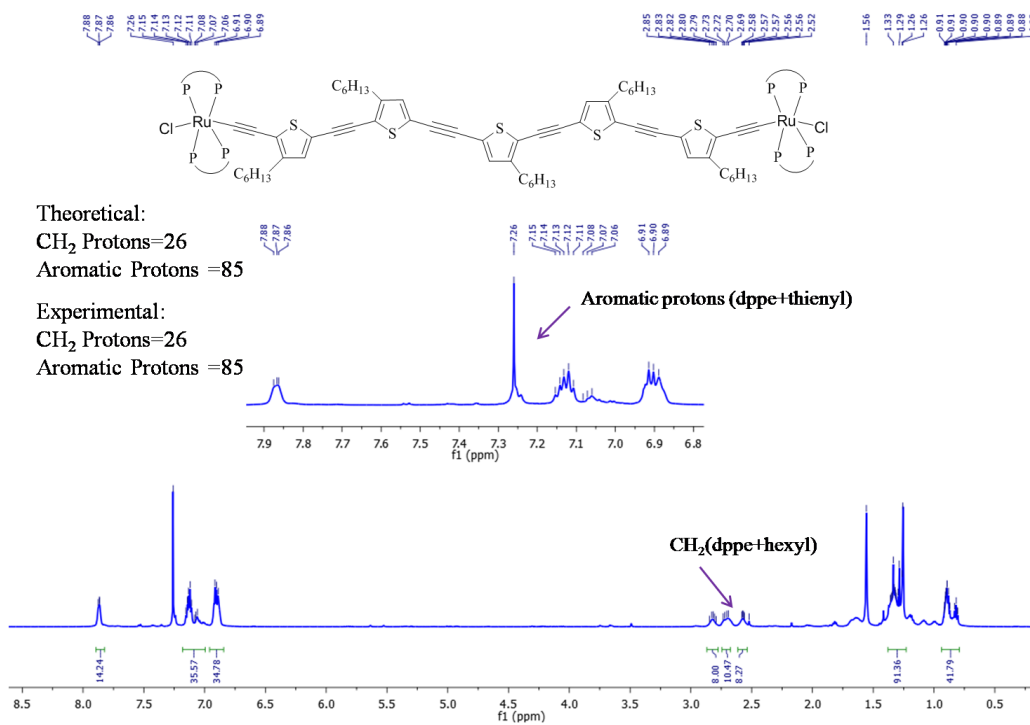


Fig. S12a: ¹H-NMR (600MHz, CDCl₃) spectrum of **O5-Ru₂**

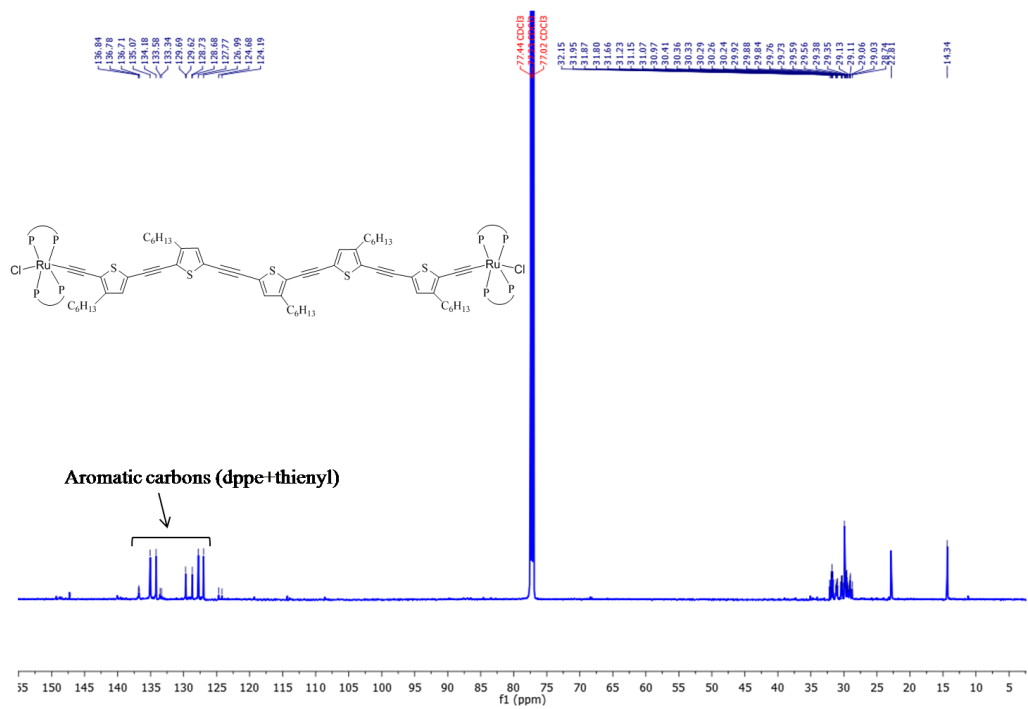


Fig. S12b: ¹³C{¹H}-NMR (150MHz, CDCl₃) spectrum of **O5-Ru₂**

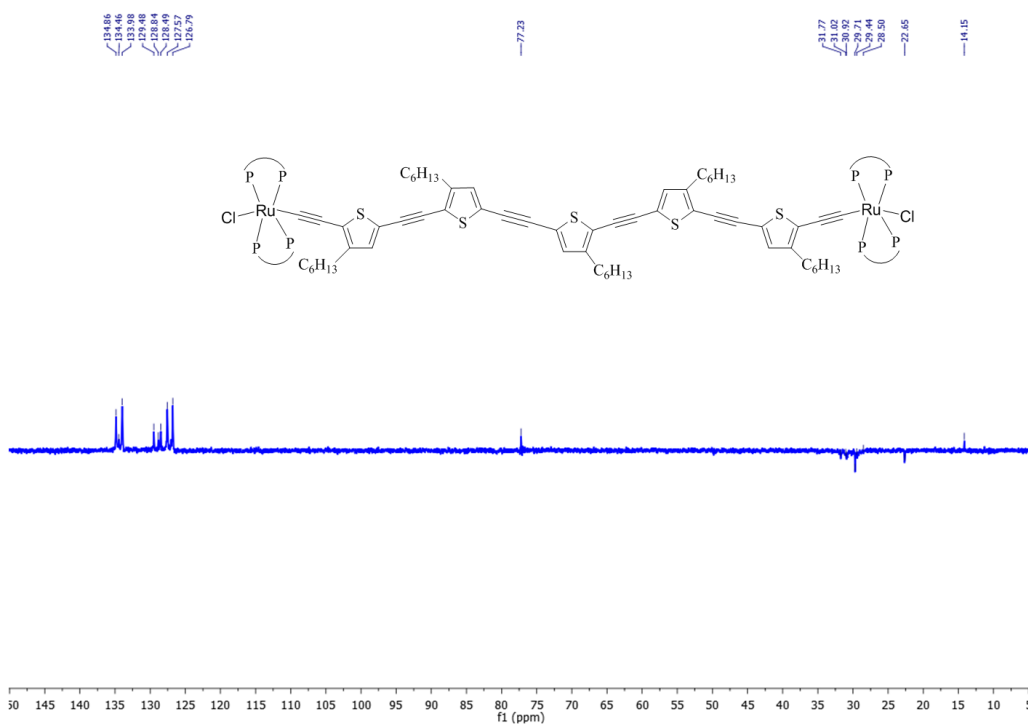


Fig. S12c: DEPT-135 (150MHz, CDCl₃) spectrum of **O5-Ru₂**

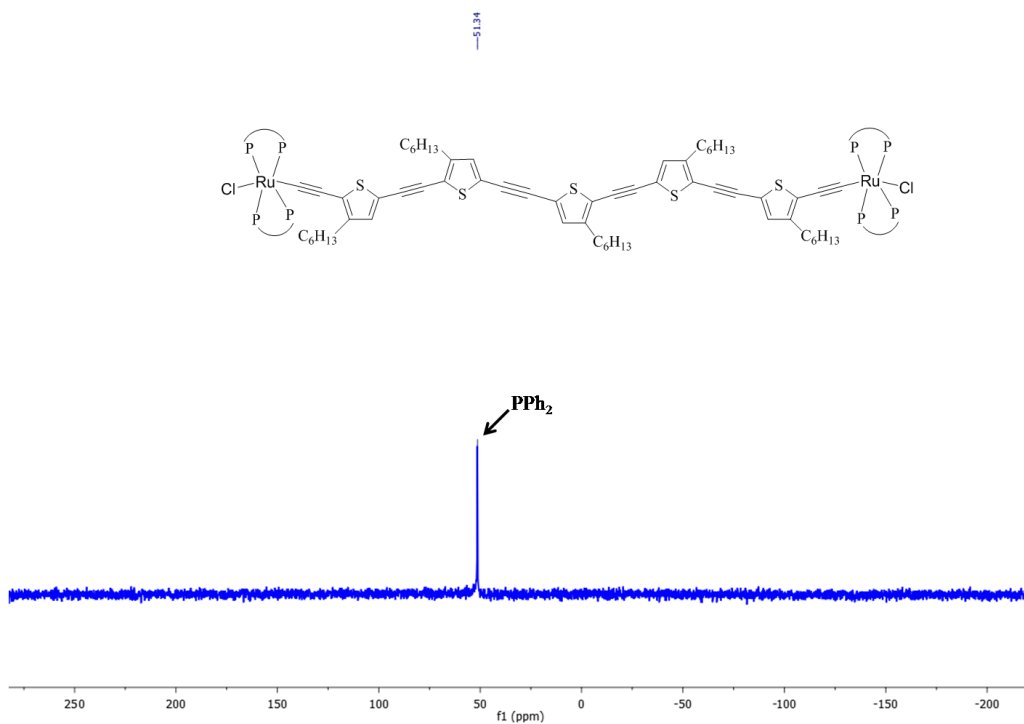


Fig. S12d: $^{31}\text{P}\{^1\text{H}\}$ -NMR (162MHz, CDCl_3) spectrum of **O5-Ru₂**

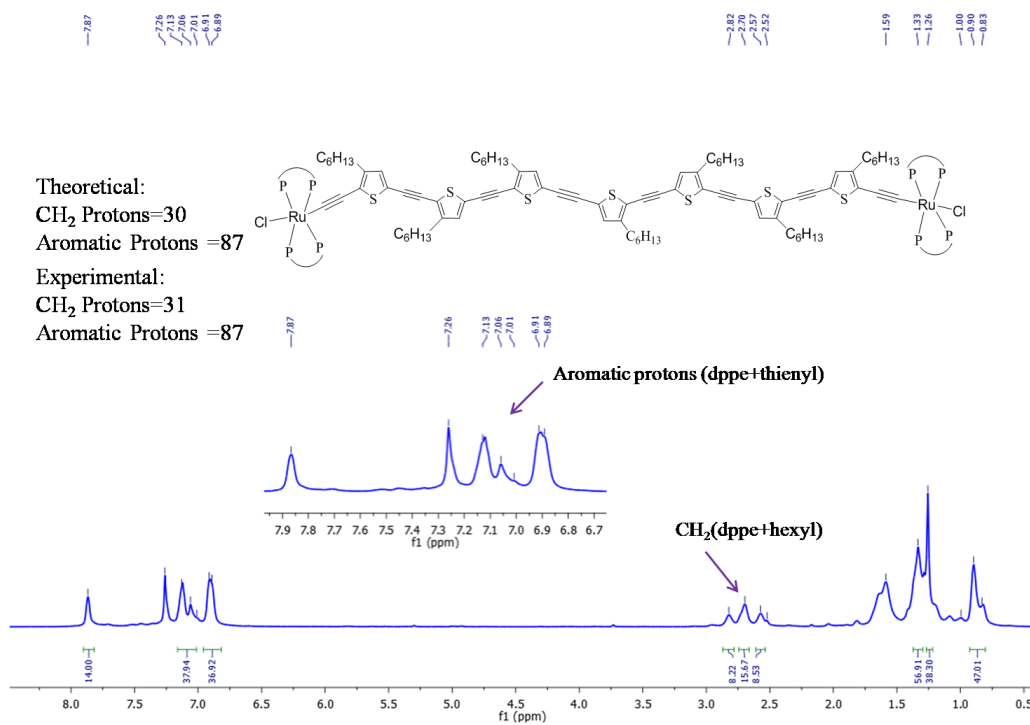


Fig. S13a: ^1H -NMR (600MHz, CDCl_3) spectrum of **O7-Ru₂**

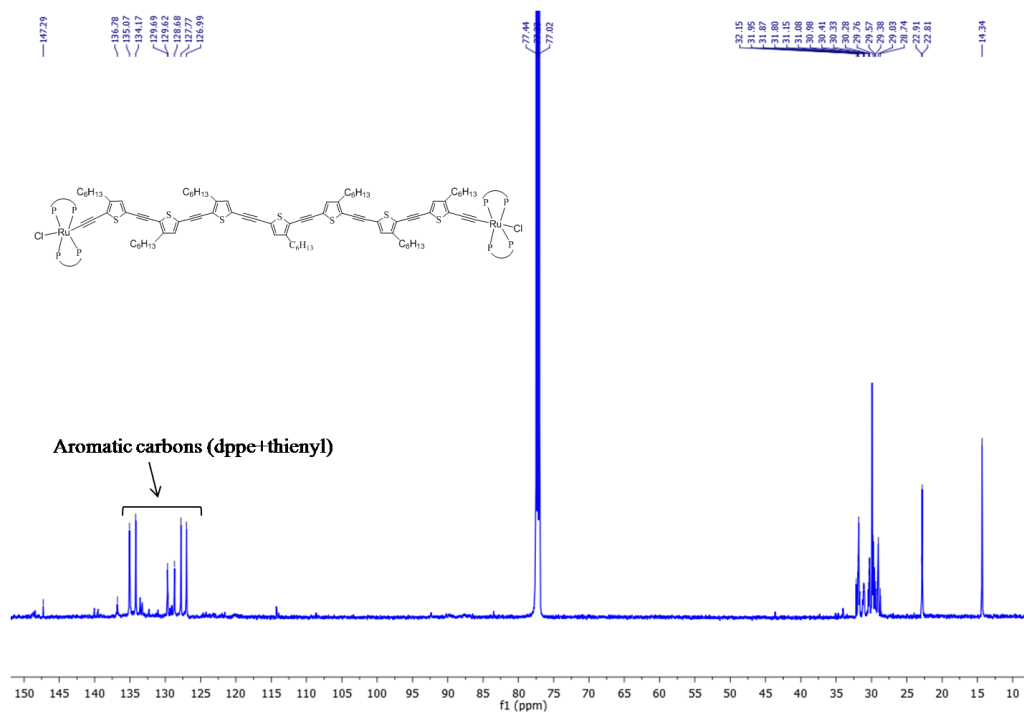


Fig. S13b: $^{13}\text{C}\{^1\text{H}\}$ -NMR (150MHz, CDCl_3) spectrum of **O7-Ru₂**

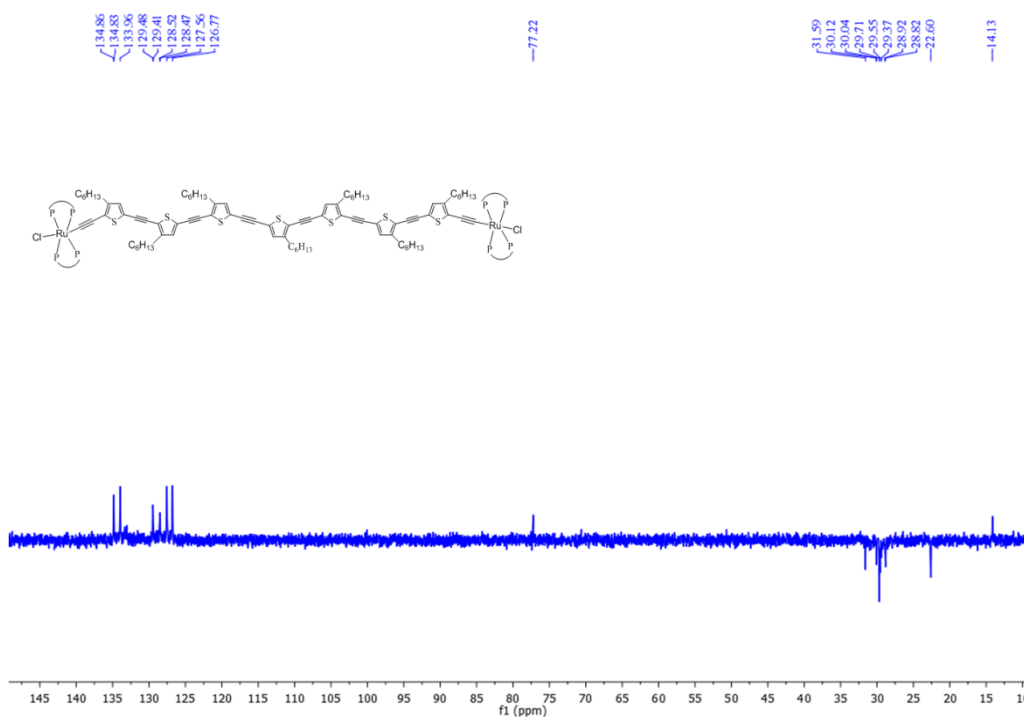


Fig. S13c: DEPT-135 (150MHz, CDCl_3) spectrum of **O7-Ru₂**

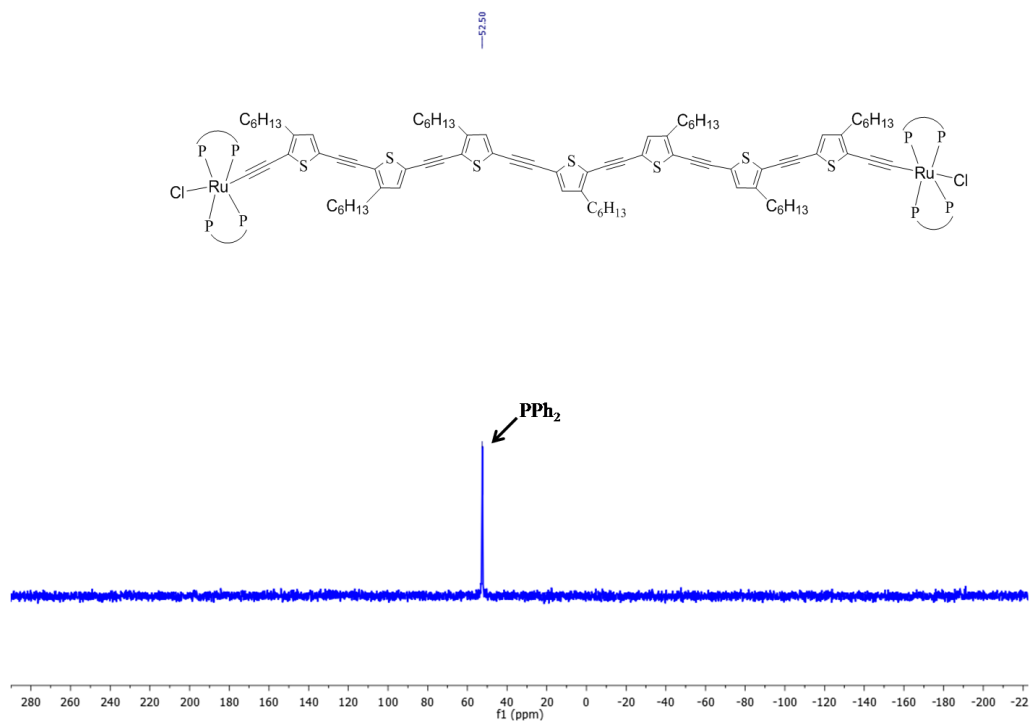


Fig. S13d: $^{31}\text{P}\{^1\text{H}\}$ -NMR (162MHz, CDCl_3) spectrum of **O7-Ru₂**

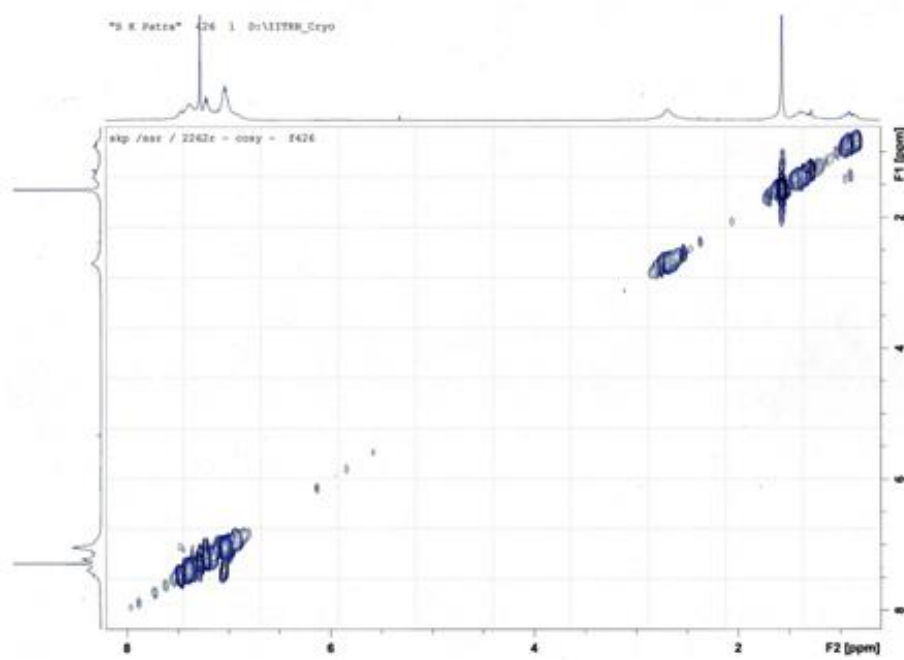


Fig. S14: ^1H - ^1H COSY NMR (600MHz, CDCl_3) spectrum of **O1-Ru₂**

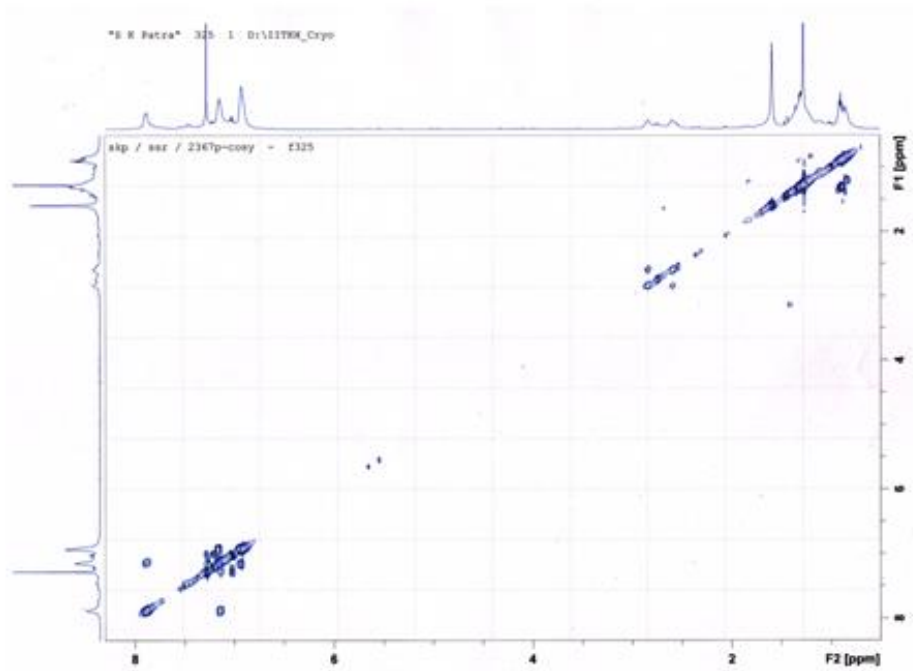


Fig. S15: ¹H-¹H COSY NMR (600MHz, CDCl₃) spectrum of O3-Ru₂

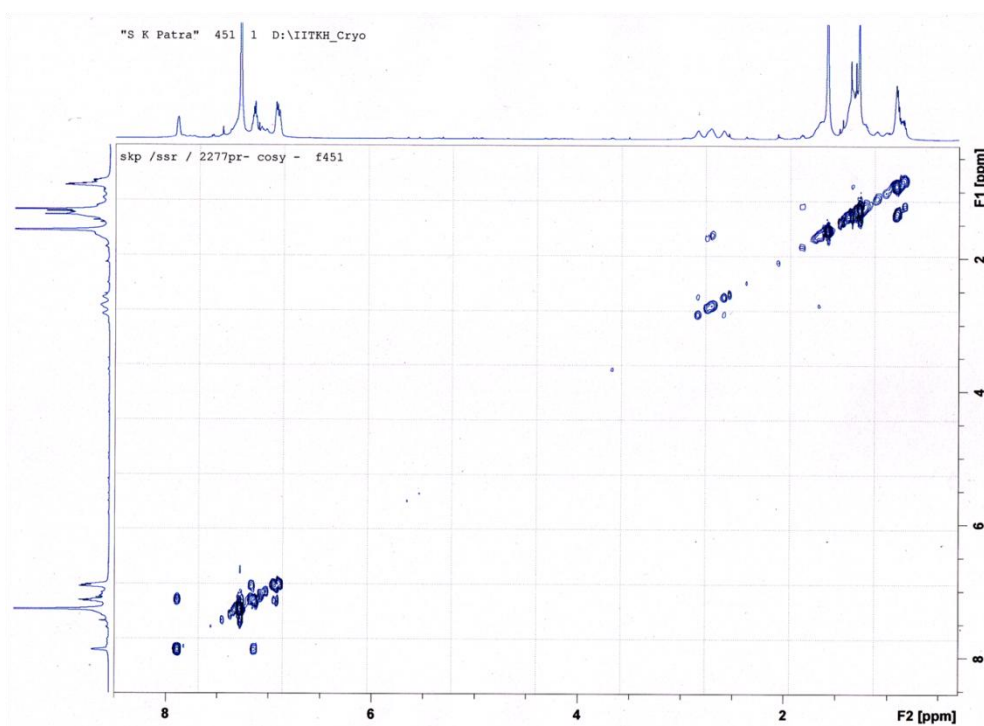


Fig. S16: ¹H-¹H COSY NMR (600MHz, CDCl₃) spectrum of O5-Ru₂

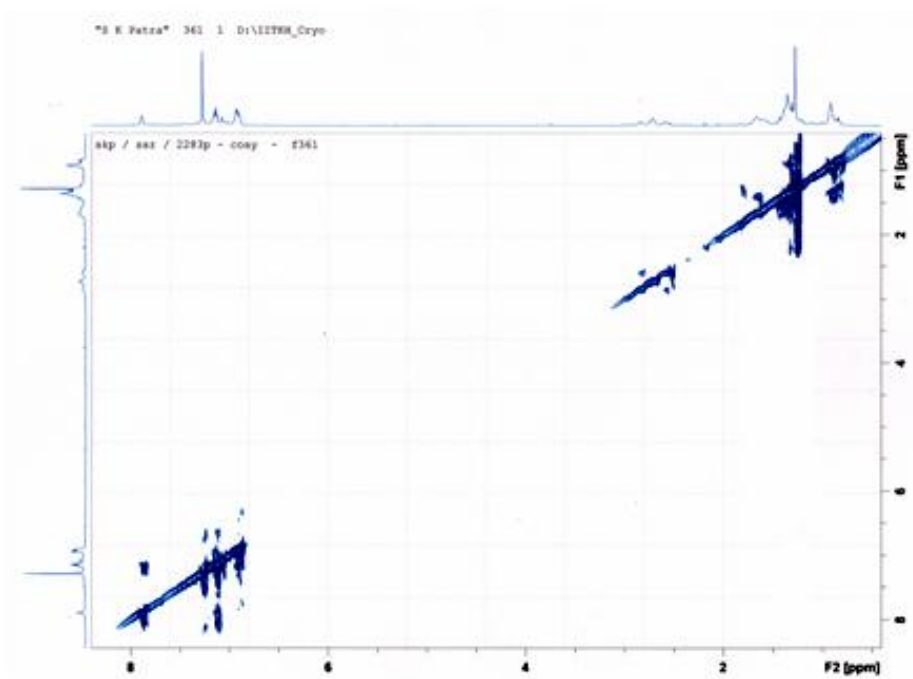


Fig. S17: ^1H - ^1H COSY NMR (600MHz, CDCl_3) spectrum of **O7-Ru₂**

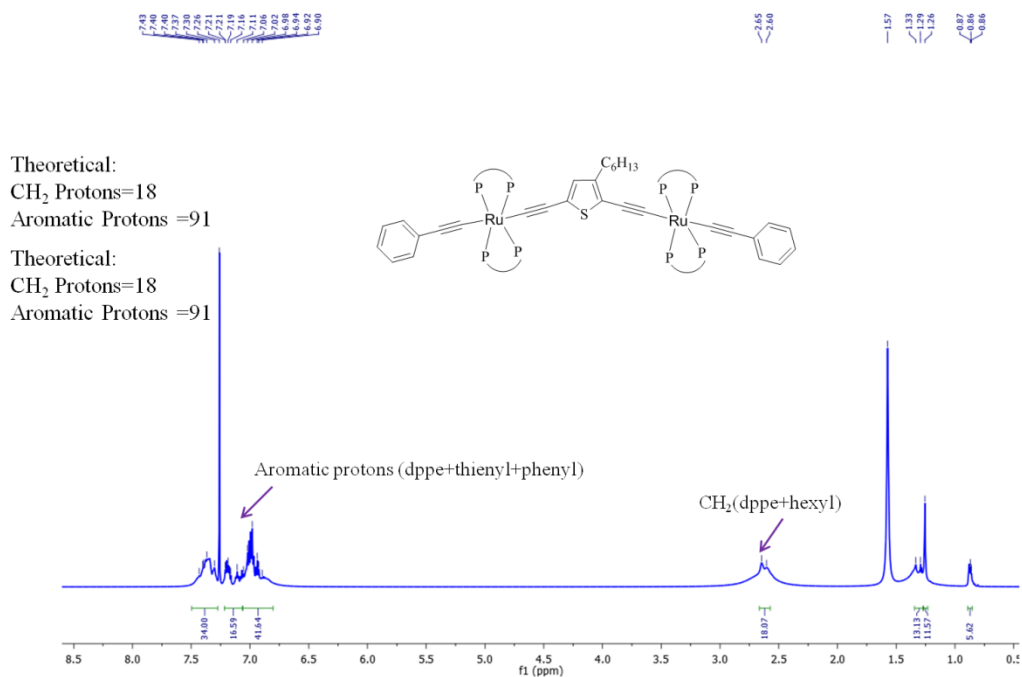


Fig. S18a: ^1H -NMR (600MHz, CDCl_3) spectrum of **O1-Ru₂-Ph**

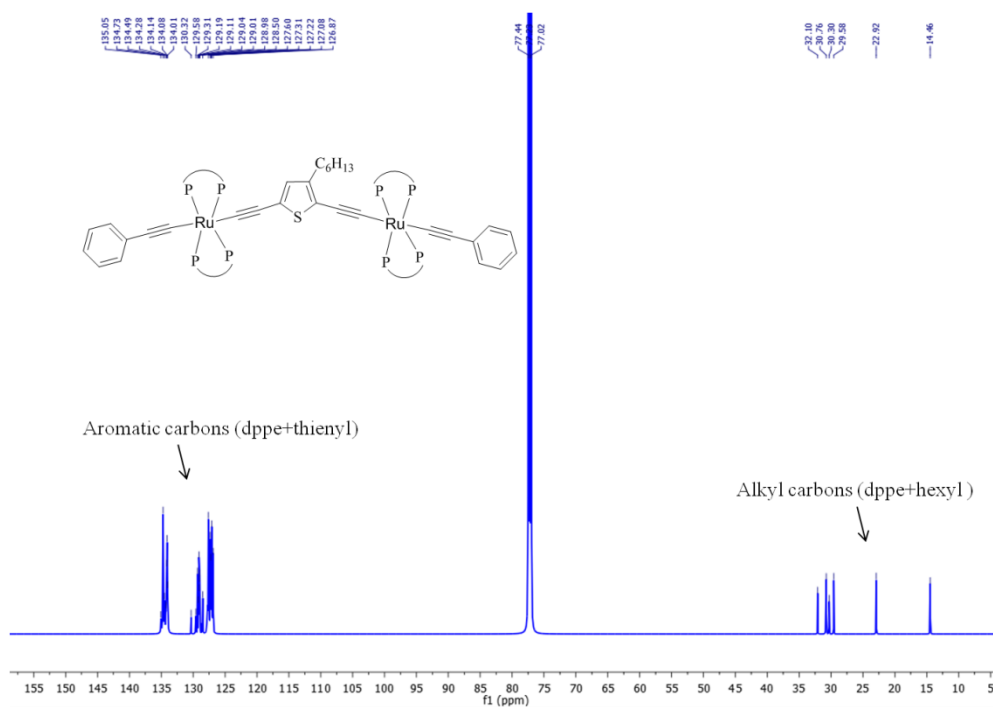


Fig. S18b: $^{13}\text{C}\{^1\text{H}\}$ -NMR (150MHz, CDCl_3) spectrum of **O1-Ru₂-Ph**

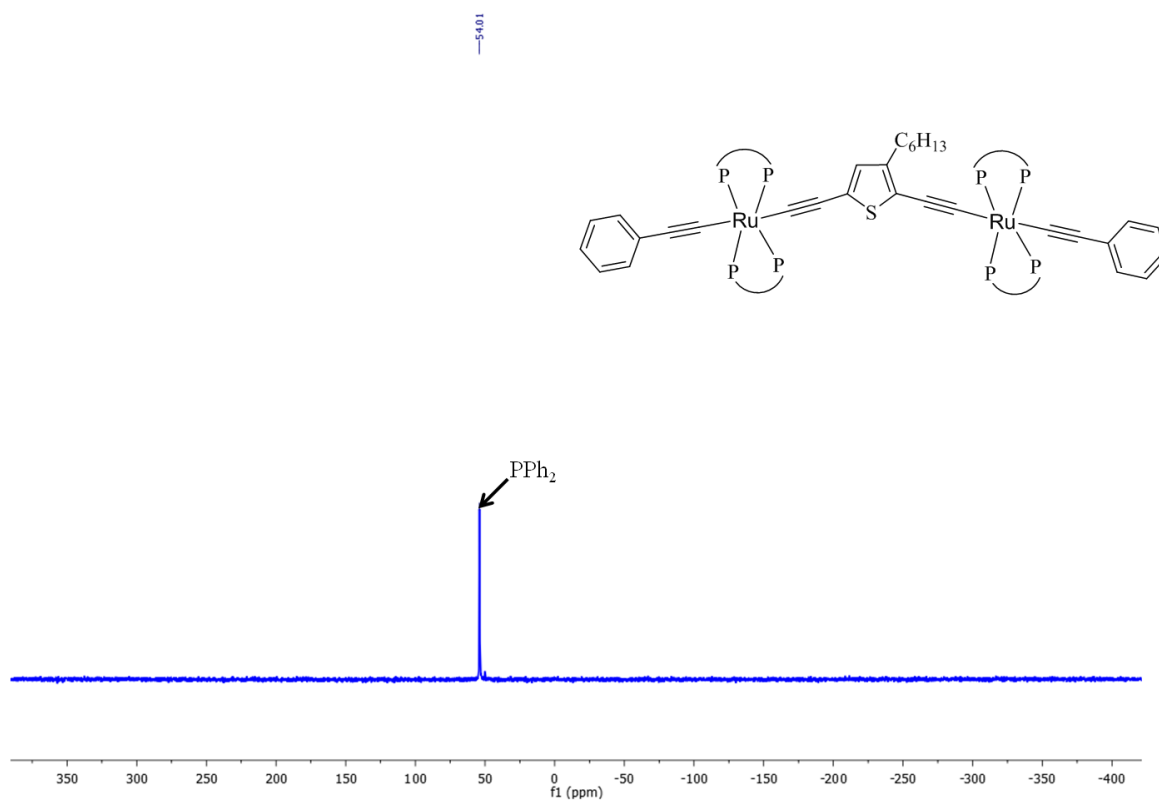


Fig. S18c: $^{31}\text{P}\{^1\text{H}\}$ -NMR (162MHz, CDCl_3) spectrum of **O1-Ru₂-Ph**

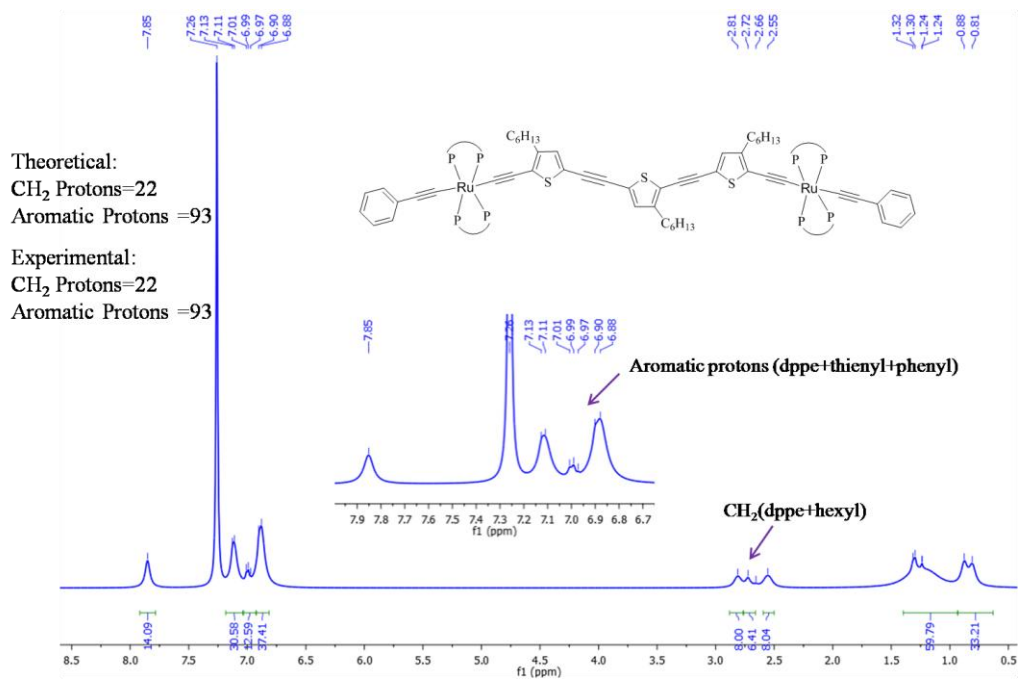


Fig. S19a: ¹H-NMR (600MHz, CDCl₃) spectrum of **O3-Ru₂-Ph**

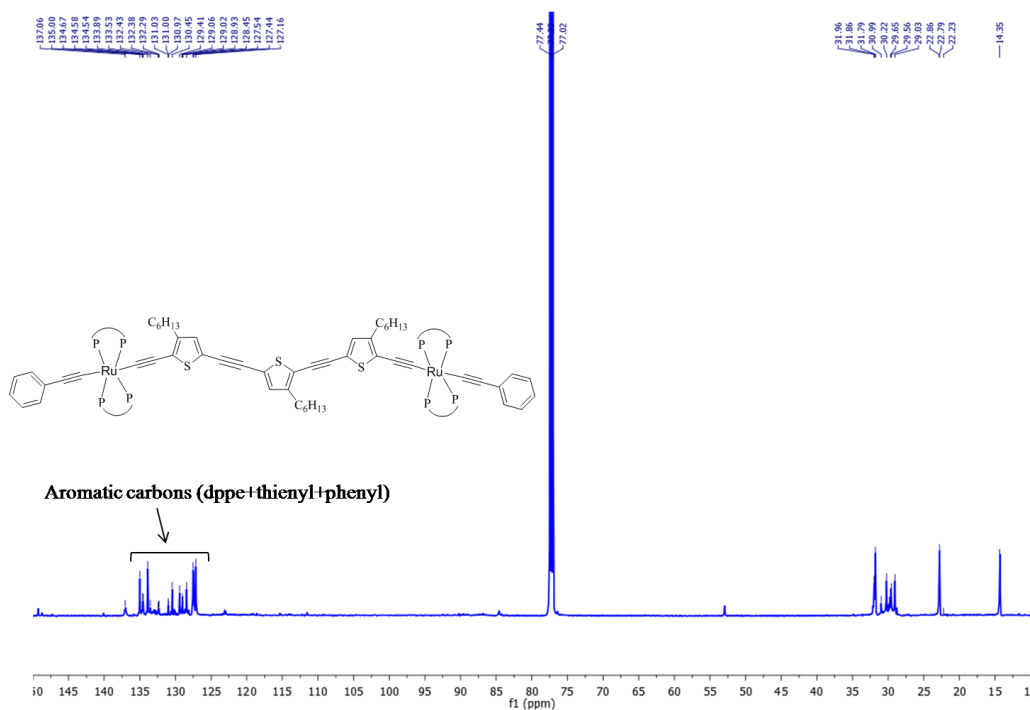


Fig. S19b: ¹³C{¹H}-NMR (150MHz, CDCl₃) spectrum of **O3-Ru₂-Ph**

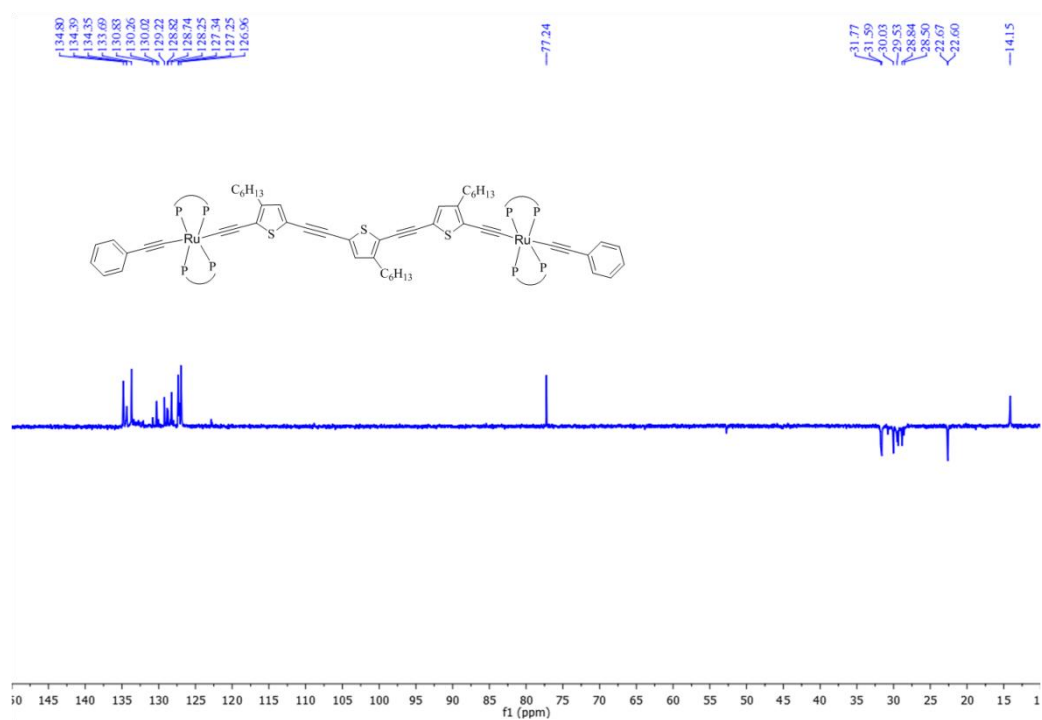


Fig. S19c: DEPT-135 (150MHz, CDCl₃) spectrum of **O3-Ru₂-Ph**

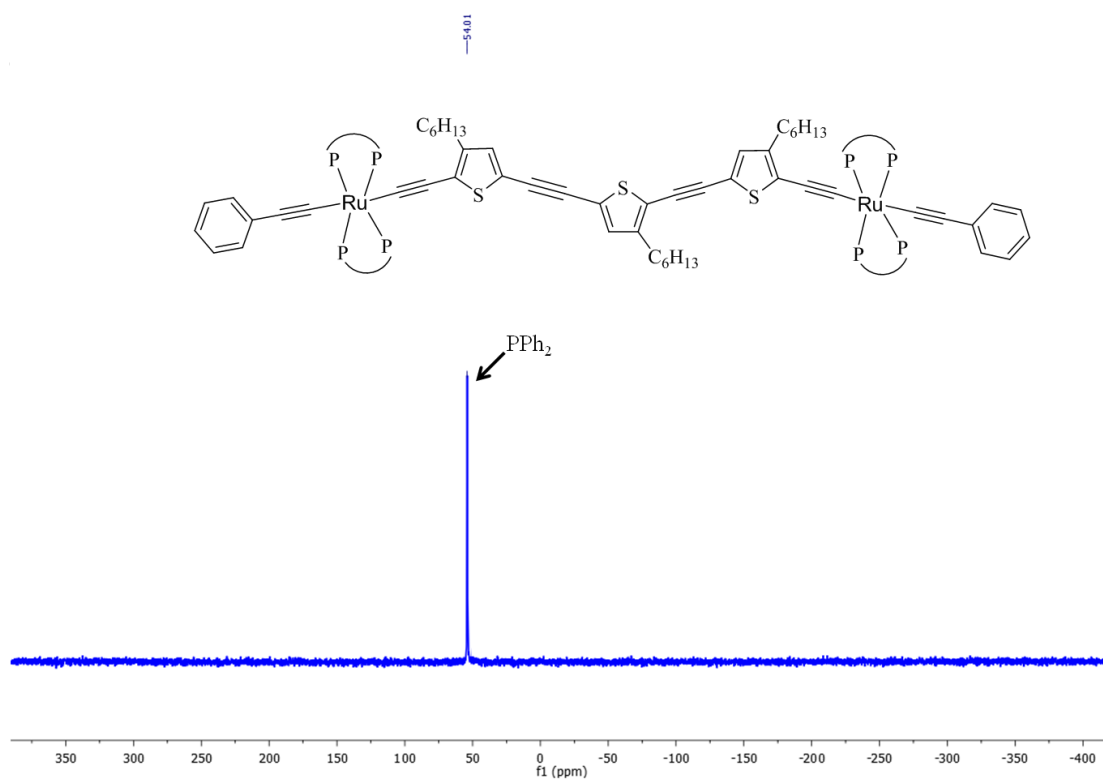


Fig. S19d: ³¹P{¹H} NMR (162MHz, CDCl₃) spectrum of **O3-Ru₂-Ph**

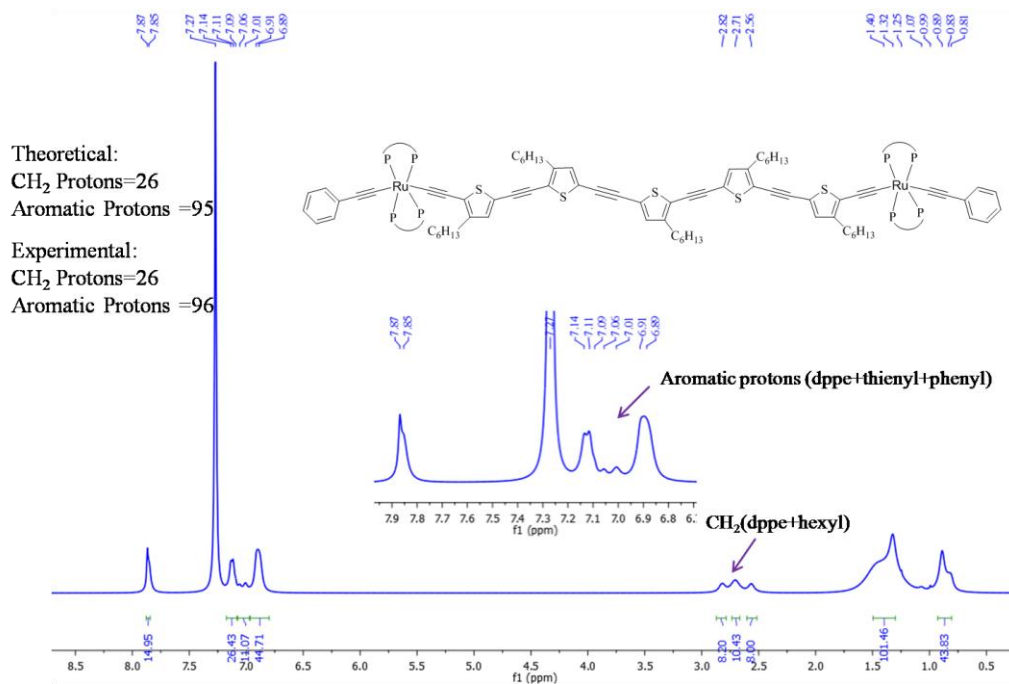


Fig. S20a: ¹H NMR(600MHz, CDCl₃) spectrum of **O5-Ru₂-Ph**

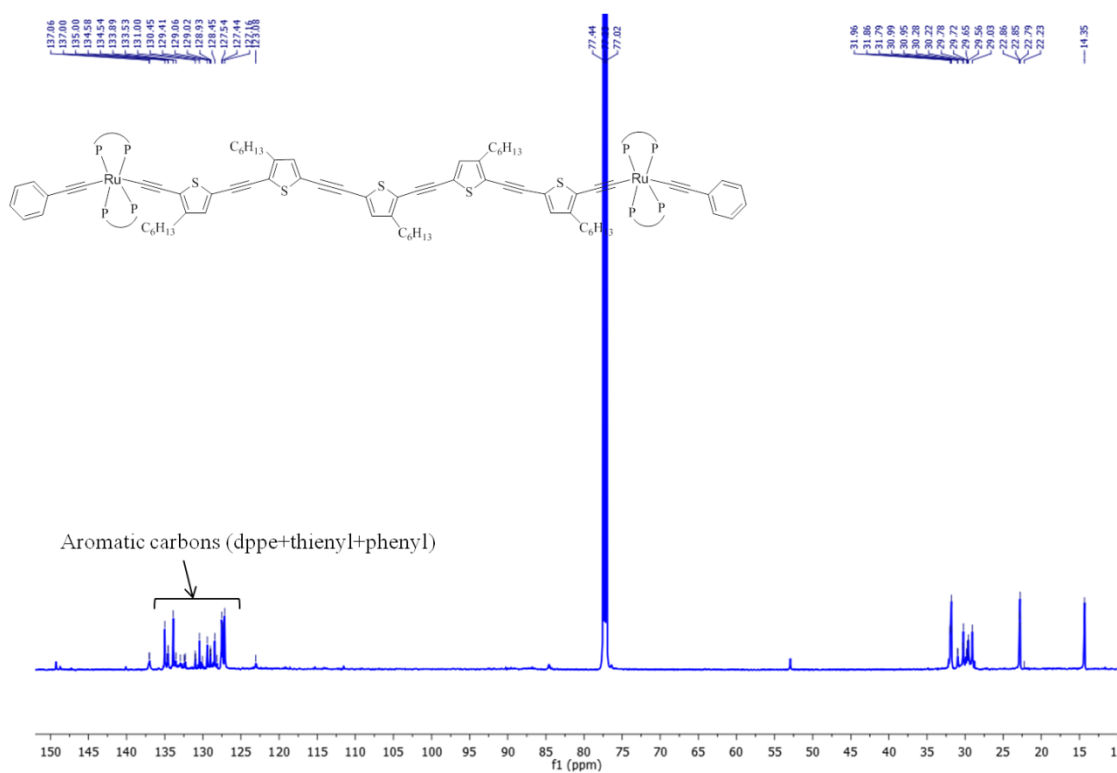


Fig. S20b: ¹³C{¹H}-NMR (150MHz, CDCl₃) spectrum of **O5-Ru₂-Ph**

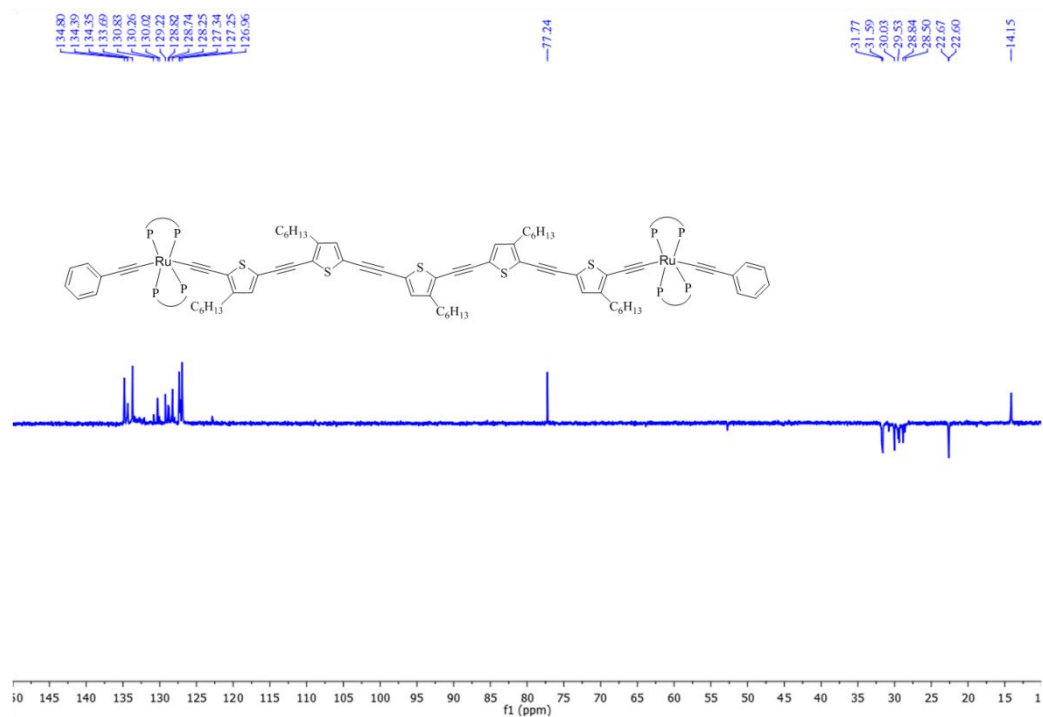


Fig. S20c: DEPT-135 (150MHz, CDCl₃) spectrum of **O5-Ru₂-Ph**

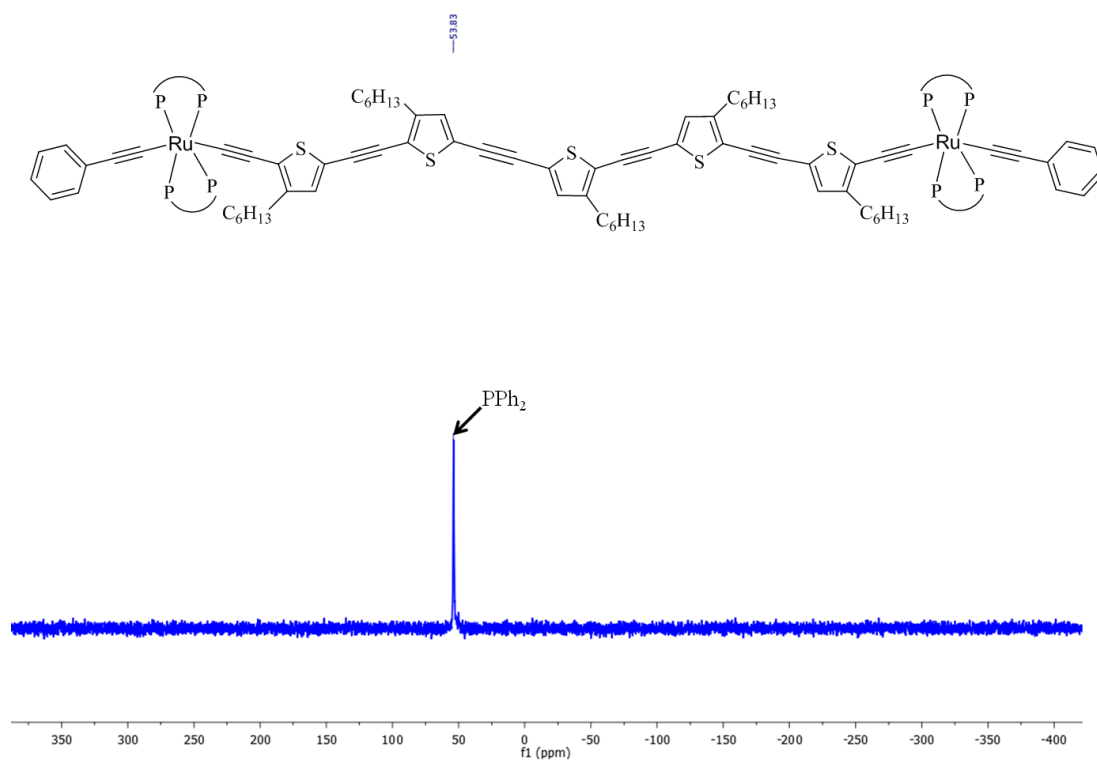


Fig. S20d: ³¹P{¹H}-NMR (162MHz, CDCl₃) spectrum of **O5-Ru₂-Ph**

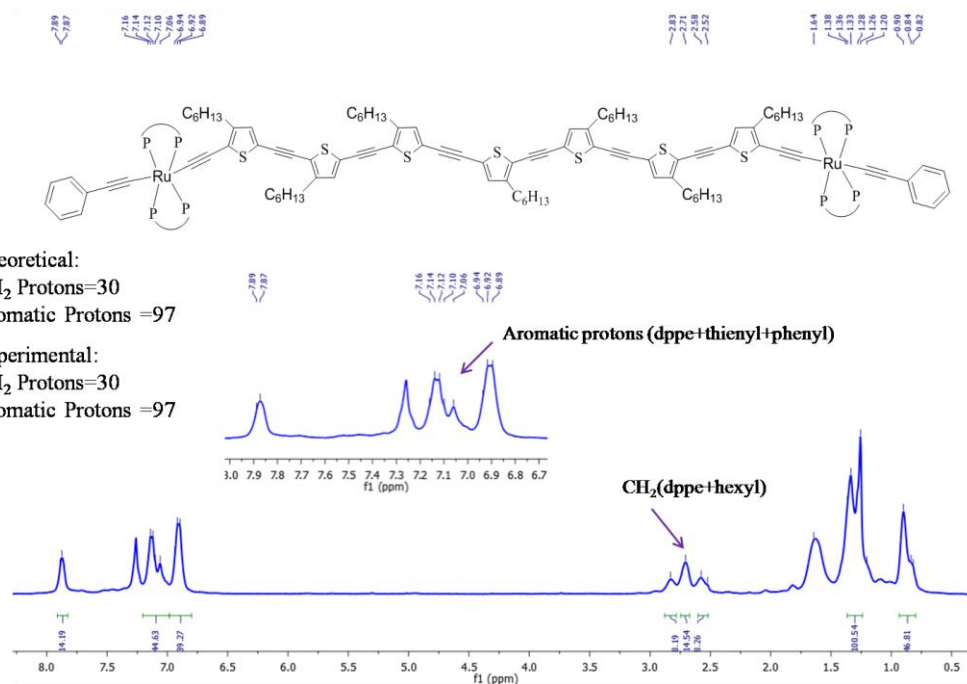


Fig. S21a: ¹H-NMR (600MHz, CDCl₃) spectrum of **O7-Ru₂-Ph**

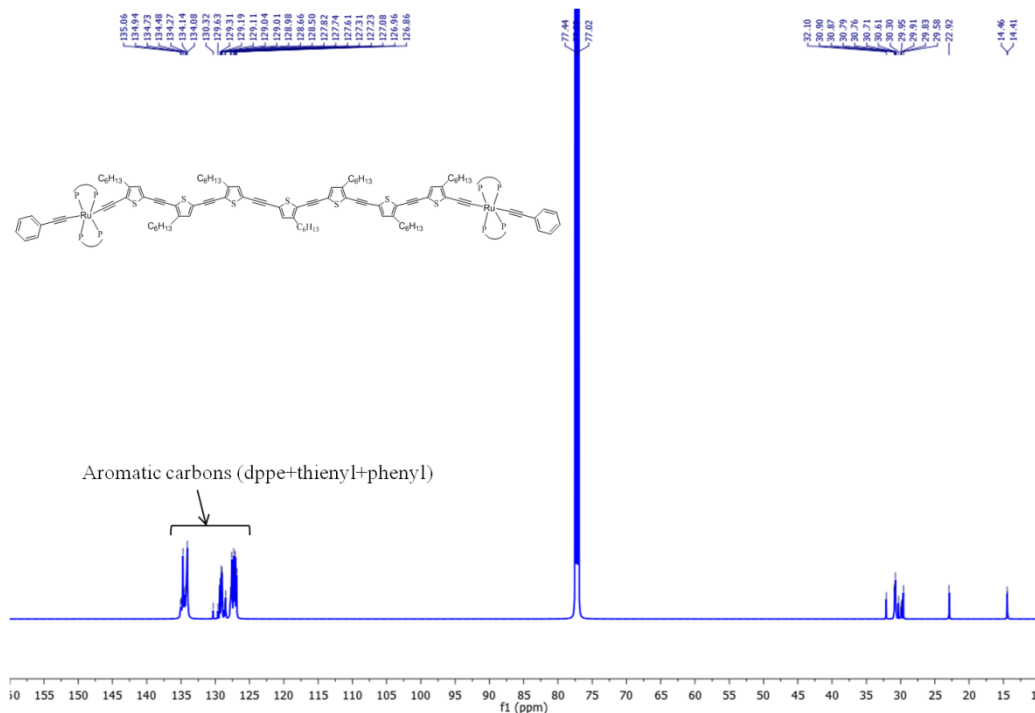


Fig. S21b: ¹³C{¹H} NMR (150MHz, CDCl₃) spectrum of **O7-Ru₂-Ph**

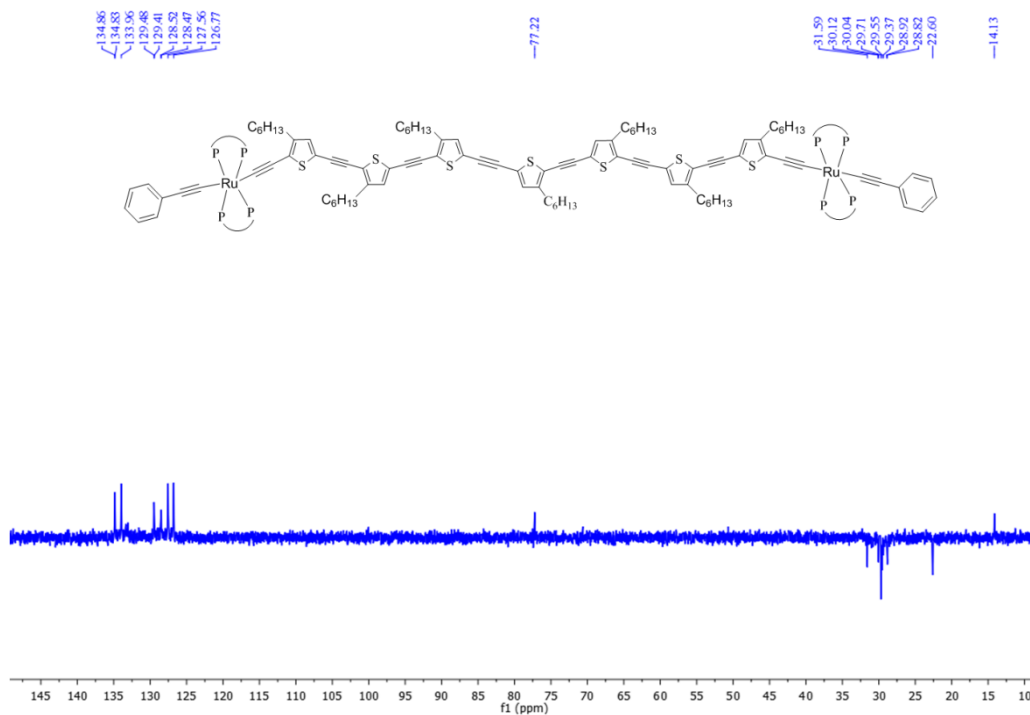


Fig. S21c: DEPT-135 (150MHz, CDCl₃) spectrum of **O7-Ru₂-Ph**

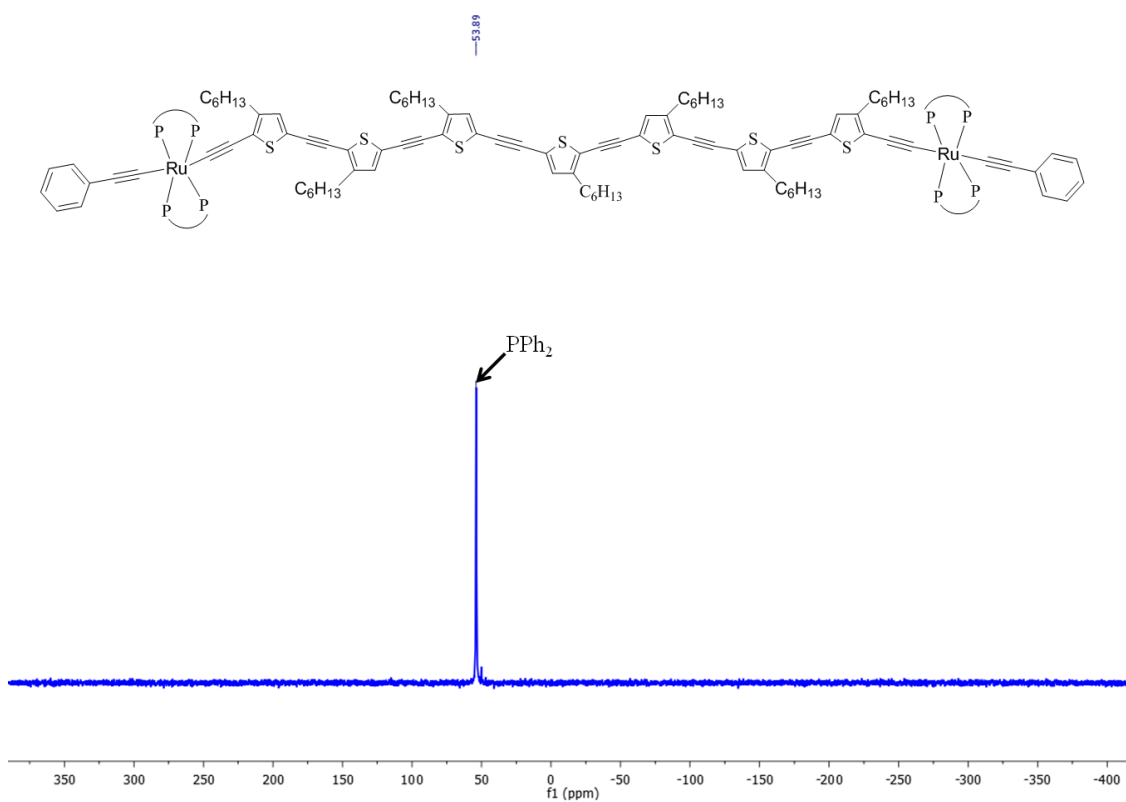


Fig. S21d: ³¹P{¹H} NMR (162MHz, CDCl₃) spectrum of **O7-Ru₂-Ph**

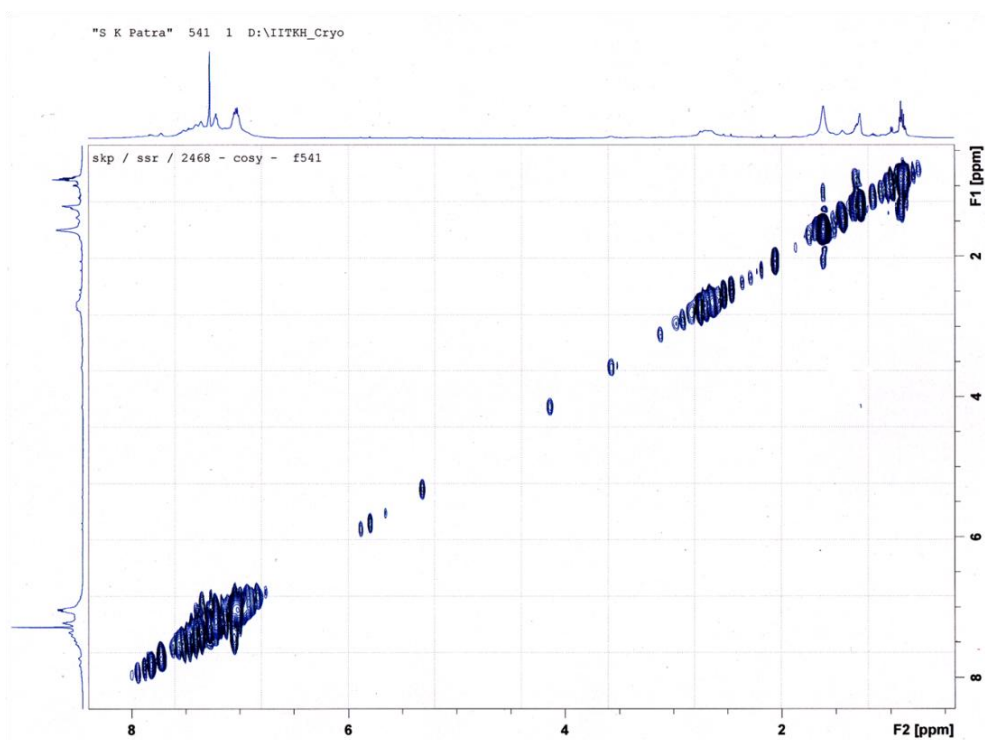


Fig. S22: ^1H - ^1H COSY NMR (600MHz, CDCl_3) spectrum of **O1-Ru₂-Ph**

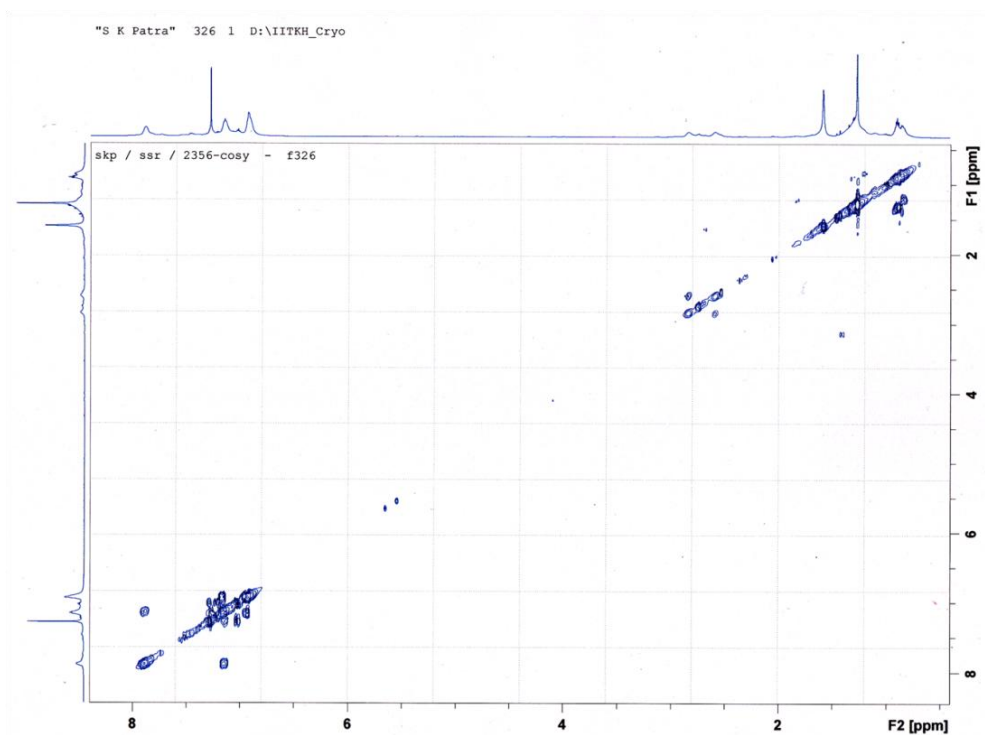


Fig. S23: ^1H - ^1H COSY NMR (600MHz, CDCl_3) spectrum of **O3-Ru₂-Ph**

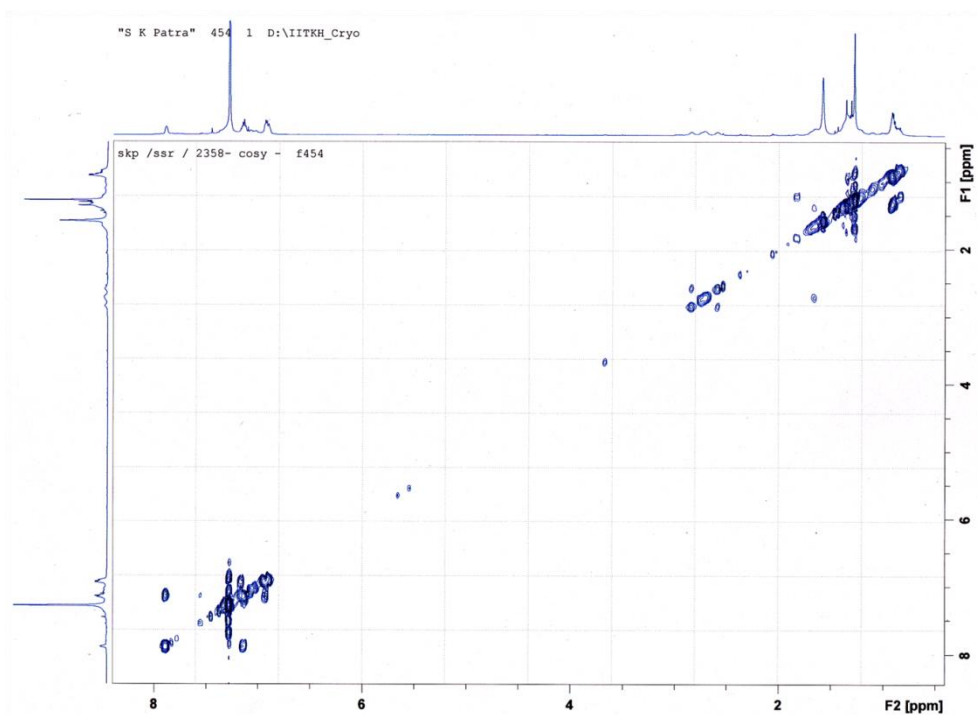


Fig. S24: ^1H - ^1H COSY NMR (600MHz, CDCl_3) spectrum of **O5-Ru₂-Ph**

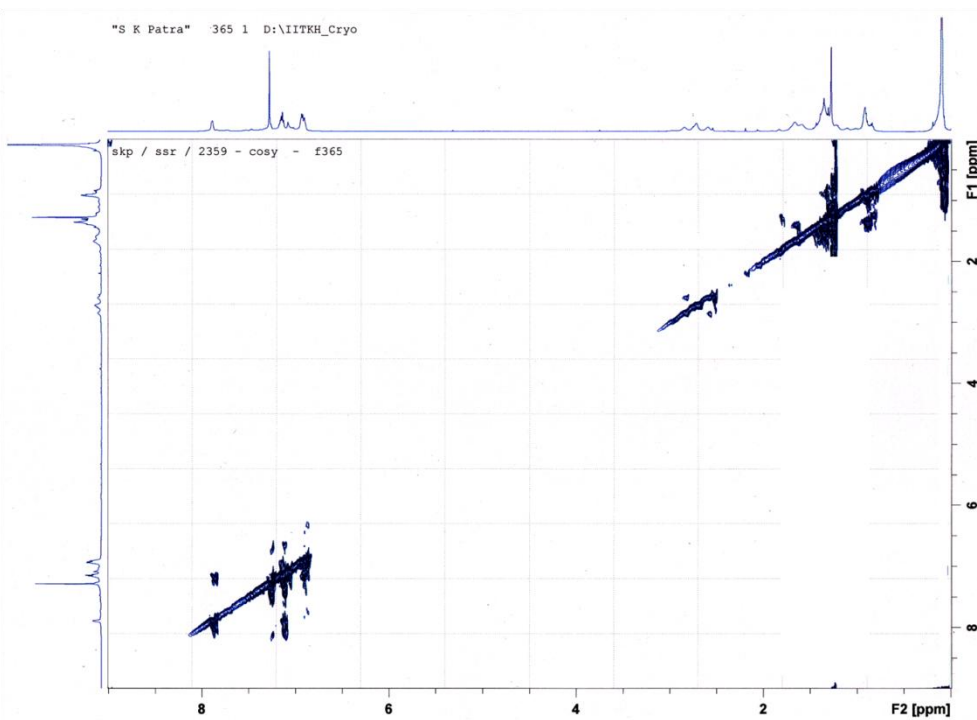


Fig. S25: ^1H - ^1H COSY NMR (600MHz, CDCl_3) spectrum of **O7-Ru₂-Ph**

1c. Mass Spectrometry

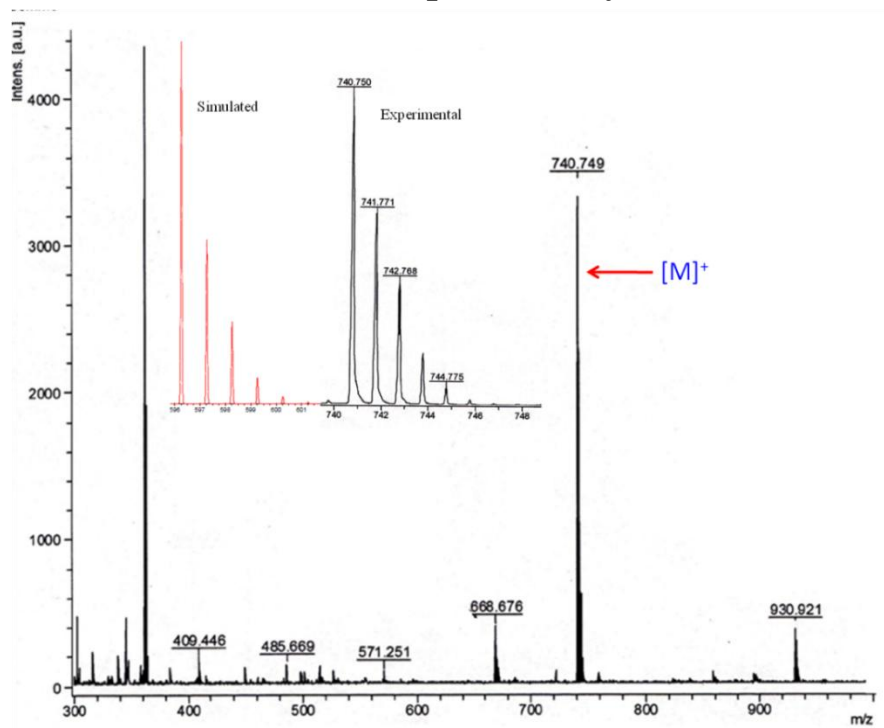


Fig. S26: MALDI-TOF spectrometry of **7** with the simulated (red) and experimental (black) isotopic distribution of the molecular ion peak.

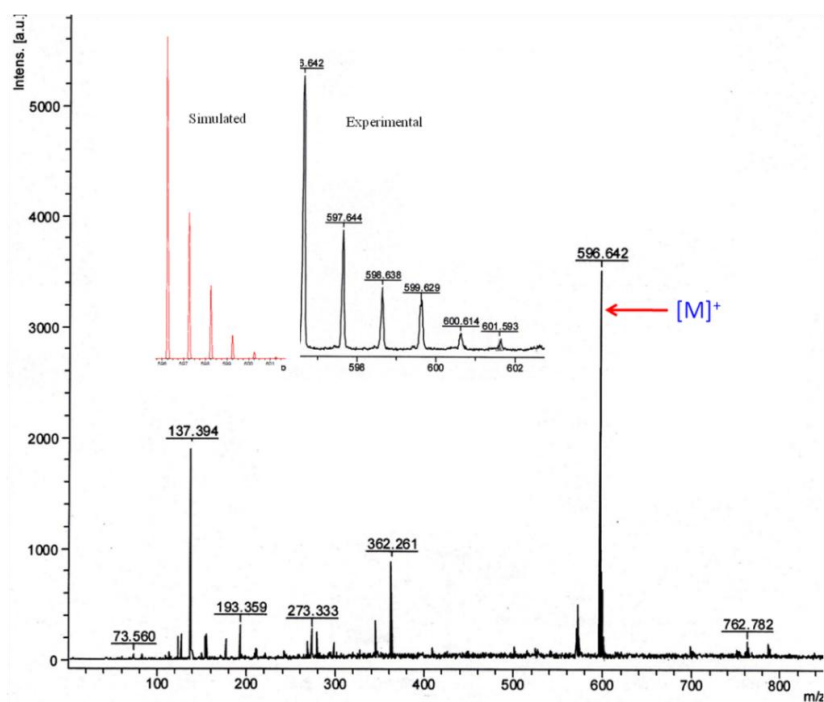


Fig. S27: MALDI-TOF spectrometry of **O3** with the simulated (red) and experimental (black) isotopic distribution of the molecular ion peak.

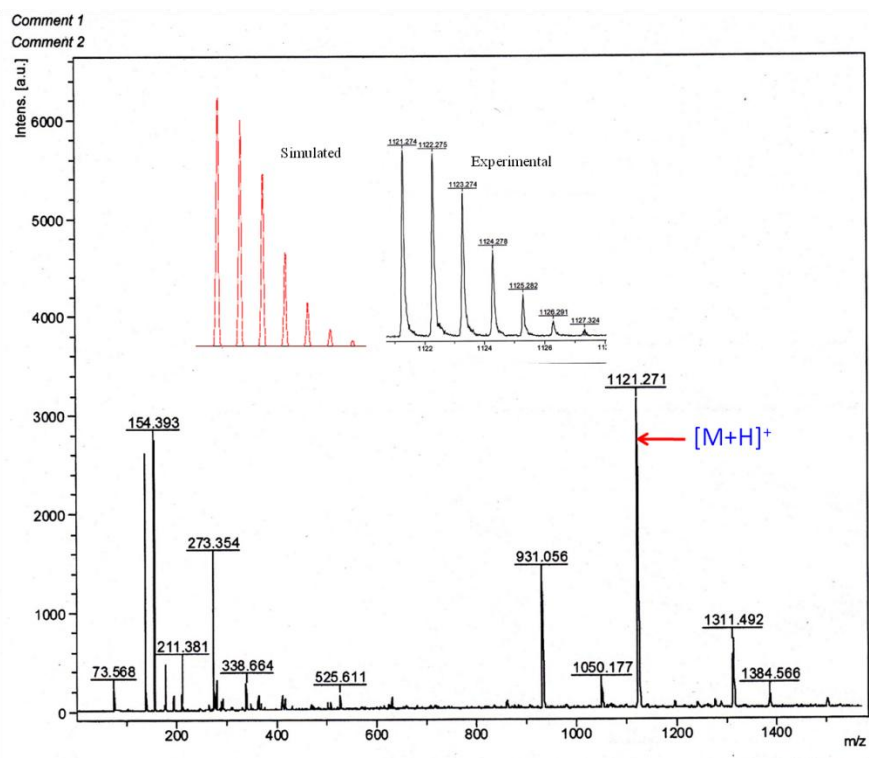


Fig. S28: MALDI-TOF spectrometry of **8** with the simulated (red) and experimental (black) isotopic distribution of the molecular ion peak.

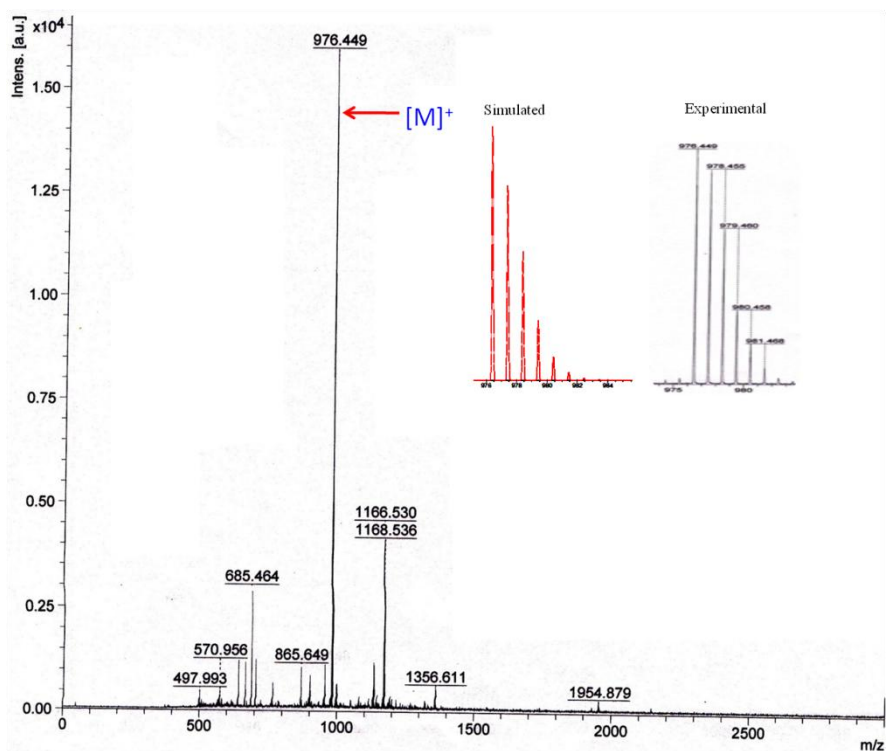


Fig. S29: MALDI-TOF spectrometry of **O5** with the simulated (red) and experimental (black) isotopic distribution of the molecular ion peak.

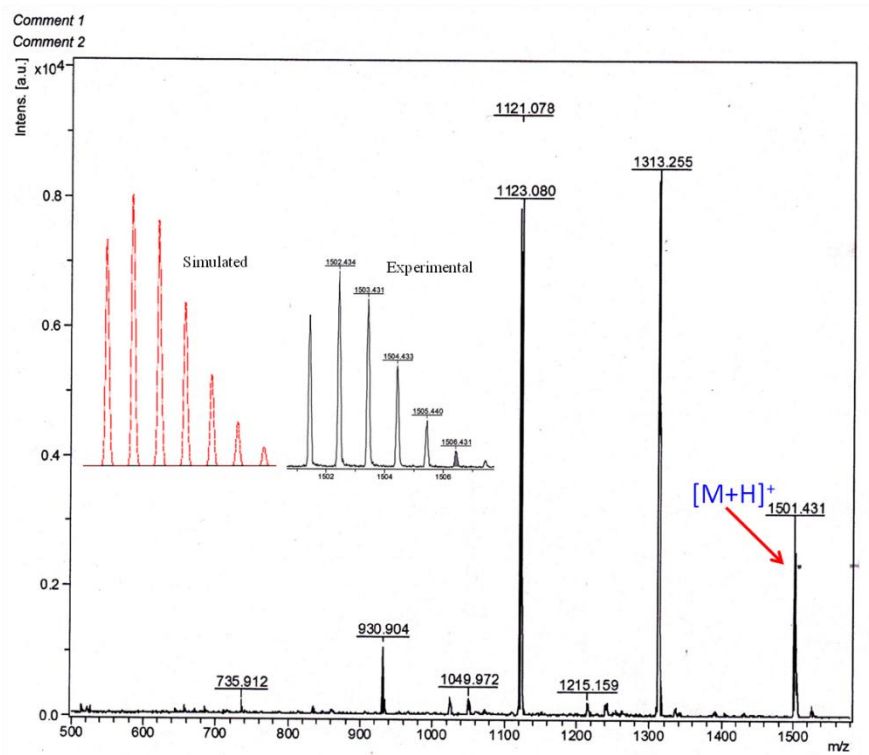


Fig. S30: MALDI-TOF spectrometry of **9** with the simulated (red) and experimental (black) isotopic distribution of the molecular ion peak.

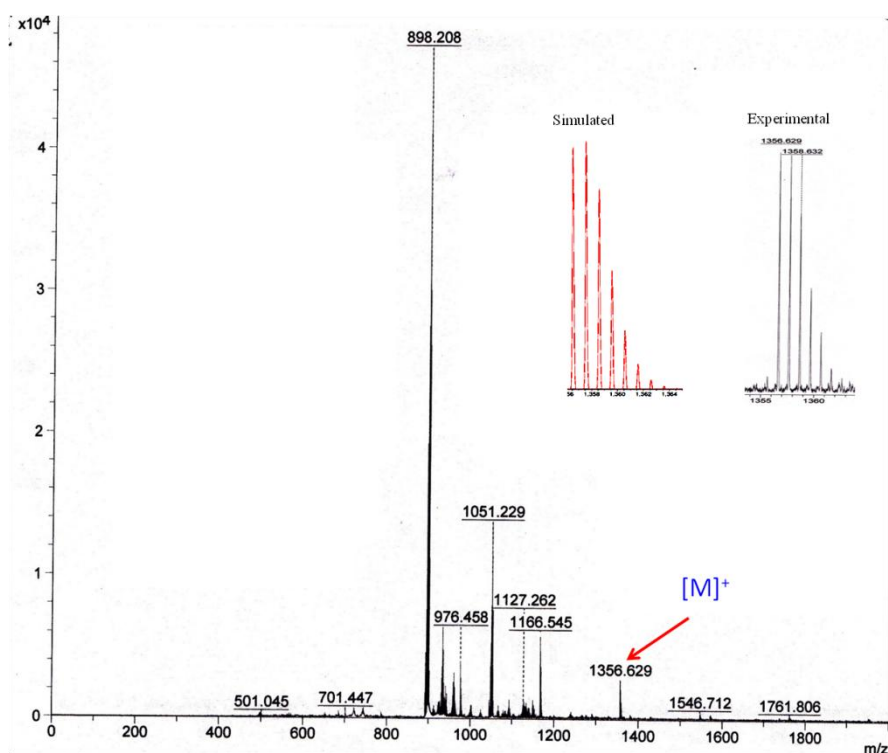


Fig. S31: MALDI-TOF spectrometry of **O7** with the simulated (red) and experimental (black) isotopic distribution of the molecular ion peak.

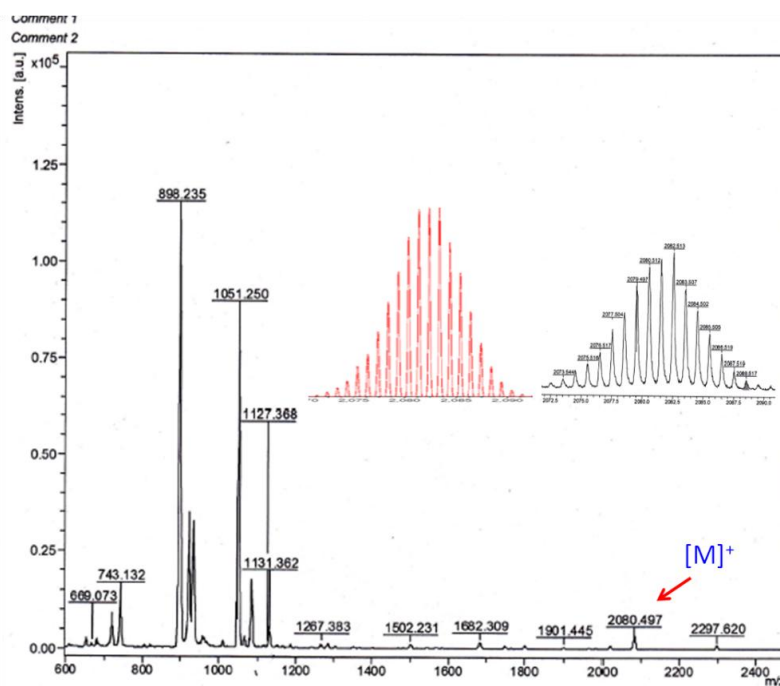


Fig. S32: MALDI-TOF spectrometry of **O1-Ru₂** with the simulated (red) and experimental (black) isotopic distribution of the molecular ion peak.

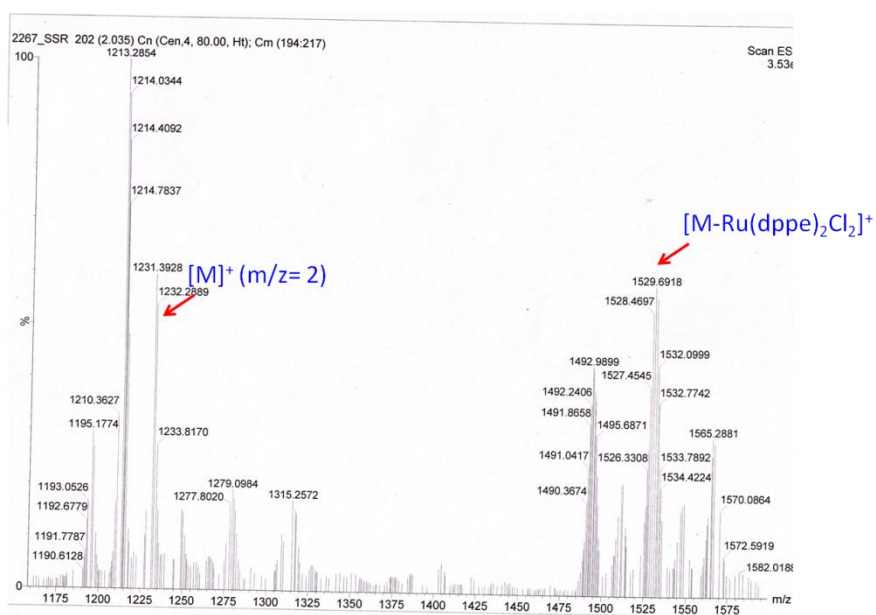


Fig. S33: Mass spectrometry (ESI⁺) of **O3-Ru₂**

1d. FTIR Spectra

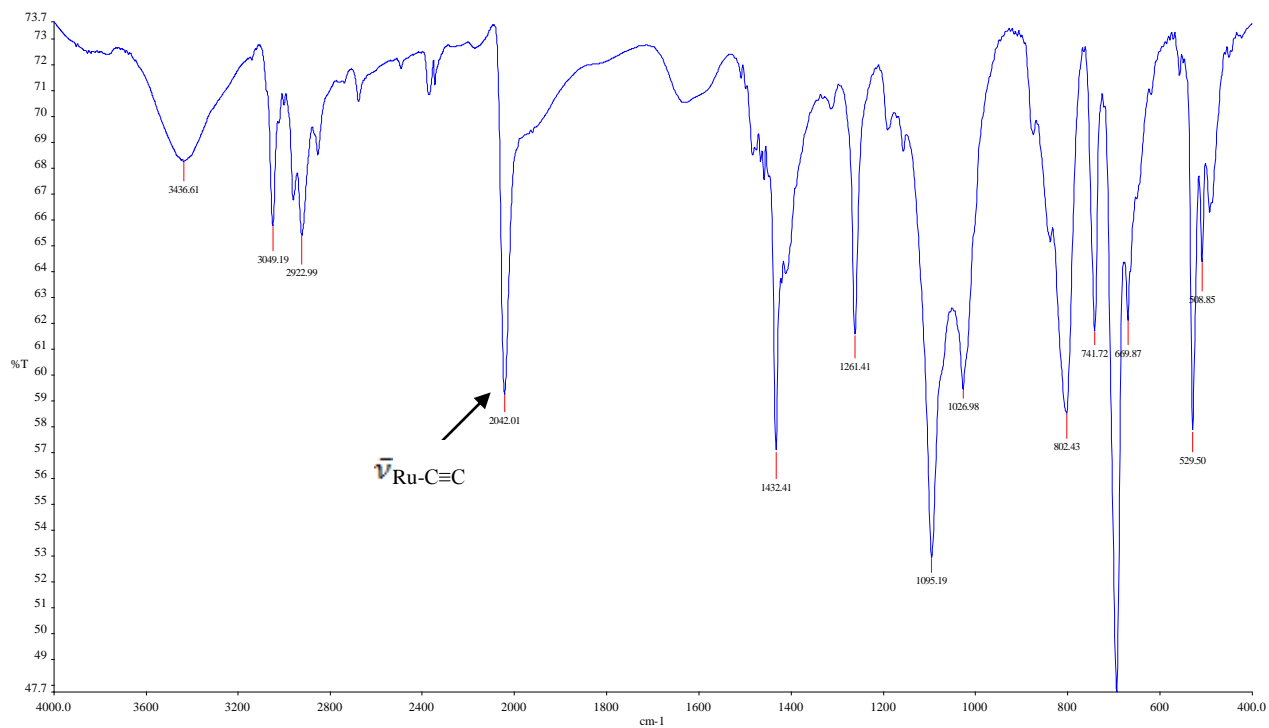


Fig. S34: FTIR spectrum of O1-Ru₂

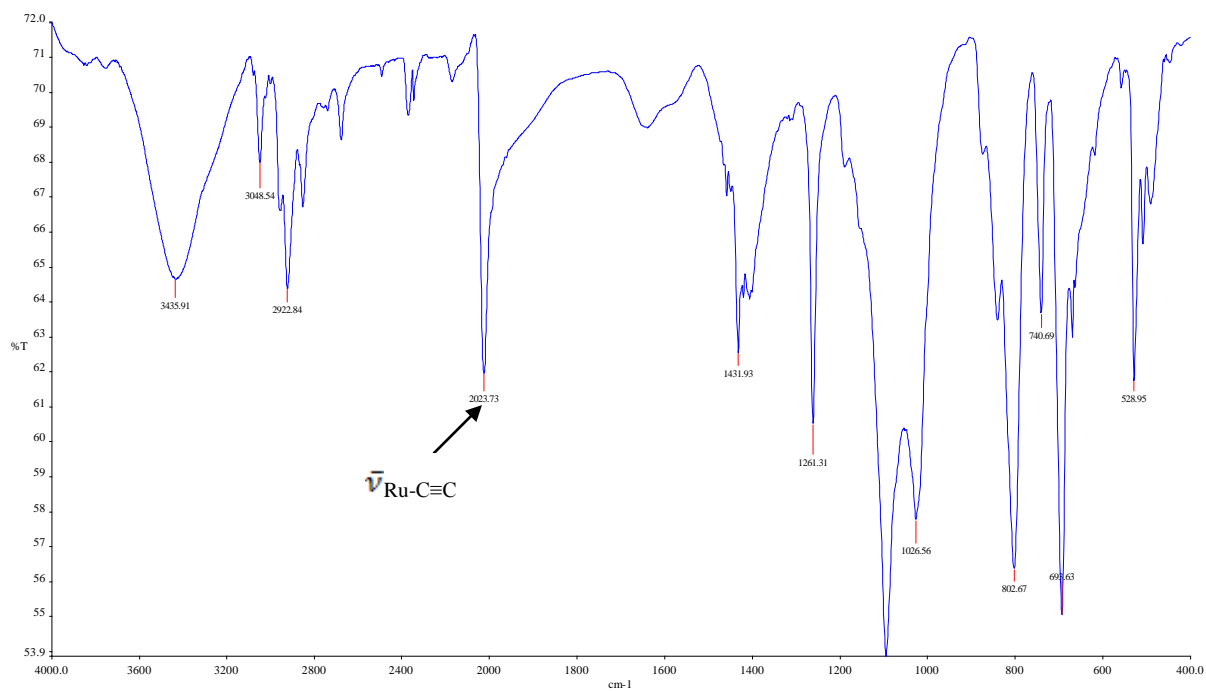


Fig. S35: FTIR spectrum of O3-Ru₂

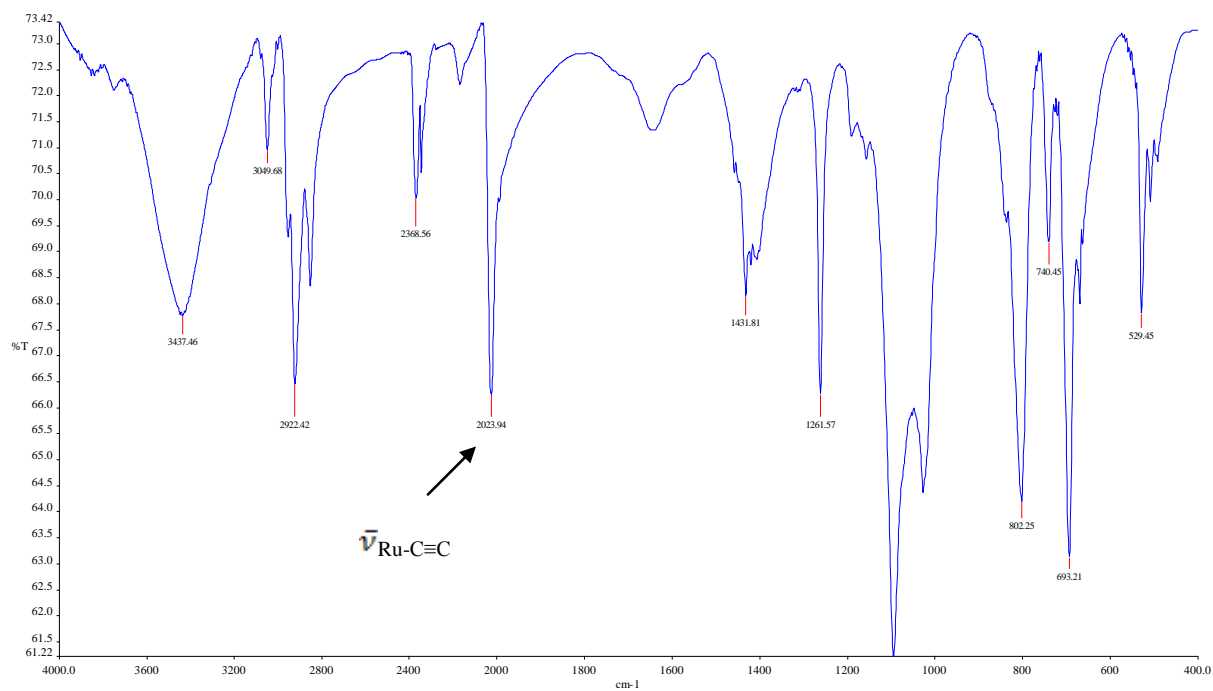


Fig. S36: FTIR spectrum of O5-Ru₂

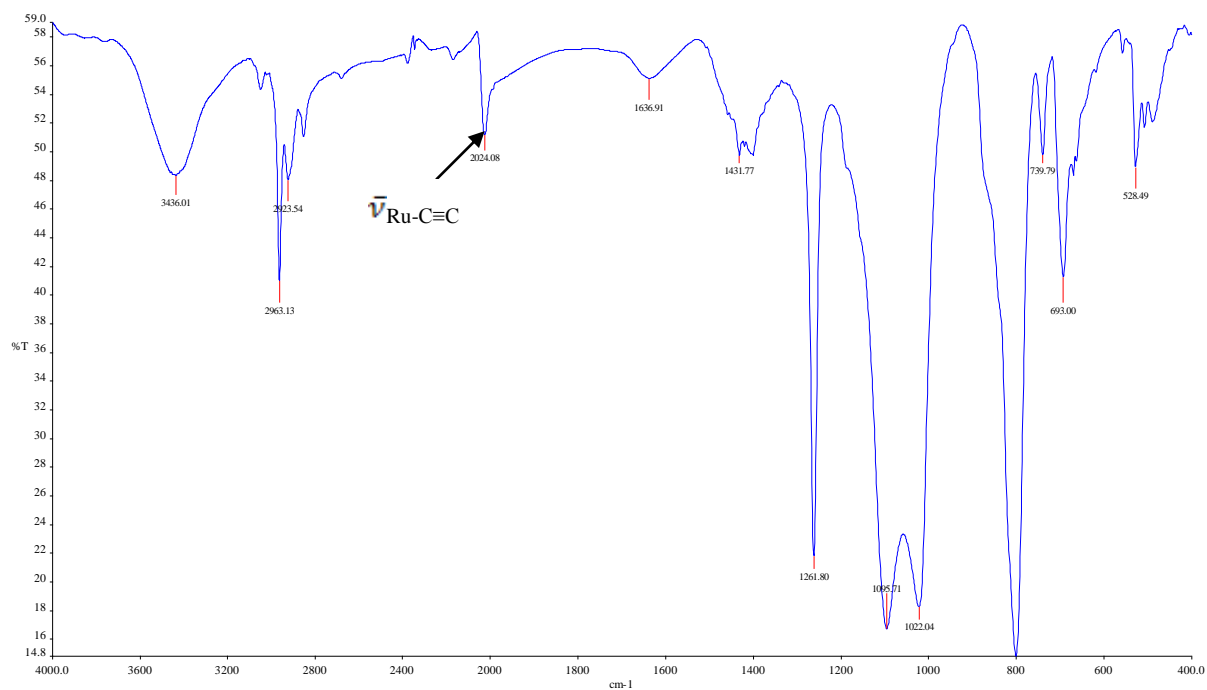


Fig. S37: FTIR spectrum of O7-Ru₂

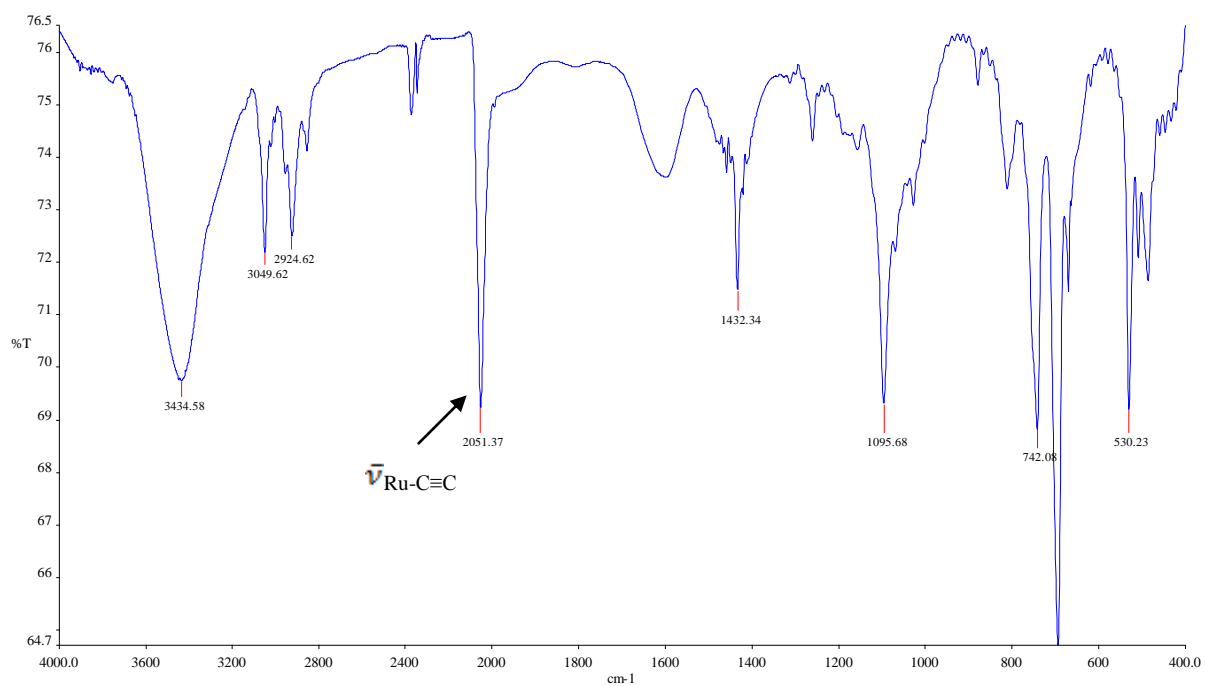


Fig. S38: FTIR spectrum of O1-Ru₂-Ph

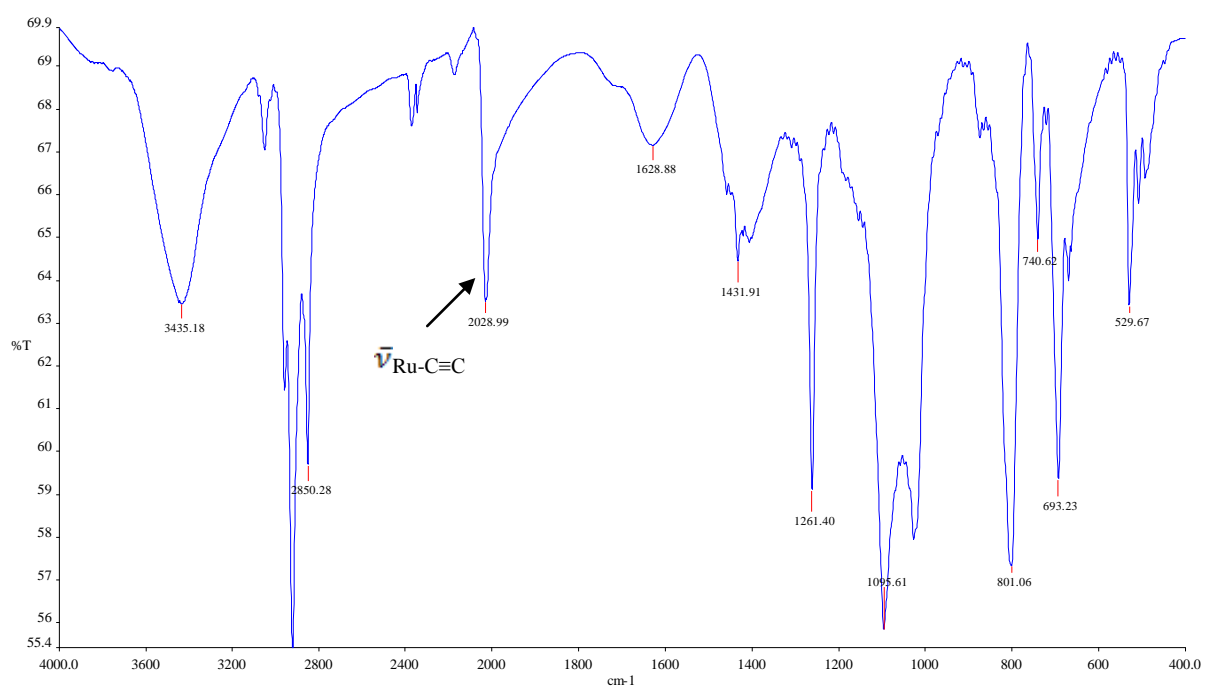


Fig. S39: FTIR spectrum of O3-Ru₂-Ph

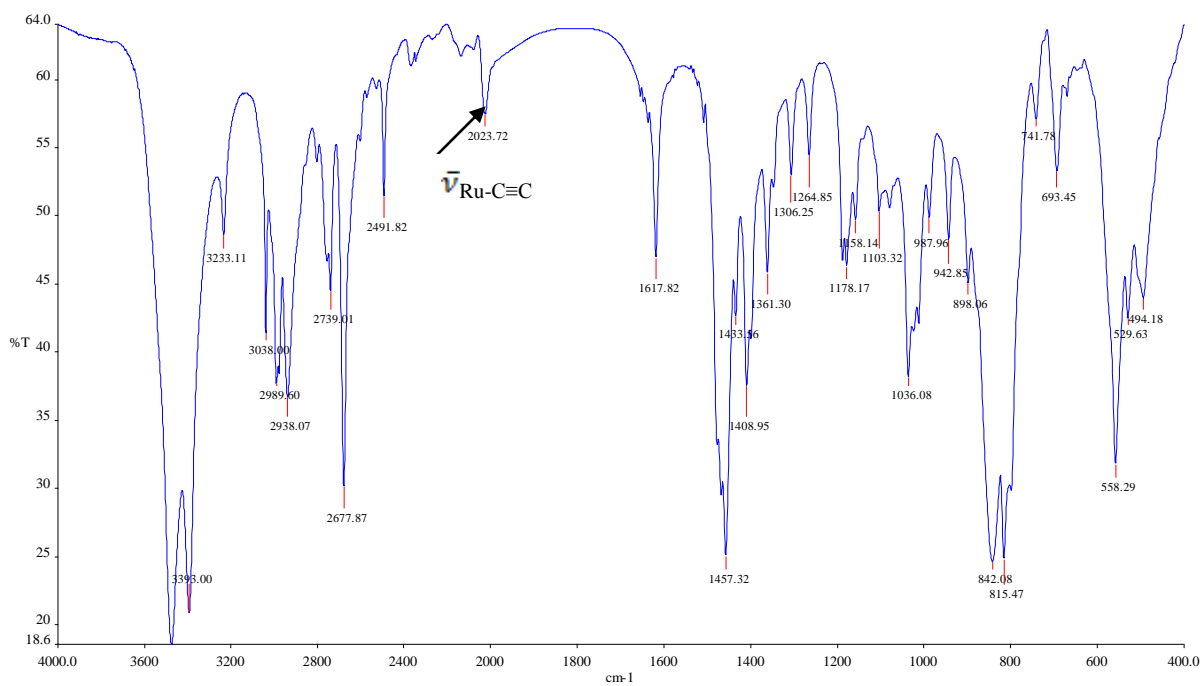


Fig. S40: FTIR spectrum of O5-Ru₂-Ph

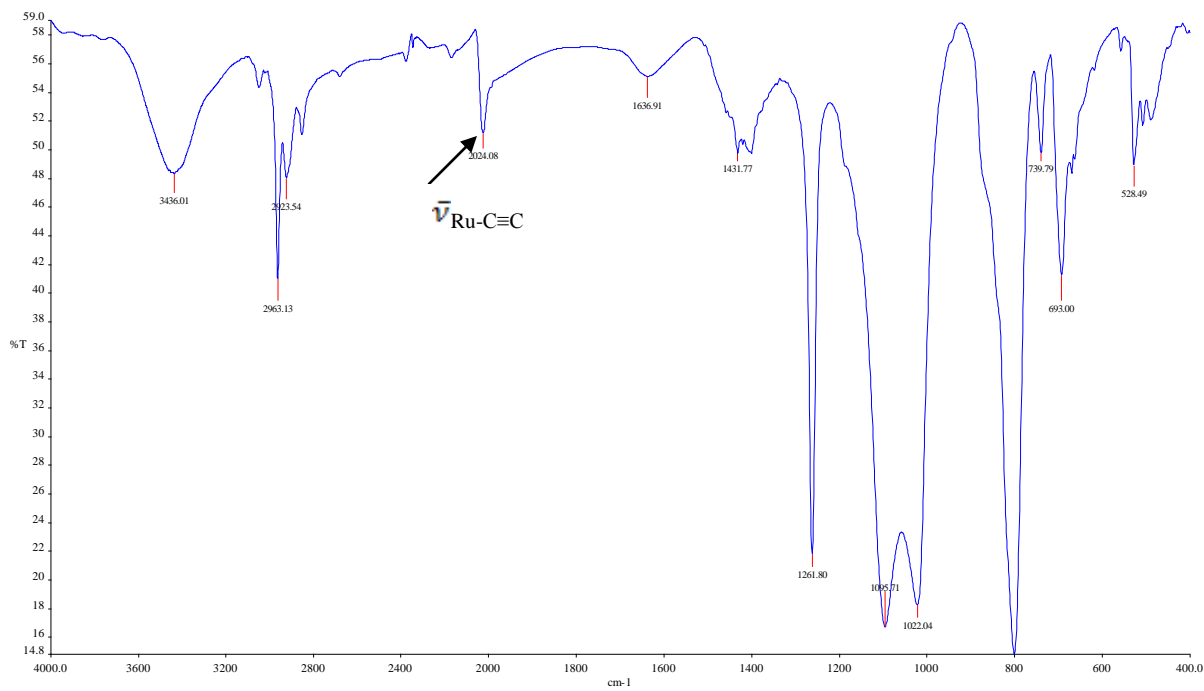


Fig. S41: FTIR spectrum of O7-Ru₂-Ph

Table S1. Selected spectroscopic parameter for ruthenium(II) diacetylide complexes

Compound	$^{13}\text{C}\{^1\text{H}\}$ (ppm, Ru-C \equiv C)	FTIR (cm^{-1} , $\bar{\nu}(\text{Ru-C}\equiv\text{C})$)	$^{31}\text{P}\{^1\text{H}\}$ (ppm, dppe ligand)
O1-Ru₂	126.9	2042	49.4
O3-Ru₂	126.9	2023	51.3
O5-Ru₂	126.9	2024	51.3
O7-Ru₂	126.9	2024	52.5
O1-Ru₂-Ph	126.9	2051	54.0
O3-Ru₂-Ph	127.1	2028	54.0
O5-Ru₂-Ph	127.1	2023	53.9
O7-Ru₂-Ph	126.9	2028	53.9

1e. CHN analysis

Complex	CHN data
O1-Ru₂	<p>DATE 07 12 16 TIME 14 09 21 OPERATOR ID CHEMISTRY</p> <p>RUN 16 ID SKP SSR 2358 WEIGHT 2.052</p> <p>SIGNALS</p> <p>ZR 8589 NR 9450 CR 27407 HR 31449</p> <p>CARBON 65.72% HYDROGEN 5.56% NITROGEN .20%</p>
O3-Ru₂	<p>DATE 07 12 16 TIME 14 29 09 OPERATOR ID CHEMISTRY</p> <p>RUN 20 ID SKP SSR 2359 WEIGHT 1.787</p> <p>SIGNALS</p> <p>ZR 8536 NR 9325 CR 25414 HR 28875</p> <p>CARBON 67.51% HYDROGEN 5.60% NITROGEN -.54%</p>

O5-Ru₂	<pre> DATE 23 11 16 TIME 14 21 52 OPERATOR ID CHEMISTRY RUN 16 ID SKP SSR2277R WEIGHT 1.916 SIGNALS ZR 7324 NR 8167 CR 25449 HR 29479 CARBON 67.31% HYDROGEN 6.06% NITROGEN .35% </pre>
O7-Ru₂	<pre> DATE 23 04 18 TIME 17 03 43 OPERATOR ID CHEMISTRY RUN 32 ID SKP SSR 2632 WEIGHT 1.738 SIGNALS ZR 6576 NR 7487 CR 24972 HR 29056 CARBON 69.64% HYDROGEN 6.25% NITROGEN -.08% </pre>

Complex	CHN data
O1-Ru₂-Ph	<pre> DATE 11 12 15 TIME 11 52 11 OPERATOR ID CHEMISTRY ID SKP SSR 2262 WEIGHT 2.152 SIGNALS ZR 5151 NR 6211 CR 24962 HR 29182 CARBON 65.68% HYDROGEN 5.58% NITROGEN .29% </pre>
O3-Ru₂-Ph	<pre> DATE 11 12 15 TIME 12 33 32 OPERATOR ID CHEMISTRY ID SKP SSR 2277 WEIGHT 2.143 SIGNALS ZR 5105 NR 6175 CR 25904 HR 31458 CARBON 69.29% HYDROGEN 7.64% NITROGEN .25% </pre>

O5-Ru₂-Ph	<p>DATE 22 05 18 TIME 14 11 16 OPERATOR ID CHEMISTRY</p> <p>RUN 18 ID SKP SSR 2358 WEIGHT 1.685</p> <p>SIGNALS</p> <p>CARBON 69.73% ZR 6565 HYDROGEN 6.53% NR 7313 NITROGEN 0.0% CR 23001 HR 27076</p>
O7-Ru₂-Ph	<p>DATE 23 04 18 TIME 17 03 43 OPERATOR ID CHEMISTRY</p> <p>RUN 32 ID SKP SSR 2632 WEIGHT 1.738</p> <p>SIGNALS</p> <p>CARBON 71.64% ZR 6576 HYDROGEN 6.25% NR 7487 NITROGEN -.08% CR 24972 HR 29056</p>

2. Photophysical Studies

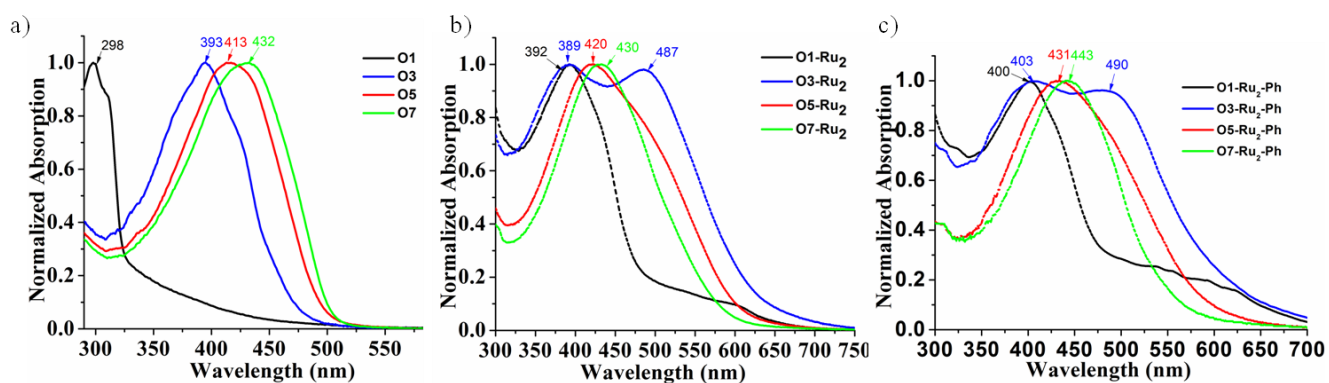


Fig. S42: Absorbance spectra of a) **O1-O7**, b) **O1-Ru₂** to **O7-Ru₂** and c) **O1-Ru₂-Ph** to **O7-Ru₂-Ph** in 1,2 DCE in $\sim 1 \times 10^{-5}$ M.

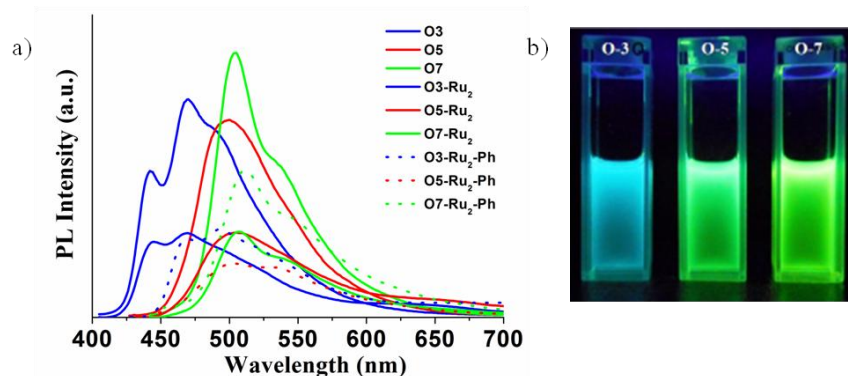


Fig. S43: a) PL spectra of **O3-O7**, **O3-Ru₂** to **O7-Ru₂** and **O3-Ru₂-Ph** to **O7-Ru₂-Ph** recorded in 1, 2 DCE. b) Visual appearance of **O3**, **O5**, **O7** in 1,2-DCE under UV illumination at 365 nm.

3. Thermal analysis

3a. TGA analysis

TGA study under N₂ atmosphere clearly indicates that all the diruthenium(II) diacetylide complexes have good thermal stability. The decomposition temperatures for **O1-Ru₂** to **O7-Ru₂** are from 290-332 °C respectively whereas for **O1-Ru₂-Ph** to **O7-Ru₂-Ph** the decomposition temperatures are from 295-340 °C respectively. The decomposition onset is defined by a 40-46 wt% loss for **O1-Ru₂** to **O7-Ru₂** corresponding to the removal of “-C≡C-Ru(dppe)₂Cl” moiety from the core of the molecular *wires*.

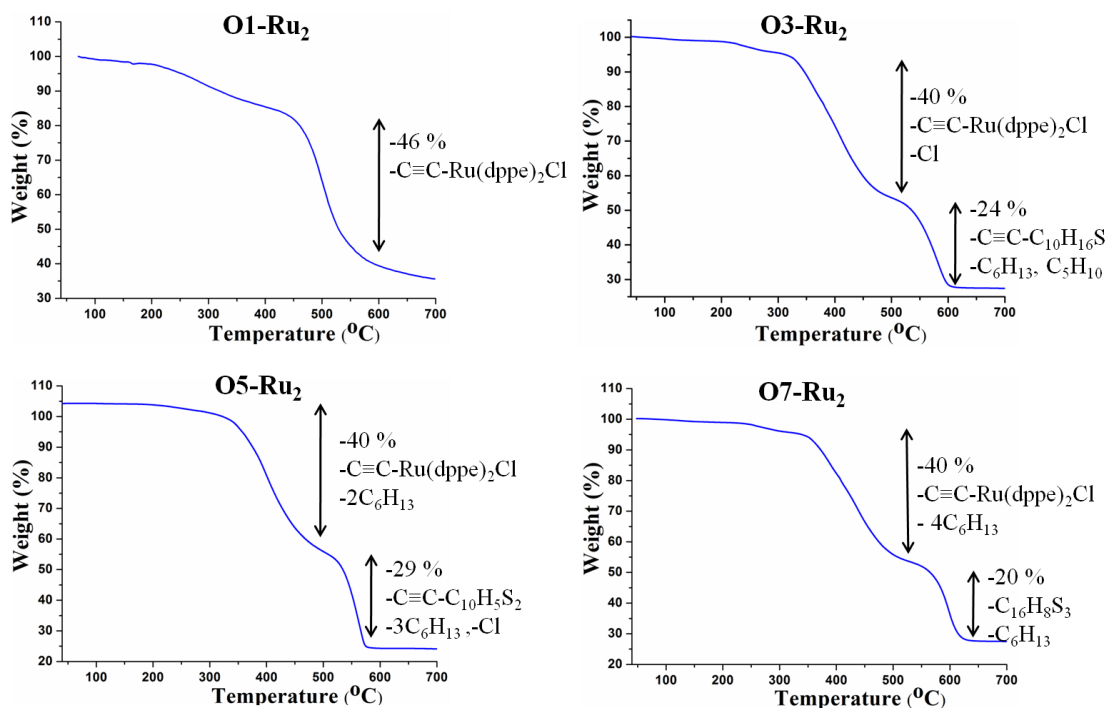


Fig. S44a: TGA Thermograms of **O1-Ru₂**, **O3-Ru₂**, **O5-Ru₂** and **O7-Ru₂** recorded at a rate of 10 °C/min under N₂ atmosphere

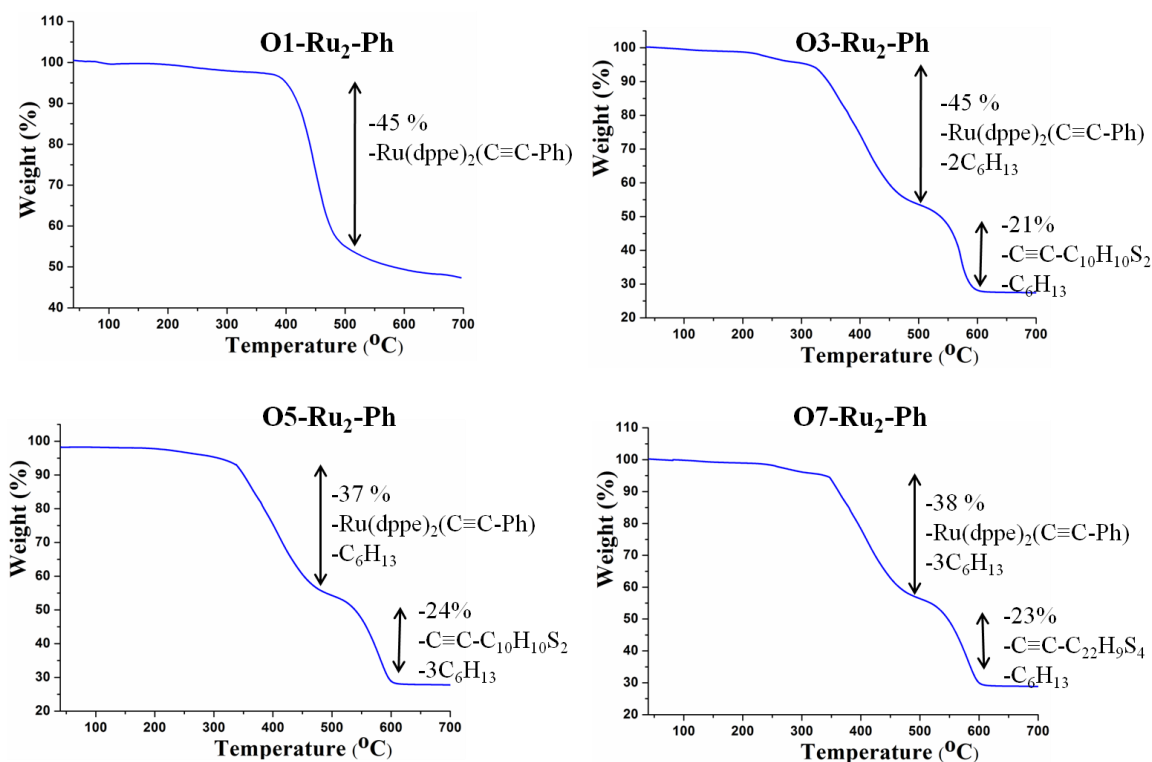


Fig. S44b: TGA Thermograms of **O1-Ru₂-Ph**, **O3-Ru₂-Ph**, **O5-Ru₂-Ph** and **O7-Ru₂-Ph** recorded at a rate of 10 °C/min under N₂ atmosphere

3b. DSC analysis

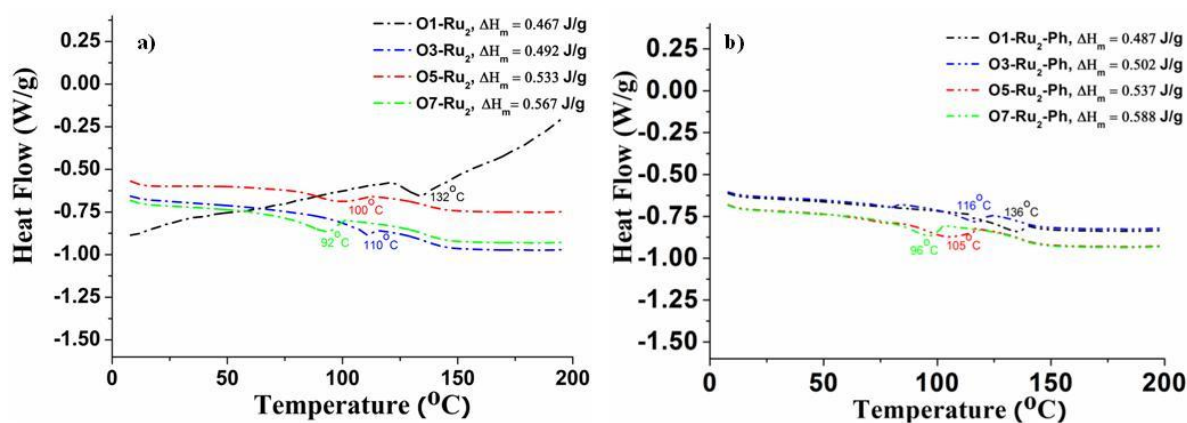


Fig. S45: DSC Thermograms of a) **O1-Ru₂** to **O7-Ru₂** and b) **O1-Ru₂-Ph** to **O7-Ru₂-Ph** recorded at a rate of 10 °C/min under N₂ atmosphere

4. Electrochemical Characterization

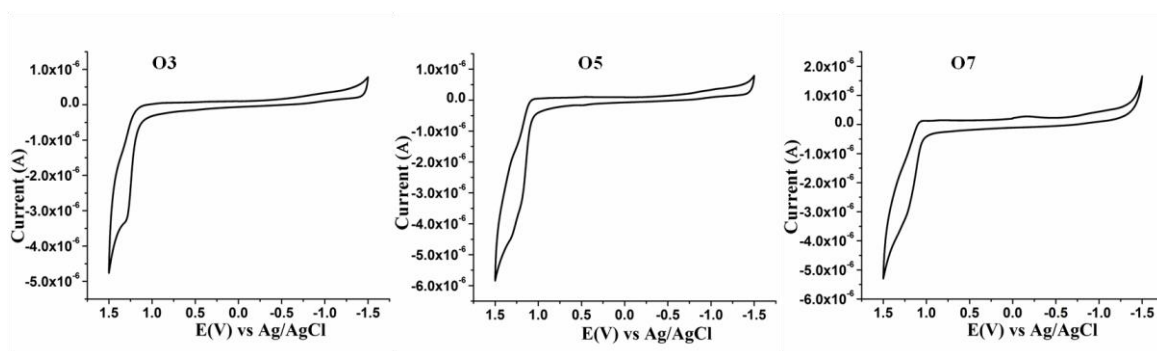


Fig. S46: Cyclic voltammograms (CV) of **O3**, **O5** and **O7** in DCM solution using TBAPF₆ as supporting electrolyte, Pt disc working electrode, and Ag/AgCl reference electrode. Scan rate at 100 mV/s.

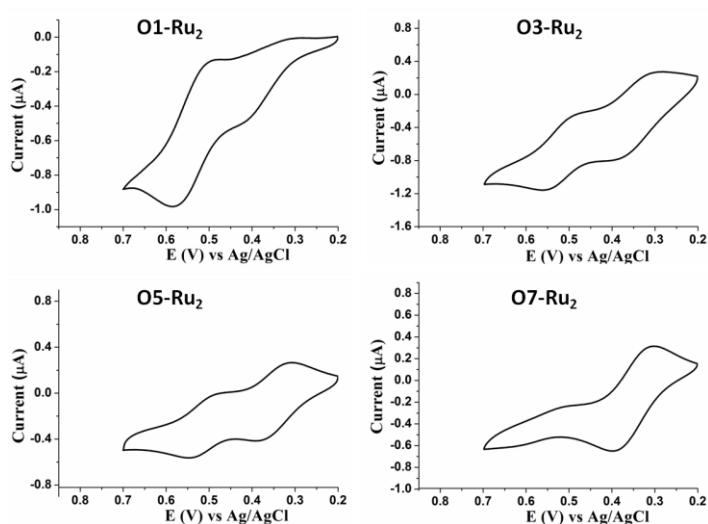


Fig. S47: Cyclic voltammograms (CV) of **O1-Ru₂**, **O3-Ru₂**, **O5-Ru₂** and **O7-Ru₂**.

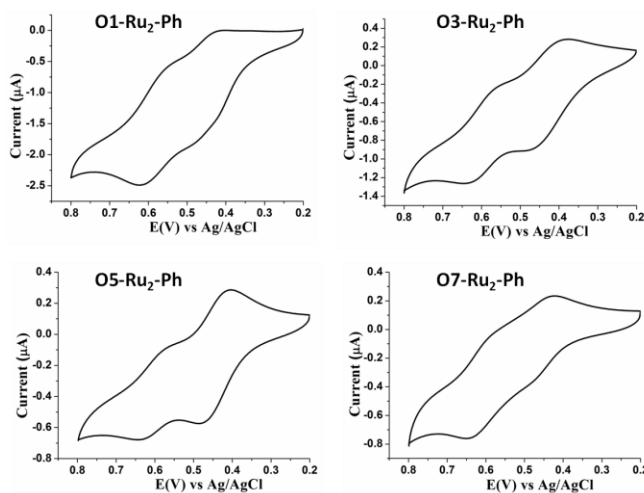


Fig. S48: Cyclic voltammograms (CV) of **O1-Ru₂-Ph**, **O3-Ru₂-Ph**, **O5-Ru₂-Ph** and **O7-Ru₂-Ph**.

5. Crystallographic data

X-ray data collections and refinement. The yellow block shaped single crystals of **12** suitable for X-ray crystallography were obtained by layering hexanes on DCM solution of **12** in a 8 mm dia glass tube. Data were collected at 293 K using graphite-monochromated Mo K α radiation ($\lambda_{\alpha} = 0.71073 \text{ \AA}$) on a Bruker-APEX-II CCD X-ray diffractometer equipped with an Oxford Instruments low-temperature attachment. The frames were indexed, integrated, and scaled using the SMART and SAINT software package,¹ and the data were corrected for absorption using the SADABS program.² Pertinent crystallographic data for **12** is summarized in Table S3. The title compound crystallizes in the monoclinic space group, P2₁/c. Two independent molecules of **12** were located in the asymmetric unit with negligible differences in their metrical parameters. CCDC 1827665 contains the supplementary crystallographic data for this paper. These data can be obtained free of charge from The Cambridge Crystallographic Data Centre via www.ccdc.cam.ac.uk/data_request/cif. The structure was solved by SHELXT³ and refined with SHELXL⁴ using Olex2 program.⁵ The molecular structure was generated by using ORTEP-3 for Windows Version 2.02.⁶ The hydrogen atoms were included in geometrically calculated positions in the final stages of the refinement and were refined according to the typical riding model. All non-hydrogen atoms were refined with anisotropic thermal parameters.

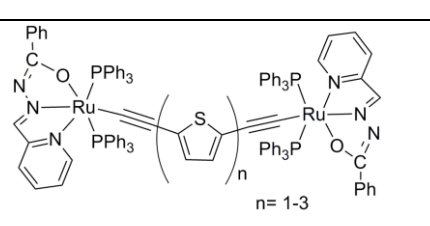
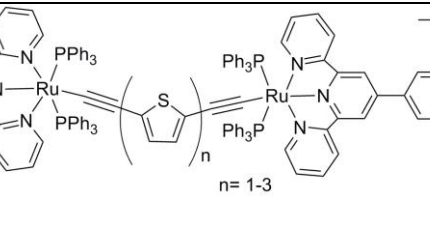
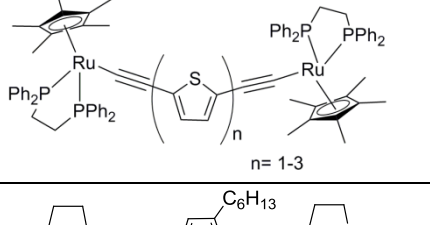
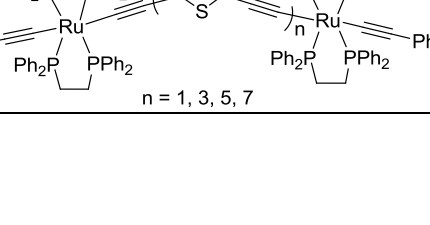
Table S2. Crystallographic data and refinement parameters for **12**.

12	
Empirical formula	C ₆₄ H ₆₃ ClP ₄ RuS
Formula weight	1124.60
Crystal system	Monoclinic
Space group	P2 ₁ /c
a, \AA	12.6925(11)
b, \AA	13.3259(11)
c, \AA	32.834(3)
α , deg	90.00
β , deg	95.886(5)
γ , deg	90.00
V, \AA^3	5524.2(8)
Z	4
ρ_{calcd} , g cm ⁻³	1.352
μ , mm ⁻¹	0.526
F(000)	2336
Reflections	
Collected	55682
independent	13726

observed [$I > 2\sigma(I)$]	6947
No. of variables	640
Goodness-of-fit	1.005
Final R indices [$I > 2\sigma(I)$] ^a	$R_1 = 0.0684$ $wR_2 = 0.1172$
R indices (all data) ^a	$R_1 = 0.1741$ $wR_2 = 0.1459$

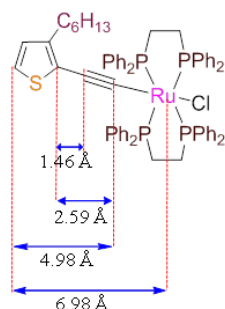
$$^a R_1 = \frac{\sum ||F_o| - |F_c||}{\sum |F_o|} \text{ with } F_o^2 > 2\sigma(F_o^2). \quad wR_2 = \frac{[\sum w(|F_o|^2 - |F_c|^2)|^2 / \sum |F_o|^4]^{1/2}}{1}$$

Table S3. Comparison of electronic communication data in the diruthenium(II) complexes with thienlethynyl bridges.

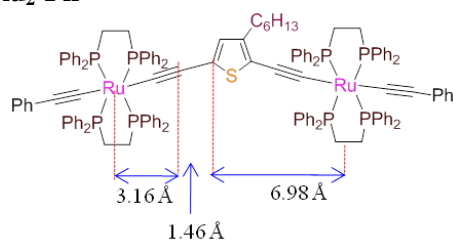
Compound	$\Delta E_{1/2}$ (V)	K_c	Reference
 n = 1-3	0.17, n=2 0.10, n=3	7.4×10^2 4.9×10^1	29
 n = 1-3	0.13, n=2 0.07, n=3	1.6×10^2 1.5×10^1	29
 n = 1-3	0.13, n=2 single wave, n=3	2.1×10^2 -	30
 n = 1, 3, 5, 7	0.12, n=1 0.17, n=3 0.16, n=5 0.15, n=7	1.1×10^2 7.5×10^2 5.0×10^2 3.4×10^2	this work

6. Estimation of intermetallic distances

From the molecular structure of **12** obtained from single crystal X-ray crystallography, the following bond distances are obtained.

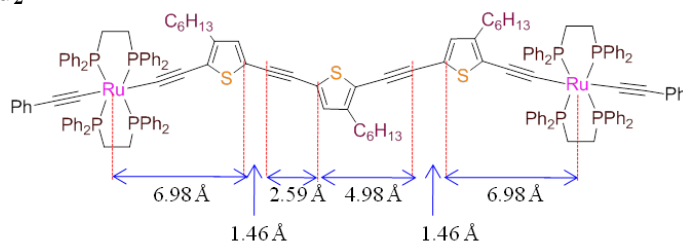


O1-Ru₂-Ph



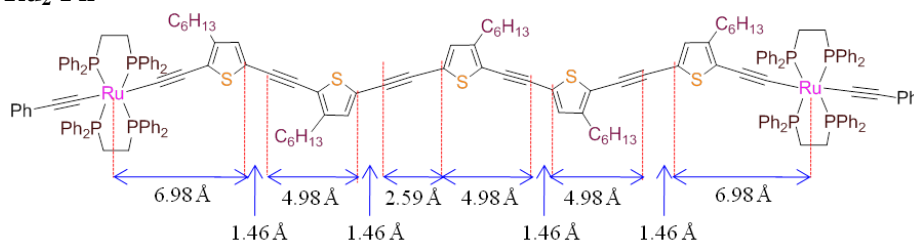
$$\text{Ru} \cdots \text{Ru} = 3.16 + 6.98 + 1.46 \text{ \AA} = 11.60 \text{ \AA}$$

O3-Ru₂-Ph



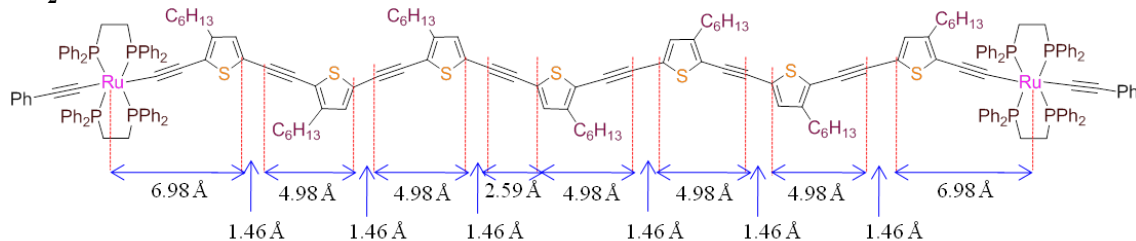
$$\text{Ru} \cdots \text{Ru} = (2 \times 6.98) + 2.59 + 4.98 + (2 \times 1.46) \text{ \AA} = 24.45 \text{ \AA}$$

O5-Ru₂-Ph



$$\text{Ru} \cdots \text{Ru} = (2 \times 6.98) + 2.59 + (3 \times 4.98) + (4 \times 1.46) \text{ \AA} = 37.33 \text{ \AA}$$

O7-Ru₂-Ph



$$\text{Ru} \cdots \text{Ru} = (2 \times 6.98) + 2.59 + (5 \times 4.98) + (6 \times 1.46) \text{ \AA} = 50.21 \text{ \AA}$$

Fig. S49: Intermetallic distances in the synthesized diruthenium(II) organometallic wires.

The calculated intermetallic distance values for the diruthenium(II) organometallic *wires* may not be absolutely accurate. However, considering the long-range distance, the obtained calculated values are sufficiently informative for our discussion. The distances are very similar as reported for mentioned in the similar thienylethynyl rod-like oligomers.⁷ The intermetallic distances calculated from the theoretical studies of the geometrical optimized structures are of well agreement with the distances measured by the above method.

Table S4. Intermetallic distances.

Complexes	Ru...Ru distance (Å)	Ru...Ru distance (Å) calculated from DFT. ^a
O1-Ru₂-Ph	11.6	11.6
O3-Ru₂-Ph	24.4	24.3
O5-Ru₂-Ph	37.3	35.6
O7-Ru₂-Ph	50.2	

^aAs truncated model systems [**O1-Ru₂-Ph-H**], [**O3-Ru₂-Ph-H**] and [**O5-Ru₂-Ph-H**], where the “-Ph” ligands of the PPh₃ moiety were replaced by “-H” atoms.

7. UV-vis-NIR measurements

The UV-vis-NIR spectra were measured on a Varian (Model- Cary 5000) UV-vis-NIR spectrometer. For the absorption measurements, the compound was dissolved in 1,2-DCE solution ($\sim 1 \times 10^{-5}$ M). To this solution, an organometallic oxidant [Cp₂Fe][BF₄] in 1,2-DCE was added and the resulting solution was quickly mixed and immediately subjected to UV-vis-NIR measurements. A very weak to negligible IVCT band in the region of 1200-2000 was observed.

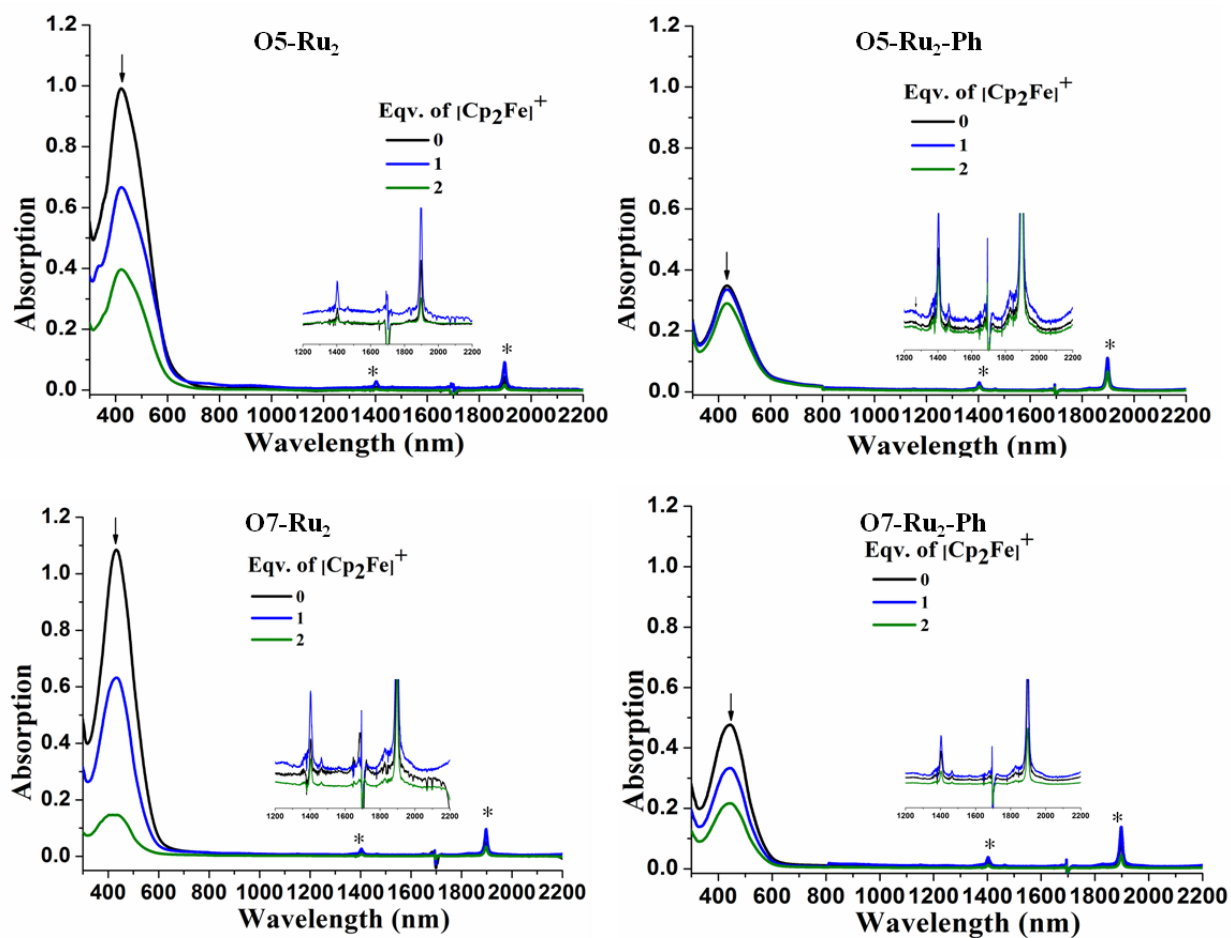


Figure S50: Stepwise electrochemical oxidation of representative diruthenium complexes **O5-Ru₂**, **O7-Ru₂**, **O5-Ru₂-Ph** and **O7-Ru₂-Ph** using [Cp₂Fe]⁺ in 1,2-DCE solvent. The insets show the enlarged plot of the NIR region. Asterisk (*) indicates artifacts.

8. Selected frontier molecular orbitals obtained from DFT calculation

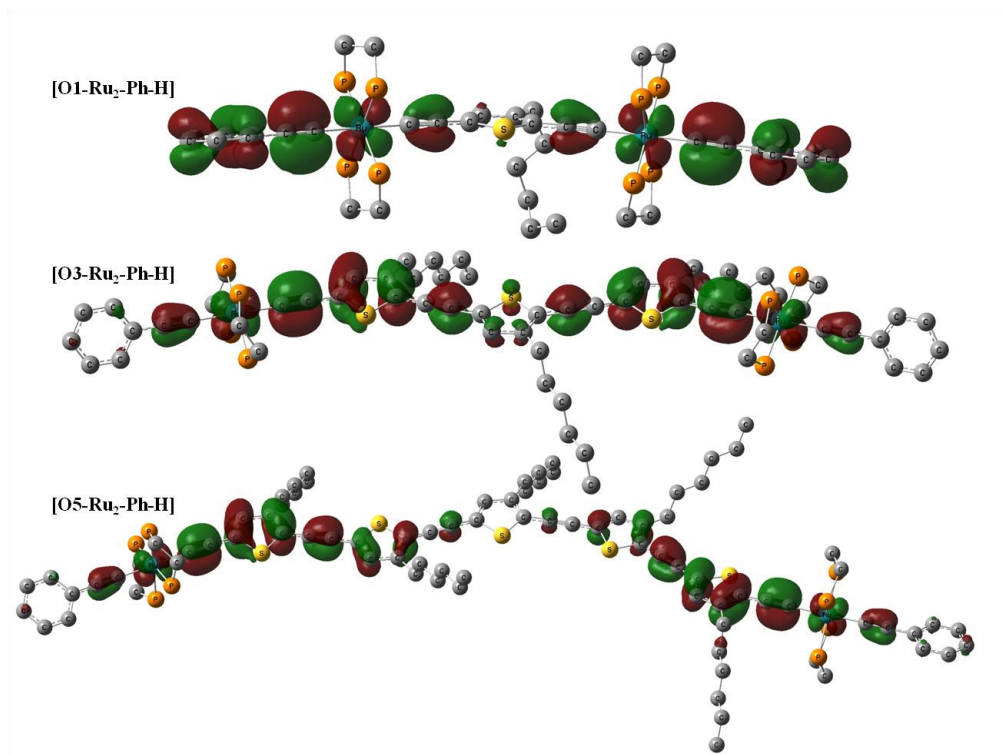


Figure S51. HOMO-1 frontier molecular orbitals of the model complexes [O1-Ru₂-Ph-H], [O3-Ru₂-Ph-H] and [O5-Ru₂-Ph-H].

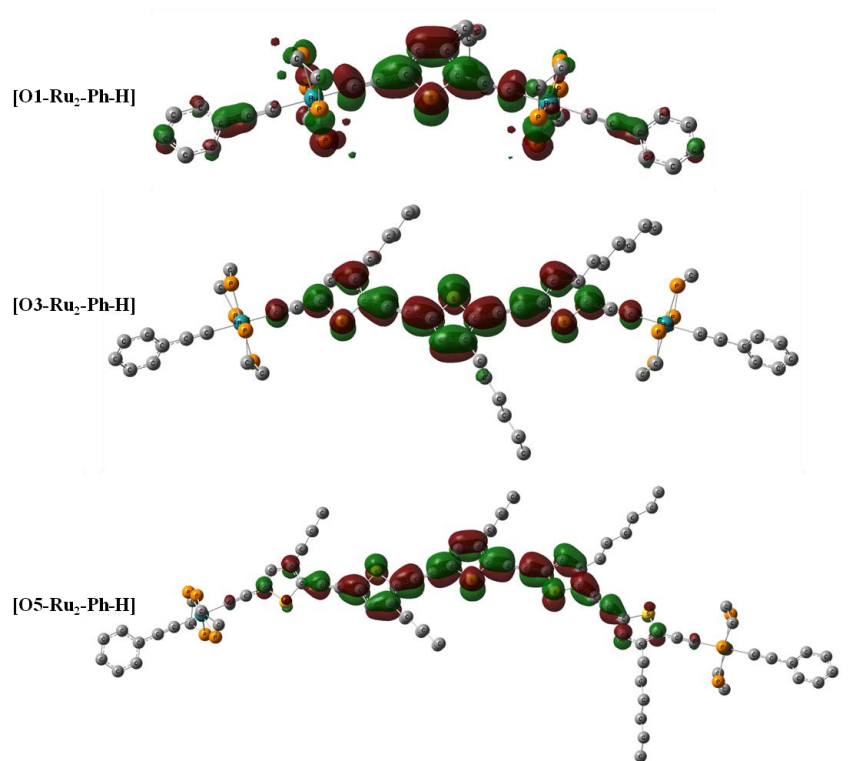


Figure S52. LUMOs of the model complexes [O1-Ru₂-Ph-H], [O3-Ru₂-Ph-H] and [O5-Ru₂-Ph-H].

9. References

1. SAINT+ Software for CCD Diffractometers, Bruker AXS, Madison, WI, 2000.
2. Sheldrick, G. M. SADABS Program for Correction of Area Detector Data, University of Göttingen, Göttingen, Germany, 1999.
3. G. M. Sheldrick, SHELXT - Integrated space-group and crystal-structure determination *Acta Cryst.*, 2015, **A71**, 3-8.
4. G. M. Sheldrick, Crystal structure refinement with SHELXL *Acta Cryst.*, 2015, **C71**, 3-8.
5. O.V. Dolomanov, L.J. Bourhis, R.J. Gildea, J.A.K. Howard and H. Puschmann, OLEX2: A complete structure solution, refinement and analysis program *J. Appl. Cryst.*, 2009, **42**, 339-341.
6. L. J. Farrugia, ORTEP-3 for windows-A version of ORTEP-III with a graphical user interface (GUI) *J. Appl. Cryst.*, 1997, **30**, 565.
7. J. M. Tour Molecular electronics. synthesis and testing of components. *Acc. Chem. Res.* 2000, **33**, 791-804.